

(i)

EFFECT OF TEMPERATURE ON THE RATE OF DECAY OF PHOSPHORESCENCE
IN ORGANIC GLASSES

A thesis presented for the
degree of Doctor of Philosophy in Chemistry
in the University of Canterbury,
Christchurch, New Zealand.

by

SMITH G. J.

1970

(ii)

ACKNOWLEDGEMENTS

I would like to thank Dr. R. F. C. Claridge for his help during the course of this work and the University Grants Committee for the award of a Postgraduate Scholarship.

I would also like to express my thanks to the technical staff of the Chemistry Department and particularly to Mr. C. Rowe and Mr. R. Hooper who designed and built most of the electronic equipment shown in Appendix II.

G. J. Smith

April, 1970

(iii)

CONTENTS

TITLE	(i)
ACKNOWLEDGEMENTS	(ii)
CONTENTS	(iii)
CHAPTER 1 <u>PHOSPHORESCENCE</u>	1
1.1 Introduction	1
1.2 Relationship Between Electronic States	3
1.3 Population of the Triplet States	4
1.4 Depopulation of the Triplet State	4
(a) Ground State Quenching	5
(b) Triplet-Triplet Annihilation	5
(c) Quenching by Impurities	6
(d) Radiative Decay or Phosphorescence	8
(e) Non-Radiative Transitions	9
1.5 Experimentally Determined Rate of Triplet State Decay	11
CHAPTER 1.1 <u>DIFFUSION AND THE TEMPERATURE DEPENDENCE OF RATE CONSTANTS</u>	13
2.1 Introduction	13
2.2 Rate of Bimolecular Reaction	14
2.3 Diffusion in a one Component Condensed Phase	18
2.4 Temperature Dependence of a Rate Constant	20
2.5 Diffusion in Binary Mixtures	22

CHAPTER III REVIEW	27
3.1 Introduction	27
3.2 Temperature Dependence of Phosphorescence	
Lifetime	27
(a) "Low Viscosity" Region	28
(b) "High Viscosity" Region	33
3.3 Pressure Dependence of Phosphorescence Lifetime	39
3.4 Rationale	40
CHAPTER IV EXPERIMENTAL	45
4.1 Introduction	45
4.2 Preparation of cells	46
4.3 Impurities	49
4.4 Choice of Phosphorescent Materials	50
4.5 Purification	51
(a) Solvents	51
(b) Naphthalene	52
(c) Mono Methyl Substituted 1,2-Benzanthracenes	53
4.6 Temperature Control and Measurements	54
4.7 Recording of Phosphorescence	56
4.8 Analysis of Data	57
4.9 Errors	62
CHAPTER V RESULTS AND DISCUSSION	65
Typical Least Squares Fit of Intensity-Time Data	65
Section I Results	66
Section I Discussion	74

(v)

Section 2 Results	77
Section 2 Discussion	83
Section 3 Results	85
Section 3 Discussion	97
Section 4 Results	100
Section 4 Discussion	103
 <u>APPENDIX I ZONE REFINING</u>	 106
 <u>APPENDIX II CIRCUIT DIAGRAMS</u>	
 <u>APPENDIX III LEAST SQUARES FITTING OF DATA TO A FUNCTION</u>	109
 <u>REFERENCES</u>	113

CHAPTER I

PHOSPHORESCENCE

1.1. INTRODUCTION

Each orbital of a molecule in its ground or unexcited state is usually occupied by two electrons, if the molecule has an even number of electrons. The Pauli Exclusion Principle demands that electrons occupying the same orbital have their spins aligned in opposite directions.

If one electron in the molecule is excited to a higher electronic level, its spin can either be oriented parallel or antiparallel to the spin of the electron remaining in the orbital from which the excited electron was removed. If the spins are antiparallel the molecule is said to be in a singlet state or if the spins are parallel the molecule is said to be in a triplet state. Alternatively the molecule can be said to have a "multiplicity" of one or three respectively.

The term "phosphorescence", usually refers to the light emitted by an excited molecule which may accompany the transition from the lowest triplet state to the ground singlet state of the molecule.

Theoretically, if angular momentum is to be conserved, transitions can only occur between states of the same multiplicity. In practice, because of a perturbation to the electron's spin quantum number due to coupling between the rotation of the electron

on its axis and its orbital motion around the nucleus, there is a finite probability of a radiative transition between triplet and singlet states. This probability is however, very much smaller than between states of the same multiplicity. This lower radiative transition probability manifests itself as a longer lived luminescence than fluorescence, which is the emission accompanying a radiative degradation between electronic states of the same multiplicity. For example, fluorescence typically has a lifetime of the order of nanoseconds whereas phosphorescence has a lifetime from 10^{-4} to 10 seconds.

Because of its long lifetime, phosphorescence is very difficult to observe in the gaseous or liquid phases due to faster competing non-radiative quenching processes. A quenching reaction is a process in which the excitation energy possessed by the triplet state is dissipated by some chemical species present in the system. Phosphorescence may often be readily observed from irradiated molecules in the solid state where molecular movement has largely been "frozen out". Under these conditions quenching reactions become very much slower than in the liquid or gaseous phases and consequently phosphorescence may compete with the quenching reactions far more successfully.

Phosphorescence has been observed in a number of solid state environments. In 1896, Schmidt⁽¹⁾ was the first to observe phosphorescence from molecules trapped in a "glassy" matrix. This technique was employed by Vavilov⁽²⁾ and later extensively used by

Lewis and Terenin⁽³⁾ in the 1940's. Today, glasses commonly used, are those formed on cooling 3-methylpentane, Methylcyclohexane - isopentane mixtures, and a variety of other organic solvent mixtures⁽⁴⁾. Oster⁽⁵⁾ and Welhuish⁽⁶⁾ have employed plastics as rigid media for phosphorescence studies. Among the plastics that have been found useful are polycarbonates, acrylics, polystyrene, and cellulose polymers. A good deal of work has also been done on the phosphorescence of molecules in the crystalline state⁽⁷⁾.

1.2 RELATIONSHIP BETWEEN ELECTRONIC STATES

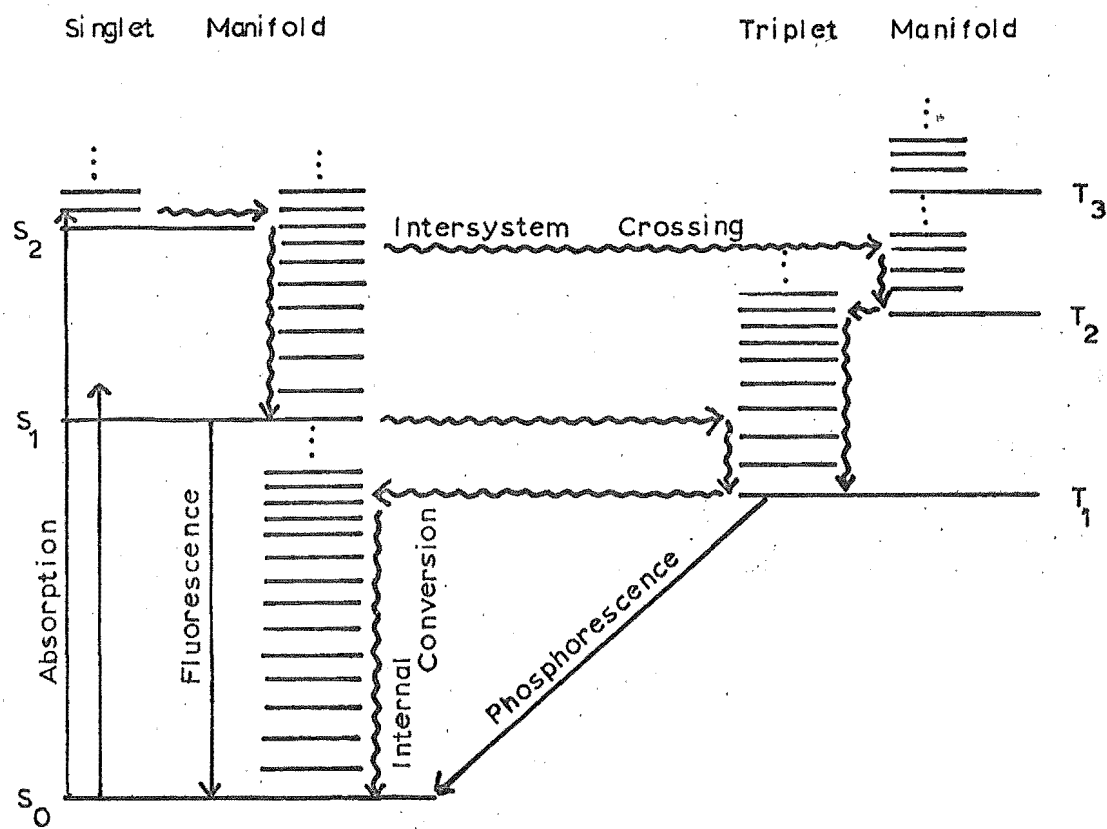
The relationship between electronic states may be most readily discussed by reference to diagram 1.1. The wavy lines refer to non-radiative processes and the straight lines refer to radiative processes.

When molecules in their ground state absorb light energy they are excited to upper singlet states. At low temperatures, molecules excited to higher vibrational levels within an electronic state quickly ($<10^{-12}$ seconds) fall into the lowest vibrational level by a non-radiative process, from where they can either undergo "intersystem crossing", to a vibrational level of an electronic state of the same energy but of different multiplicity, or "internal conversion", to a lower electronic level of the same multiplicity.

Phosphorescence is generally only observed from a transition between the lowest triplet state and the ground state. This is presumably because the rate of intersystem crossing and

DIAGRAM 1.1

Energy Level Diagram



internal conversion within the higher energy states is faster than radiative and non-radiative processes between the first excited triplet state and ground state.

1.3 POPULATION OF THE TRIPLET STATE

From the fact that phosphorescence is observed, it may be deduced that the process, $T_1 \rightsquigarrow S_0$, is slower than the process, $S_1 \rightsquigarrow T_1$. The $S_1 \rightsquigarrow T_1$ transition appears to be the principal means of populating the lowest triplet state where the exciting illumination is of low or medium intensity. In fact, for anthracene, it has been estimated that only about 0.01% of the triplet state population is due to the direct spin-forbidden excitation $T_1 \leftarrow S_0$.

The process of excitation may be summarised as follows:



1.4 DEPOPULATION OF THE TRIPLET STATE

The work described in this thesis is concerned with some of the mechanisms that are important in the depopulation of the triplet state.

Generally the mechanisms which contribute to the depopulation of the triplet state may be summarized by the kinetic equation proposed by Linschitz⁽⁸⁾.

$$-\frac{d[T_1]}{dt} = k_p [T_1] + k_{QP}[T_1] + k_{TT}[T_1]^2 + k_{TS_0}[T_1][S_0] + \sum_i k_{QM_i}[T_1][M_i]$$

Where $[T_1]$ refers to the concentration of the lowest triplet state.

$[S_0]$ refers to the concentration of the ground state,

$[M_i]$ refers to the concentration of the i th quenching species,

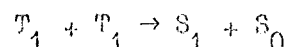
and the subscripted k 's refer to the rate constants of the different mechanisms of deactivation.

(a) Ground State Quenching:

The term $k_{TS_0} [T_1] [S_0]$ describes the contribution to the rate of decay of the triplet state by quenching of the triplet state with the ground state. For most molecules this term is found to be negligible. (9)

(b) Triplet - Triplet Annihilation:

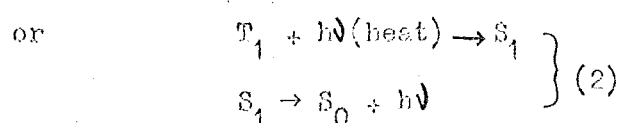
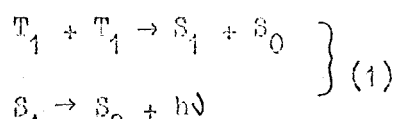
The term $k_{TT} [T_1]^2$ is usually negligible at low solution concentrations and low intensity exciting illuminations, because under these conditions $[T_1]$ is small. It is associated with the reaction:



This reaction is important as a source of the emission known as "delayed fluorescence" which has been extensively studied by G.A. Parker who has also written reviews on the subject (10).

This emission has the same spectral characteristics as fluorescence, but a lifetime comparable to that of phosphorescence.

The usual mechanisms proposed for its production are:



Mechanism (1) can be important at low temperatures provided $[T_1]$ is great enough and the viscosity of the medium low enough to make a diffusion controlled $T + T$ reaction competitive with normal radiative or non-radiative deactivation to the ground state.

Mechanism (2) is only important near or above room temperature where there is sufficient thermal energy to allow some thermal population of higher vibrational levels of the lowest triplet state, from where intersystem crossing to the first excited singlet state can take place.

(c) Quenching by Impurities:

$\sum_i k_{QMi} [M_i] [T_1]$ expresses the contribution to the rate of decay of the triplet state made by quenching reactions of species M_i with T_1 .

There are several types of quenching reactions that are possible, some of which are very efficient. This imposes stringent standards of purity on the reagents used in studies of phosphorescent lifetimes, as traces of some impurities can have a significant effect on the rate of decay by quenching.

(i) Since the triplet state is a biradical, it is very reactive, particularly with other radical species. The type of reaction envisaged in this kind of quenching is an addition:



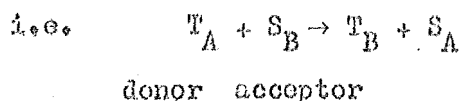
followed by some further reaction to produce a more stable product. This type of quenching demands triplet - quench encounter and hence is not important in a completely rigid medium. However, as the

temperature increases, the viscosity of the medium decreases and if a quenching species is present, diffusion controlled reactions between it and the triplet state species become important, with a consequent increase in the rate of decay of the triplet state.

One of the most effective quenchers in this category is oxygen. This is because oxygen, in its ground state, is a biradical and also being quite small, it has a high mobility.

(ii) Another way a molecule can quench the triplet state is by perturbing the triplet state and increasing the spin-orbit coupling so that the spin selection rule is partially broken down, with a consequent increase in transition probability between states of different multiplicity. The type of species likely to have this effect are heavy atoms or paramagnetic species such as transition metal ions, oxygen or nitric oxide.

(iii) Another quenching mechanism is radiationless energy transfer to a singlet state of a molecule having a triplet state of lower energy than that being studied.



where the energy of T_A is greater than the energy of T_B .

Such a reaction is spin allowed and highly efficient.

This type of reaction was first observed by Terenin and Ermolceev⁽¹¹⁾ in studying naphthalene in a rigid ethanol matrix at 77°K. The solution was irradiated by light at 3660 Å and no phosphorescence was observed because naphthalene does not absorb at this wavelength. However, when benzaldehyde was introduced,

phosphorescence characteristic of naphthalene was observed after further irradiation with light at 3660\AA . This suggested that benzaldehyde has been excited to its triplet state and then donated its energy to naphthalene, which had then been excited to its triplet state. Excitation of naphthalene could not have been achieved by singlet \rightarrow singlet energy transfer because the singlet state of benzaldehyde is of lower energy than that of naphthalene.

This type of energy transfer can operate over comparatively long distances (up to about 50\AA).

(a) Radiative Decay or Phosphorescence:

The term, $k_p[T_1]$, refers to the contribution of radiative decay to the degradation of the triplet state.

Because of spin-orbit coupling, the singlet states of a molecule have some triplet character and likewise the triplet states have some singlet character. The triplet state is described by an eigenfunction of a Hamiltonian made up of a pure triplet state component and a spin-orbit perturbation.

$$\text{i.e. } (\hat{H}_0 + \hat{H}_{SO})^3\psi_1 = \beta_{E_1}^3\psi_1$$

where \hat{H}_0 is the Hamiltonian operator of the pure triplet state and \hat{H}_{SO} is the Hamiltonian operator of the spin-orbit interaction, $^3\psi_1$ is the wavefunction of the first or lowest "triplet" state and β_{E_1} , is its energy. $^3\psi_1$ may be expressed in terms of the first-order perturbation theory as:

$${}^3\psi_1 = {}^3\psi_1^0 + \sum_k a_k {}^1\psi_k^0$$

where ${}^3\psi_1^0$ is the wavefunction of the first pure triplet state, ${}^1\psi_k^0$ is the wavefunction of the kth pure singlet state, a_k is a coefficient and the sum is taken over the entire singlet manifold.

From perturbation theory:

$$a_k = \frac{\int ({}^3\psi_1^0)^* \hat{H}_{SO} {}^1\psi_k^0 d\tau}{|{}^3E_1 - {}^1E_k|}$$

the integration being taken over the entire configurational space, τ .

Similarly, the wavefunction for the ground state may be written as:

$${}^1\psi_0 = {}^1\psi_0^0 + \sum_i b_i {}^3\psi_i^0$$

The radiative transition probability of a molecule, as derived from time dependent perturbation theory, is proportional to the square of the matrix element of the dipole moment of the molecule, \bar{M}_{T_1, S_0} .

$$\text{i.e. } \bar{M}_{T_1, S_0} = \int ({}^3\psi_1^0)^* \vec{r} {}^1\psi_0^0 d\tau$$

$$= \sum_k a_k \bar{M}_{S_k, S_0} + \sum_i b_i \bar{M}_{T_i, T_1} \neq 0$$

(e) Non-radiative Transition:

The term, $k_{QP}[T_1]$, refers to the degradation of the triplet state by a non-radiative transition to the ground state. This is often considered to be essentially an intramolecular

process, although the environment acts as an energy sink to the transition.

This is the approach taken by Robinson and Froehl⁽¹²⁾. They assume a perturbation, H' , makes the system non-stationary with respect to a radiationless transition between the zeroth vibrational level of a triplet state and a lower singlet state, made degenerate with the zeroth vibrational level of the triplet state by the addition of primarily molecular vibrational energy. The singlet state interacts with the environment in such a way as to lose the excess vibrational energy in the singlet state, making the $T \rightarrow S^*$ process irreversible. The origin of the perturbation, H' , is considered to be interactions among the electrons and nuclei of the system. Other workers have suggested it could also arise from the dependence of the electronic states on nuclear displacement.

The transition probability, p , between the states ψ_i , initial, and ψ_f , final, of the type described above is:

$$p = (2\pi/\hbar) \rho_E (\int \psi_f^* \hat{H} \psi_i d\tau)^2$$

where ρ_E is the density of states. By separating the wavefunctions into electronic and vibrational parts and summing the probability, p , over the whole system, it can be shown that the rate of non-radiative transition $T \rightarrow S^*$ is:

$$\begin{aligned} k &= (2\pi/\hbar) \rho_E J^2 \sum (\int \phi_f^* \hat{H} \phi_i d\tau)^2 \\ &= (2\pi/\hbar) \rho_E J^2 E(E) \end{aligned}$$

where J is an electronic matrix element and $F(E)$ is the Franck-Condon factor, which is the sum of the squares of the vibrational overlap integrals. As the energy separation between electronic states increases, $F(E)$ decreases. This explains the slow non-radiative transition $T_1 \rightarrow S_0$ compared with non-radiative intersystem crossing between higher excited states.

Siebrand⁽¹³⁾, Lin⁽¹⁴⁾, Ross⁽¹⁵⁾ and others have extended this approach by trying to obtain values for $F(E)$ by considering the molecular vibrations they believe to be important in the radiationless transition.

1.5 EXPERIMENTALLY DETERMINED RATE OF TRIFLET STATE DECAY

In all experimental measurements of phosphorescence lifetimes done in this work the rate constant determined is either:

$$k_{\text{exp}} = k_p + k_{Qp} + k_{Qm} [\text{m}]$$

when a quenching species, m, is present

or:

$$k_{\text{exp}} = k_p + k_{Qp}$$

in the absence of a quench.

The only way to separate the radiative rate constant from the non-radiative rate constant is by measuring the absolute phosphorescence and fluorescence quantum yields, Φ_p and Φ_F respectively. The quantum yield of a process, is the ratio of the number of quanta involved in that process to the number of

quanta initially absorbed by the system. So for systems where no quenching species are present:

$$\frac{k_{\text{exp}}}{k_p} = \frac{k_p + k_{Qp}}{k_p} = \frac{1 - \phi_F}{\phi_p}$$

hence: $k_p = \frac{k_{\text{exp}} \phi_p}{1 - \phi_F}$

In this project however, it was not necessary to separate the measured rate constant into its component rate constants, and therefore it was not necessary to determine the absolute phosphorescence and fluorescence quantum yields.

CHAPTER IIDIFFUSION AND THE TEMPERATURE DEPENDENCE OF RATE CONSTANTS2.1 INTRODUCTION

The work described in this thesis is concerned with the temperature dependence of the rate of decay of triplet state species embedded in organic glasses. This chapter is principally intended to show what this temperature dependence is and hence the information that can be derived from it.

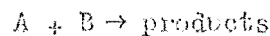
In all the systems studied, the phosphorescence decays were exponential, implying that either the reaction being studied was unimolecular, or in the case of the solutions saturated with oxygen, pseudo-first order.

All kinetic processes involve the surmounting of an energy barrier or perhaps a number of energy barriers. The speed at which the process proceeds at a given temperature depends on the magnitudes of the energy barriers.

Some of the reactions studied in this project appeared to be "diffusion controlled". i.e. The energy barrier to diffusion limits the speed of the reaction. An example of this kind of reaction was the quenching of the phosphorescence of naphthalene with oxygen. This reaction, although bimolecular, was pseudo-first order because of the large excess of oxygen present in the solutions saturated with oxygen. In other reactions studied, some other type of energy barrier appeared to limit the rate of reaction.

For example, the decays of phosphorescence of the mono-methyl substituted 1, 2-benzanthracenes in the absence of oxygen.

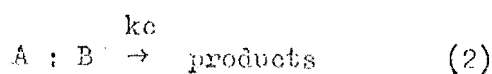
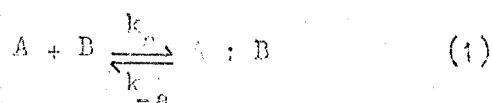
The first sections of this chapter are devoted to establishing the temperature dependence of the rate of the disappearance of a species, A, in a simple bimolecular reaction of the type:



This is followed by an examination of the effect of any concurrent unimolecular reactions of species A on the temperature dependence of the rate of disappearance of A. The final section in this chapter deals with the dependence of the energy barrier to diffusion in a binary mixture, on the composition of the mixture.

2.2 RATE OF A BIMOLECULAR REACTION

In a simple bimolecular reaction involving two reactants, A and B, there are two distinct steps involved. Firstly the reactants must come together and secondly, there is a redistribution of energy and bonds. These processes may be written as:



The species written A : B is termed an "encounter" between A and B. i.e. A and B are in such a position in space where reaction between them can take place if the energy requirements of reaction (2) are satisfied. k_a and k_{-a} are the rate constants for the diffusive approach and separation of the reactants respectively. k_c is the

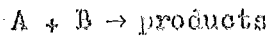
rate constant for the chemical change to the products.

k_a and k_{-a} can be related to a quantity, D_{AB} , which is the diffusion coefficient of molecule A relative to molecule B. Chandrasekhar⁽¹⁶⁾ has shown that:

$$D_{AB} = D_A + D_B$$

where D_A and D_B are the diffusion coefficients of molecules A and B respectively.

An equation for the rate of the overall reaction



in terms of D_{AB} and the energy barrier to reaction (2), may be derived in the way outlined below. This treatment is due to Waite⁽¹⁷⁾.

Consider the conditional probability of a molecule A_i being in an infinitely small volume element dv_A at r_A , t and a molecule B_j being in a similar volume element dv_B at r_B , t. (t is the time and r_A and r_B refer to spatial positions within the system).

This probability may be expressed as:

$$p_{ij}(r_A, r_B, t) dv_A dv_B / V^2$$

The rate of change in this probability when A_i and B_j are subject to diffusion and being consumed by reaction, is:

$$\frac{dp_{ij}}{dt} = D_{AB} \left[\frac{\partial^2 p_{ij}}{\partial r^2} + \frac{2}{r} \frac{\partial p_{ij}}{\partial r} \right] + \left(\frac{\partial p_{ij}}{\partial t} \right)_{\text{chem.}} \quad 2(i)$$

where $r = |r_A - r_B|$

The first term of the right hand side of the expression

describes the rate of change of p_{ij} in the six dimensional volume element, $dv_A dv_B$, due to the probability that A_i may diffuse in or out of dv_A and that B_j may diffuse in or out of dv_B . The second term on the right expresses the rate of change of p_{ij} due to chemical reaction of A_i or B_j .

The total rate of reaction is the sum over every AB pair of the probability flux of A into B. Since all of the p_{ij} are identical, this is given by:

$$\frac{d[A]}{dt} = \frac{d[B]}{dt} = \left(\frac{N_A^0}{V} \right) \left(\frac{N_B^0}{V} \right) 4\pi r_{AB}^2 D \left(\frac{\partial p_{ij}}{\partial r} \right) \Big|_{r=r_{AB}} \quad 2(i)$$

where r_{AB} is the "encounter" distance, N_A^0 and N_B^0 are the initial numbers of species A and B respectively in the system. If equation 2(i) can be solved for p_{ij} using the boundary conditions:

- (a) $p_{ij} = 1$ at $t = 0$ (random initial distribution)
- (b) $p_{ij} \rightarrow p_{\text{equilibrium}}$ at $t \rightarrow \infty$
- (c) as $r \rightarrow \infty$, p_{ij} becomes independent of r and equal to its average over the system.
- (d) a boundary condition at $r=r_{AB}$ (This boundary condition is discussed below).

$(\partial p_{ij} / \partial r)_{r=r_{AB}}$ can then be determined and substituted in equation 2(ii) to give the rate of reaction. The boundary condition at $r = r_{AB}$ due to Collins and Kimball⁽¹⁸⁾ is derived in the following way. The probability that B is in a shell of thickness Δr ,

surrounding molecule A, such that the encounter radius is r_{AB} , is:

$$\frac{4\pi r_{AB}^2 \Delta r p(r_{AB}, t)}{V}$$

The probability of the energy and steric requirements of reaction (2) being satisfied is:

$$\mathcal{J}_p \exp(-E_a/RT)$$

where \mathcal{J}_p , p , E_a are the collision frequency during encounter, the steric factor and the chemical activation energy respectively.

The probability of chemical reaction during time t , is the product of the probability of molecule A and B being in a spatial position where chemical reaction is possible, and the probability of the energy and steric requirements of reaction (2) being satisfied.

i.e.
$$\frac{4\pi r_{AB}^2 \Delta r p(r_{AB}, t)}{V} \times \mathcal{J}_p \exp(-E_a/RT)$$

By equating this, with the probability net flux, J_i , of A_i into B_j during dt :

$$J_i dt = \frac{4\pi r_{AB}^2 D_{AB}}{V} \left(\frac{\partial p_{ij}}{\partial t} \right) dt$$

$r = r_{AB}$

the boundary condition is obtained as:

$$\left(\frac{\partial p_{ij}}{\partial t} \right)_{r_{AB}, t} = \beta p(r_{AB}, t)$$

where

$$\beta = \Delta x / p \exp(-E_a / RT)$$

$$D_{AB}$$

It follows by applying this boundary condition to equation 2(i), determining $p_{3,j}$ and hence $\left(\frac{\partial p_{1,j}}{\partial x}\right)_{x=x_{AB}}$, and substituting this in equation 2(ii), that the rate of disappearance of A due to bimolecular reaction after a steady state has been attained is:

$$\frac{dp_A}{dt} = 4\pi r_{AB}^2 v_{AB} (\beta / [1 + r_{AB} \beta]) [A] [B]$$

If $[B] \gg [A]$, the reaction is pseudo-first order in A with an apparent rate constant of

$$k = C_4 \pi r_{AB}^2 v_{AB} (\beta / [1 + r_{AB} \beta]) \quad 2(iii)$$

where C is a constant equal to $[B]$

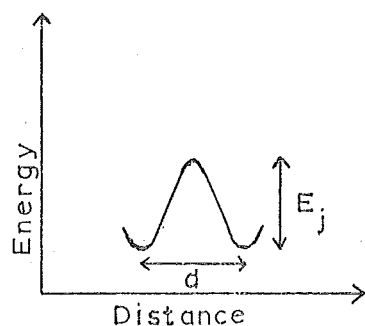
2.3 DIFFUSION IN A ONE COMPONENT CONDENSED PHASE

In this section Eyring's Transition State Theory of Rate Processes is applied to determine the temperature dependence of diffusion coefficients in a condensed phase. This treatment is due to Eyring⁽¹⁹⁾.

In a dilute solution, a diffusing solute molecule is pictured as undergoing a series of jumps from one equilibrium position to the next. To gain each equilibrium position the solute molecule is required to slip past solvent molecules. This process involves the crossing of an associated energy barrier. This may

be represented diagrammatically as shown below.

DIAGRAM 2.1



d is the distance between successive equilibrium positions.

E_j is the height of the energy barrier. If v_f is the jump frequency, it may be shown that

$$D = d^2 v_f \quad 2(iv)$$

Since v_f is the rate at which a diffusing molecule crosses the energy barrier of height, E_j , it may be expressed in terms of the partition function, Q , of the molecule in its equilibrium position, Q' , in some activated state during the jump and the magnitude of the energy barrier, E_j .

$$v_f = \frac{K k' T}{h} \left(\frac{Q'}{Q} \right) \exp(-E_j / RT) \quad 2(v)$$

K is known as the transmission coefficient and is an empirical constant which allows for the probability of a molecule, although having reached the "activated" state between equilibrium positions, returning to its original position.

So from equations 2(iv) and 2(v)

$$D = Kd^2 \left(\frac{k' T}{h} \right) \left(\frac{Q'}{Q} \right) \exp(-E_j/RT) \quad 2(vi)$$

where $\left(\frac{Q'}{Q} \right) = h / (2\pi\mu k' T)^{\frac{1}{2}} v_f^{\frac{1}{3}}$

μ is the reduced mass of the molecule, v_f is the free volume in which the molecule resides and k' is the Boltzmann constant.

Hence the temperature dependence of the diffusion coefficient is:

$$D = L(T) \exp(-E_j/RT) \quad 2(vii)$$

where $L(T)$ is a function of temperature.

In a diffusion controlled reaction involving oxygen, it is assumed that the diffusion coefficient of oxygen is much larger than that of the other species involved in the reaction. Hence:

$$D_{AB} \approx D_{O_2}$$

and so E_j is virtually the energy barrier to the diffusion of oxygen.

2.4 TEMPERATURE DEPENDENCE OF THE RATE CONSTANT

Combining the results obtained in the previous two sections (equations 2(iii) and 2(vii)), an expression for the temperature dependence of the rate constant for a bimolecular reaction is obtained.

viz., $\frac{1}{k} = \frac{1}{C\Delta r \exp(-E_a/RT) 4\pi r_{AB}^2 \mathcal{V}_P} + \frac{1}{4\pi r_{AB} L \exp(-E_j/RT)}$

Since $\mathcal{V} = \mathcal{V}' \exp(-E_j/RT)$; let $E_a + E_j = E_b$

and then the equation has the form:

$$\frac{1}{k} = A' \exp(-E_b/RT) + B' \exp(-E_j/RT)$$

Although the pre-exponential terms in this equation are functions of temperature, their contributions to the temperature dependence of the whole expression are negligible by comparison with the contributions of the exponential terms.

As mentioned before, the decays of phosphorescence intensity and hence of the triplet state, were all exponential, suggesting that all the reactions were either first order or pseudo-first order. The equation describing the decay of the triplet state is therefore:

$$-\frac{d[T]}{dt} = k_u [T] + k_{Qm} [T][m]$$

where $[T]$ is the triplet state concentration and $[m]$ the quenching species concentration. k_{Qm} is the rate constant for a bimolecular reaction. The temperature dependence for these rate constants for these rate constants has been established in sections 2.2, 2.3 and 2.4. k_u is the sum of rate constants for unimolecular reactions of the triplet state occurring in the systems studied.

$$\text{i.e. } k_u = \sum_i k_i$$

The temperature dependence of each of these rate constants is given by the following equation:

$$k_i = A_i \exp(-E_i/RT)$$

where E_i is the energy barrier to the reaction having a rate constant, k_i . The experimentally determined rate constants were:

$$k_{\text{exp}} = k_u + k_{Qm}[m]$$

Therefore the temperature dependence of k_{exp} is given by:

$$k_{\text{exp}} = \sum_i A_i \exp(-E_i / RT) + [A' \exp(E_b / RT) + B' \exp(E_j / RT)]^{-1} \quad 2(\text{viii})$$

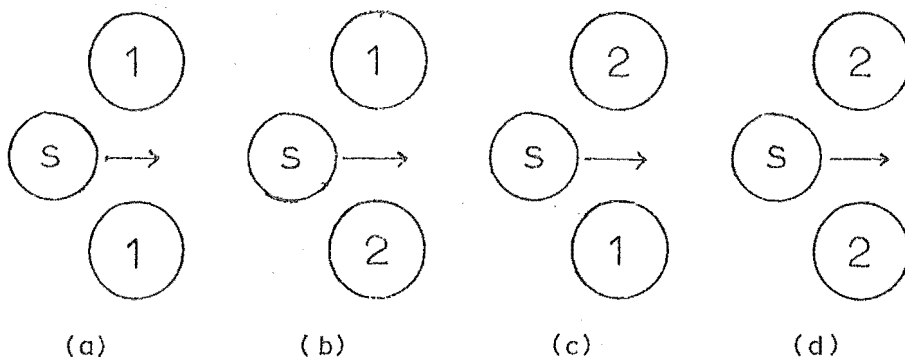
In most cases where the bimolecular rate constant, k_{exp} , makes a contribution to k_{exp} , $E_j \gg E_b$, so equation 2(viii) reduces to

$$k_{\text{exp}} = \sum_i A_i \exp(-E_i / RT) + (1/B') \exp(-E_j / RT) \quad 2(\text{ix})$$

If an Arrhenius plot was constructed, ($\log_e k_{\text{exp}}$ against $\frac{1}{T}$) it would appear as a series of straight line segments of different slope, each segment corresponding to one term in the sum; equation 2(ix). Inspection of the Arrhenius plot constructed from data obtained from a given system therefore gives the number of reactions occurring in the system over the temperature range covered. Analysis of the data in terms of equation 2(ix) gives the magnitudes of the energy barriers to the reactions.

2.5 DIFFUSION IN BINARY MIXTURES

The main principles discussed in the earlier section on diffusion in one component condensed systems apply here. However, in a binary mixture the energy barriers encountered by a diffusing molecule will not all have the same magnitude. This is because a number of different transition environments are possible for a diffusing molecule in a binary mixture. If we consider a simple two dimensional, three body model the different types of situations that are possible are shown in the diagram below.

DIAGRAM 2.2

Interactions (b) and (c) are identical and therefore according to this simple model there will be energy barriers to diffusion of three different magnitudes. The average energy barrier experienced by diffusing molecules will be:

$$\frac{\sum_i p_i E_i}{s'}$$

where p_i is the probability of a solute molecule encountering environment i , E_i is the energy barrier to diffusion in environment i and s' is the number of moles of solute molecules, s.

Regarding all but nearest neighbour interactions as negligible and assuming the probabilities of the situations shown in diagram 2.2 are independent of the free energies of the situations, the probabilities, p_i , are obtained as follows. Consider a solution consisting of $N_1 + N_2 + S'$ moles of sites,

Where N_1 is the number of moles of component 1

N_2 is the number of moles of component 2

S' is the number of moles solute molecules

For very dilute solutions of S_1 , the number of moles of solutes in the solution is:

$$N_1 + N_2 + S' \approx N_1 + N_2$$

The probability, P_a , of situation (a) in diagram 2.2 is:

$$P_a = \left(\frac{x_1^2}{(x_1 + x_2)^2} \right) \times \frac{S'}{N_1 + N_2}$$

Similarly $P_b = P_c = \frac{1}{2} \left(\frac{x_1 x_2}{(x_1 + x_2)^2} \right) \times \frac{S'}{N_1 + N_2}$

and $P_d = \left(\frac{x_2^2}{(x_1 + x_2)^2} \right) \times \frac{S'}{N_1 + N_2}$

Therefore the average molar energy barrier to diffusion is:

$$\begin{aligned} E_{av} &= E_a x_1^2 + E_b x_1 x_2 + E_d x_2^2 \\ &= x_1^2 (E_a - E_b + E_d) + x_1 (E_b - 2E_d) + E_d \end{aligned}$$

Where x_1 is the molefraction of component 1.

This model therefore predicts a parabolic relationship between the energy barrier to diffusion and the composition of the solution.

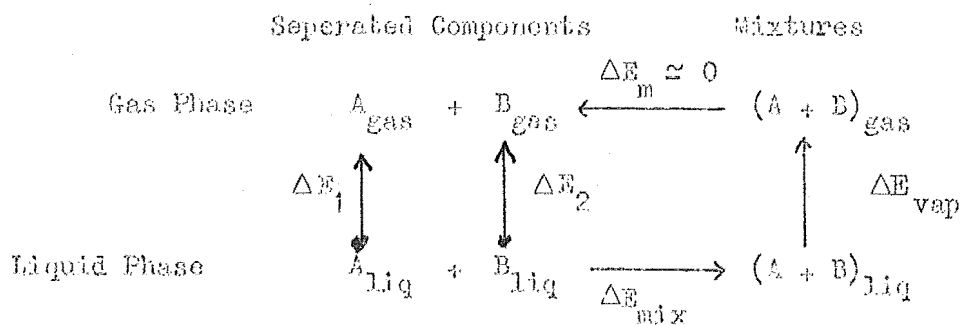
The same conclusion is reached by the following semi-empirical method. For a molecule to diffuse, a hole must be available; this hole is not necessarily the full size of a molecule but will be some fraction, represented by the additional volume required by the activated state as compared with the initial state. The work required to make a hole in the solvent the size of a solvent molecule is equal to the

energy of vapourization, ΔE_{vap} . So the free energy of activation for diffusion may be expected to be some fraction of the energy of vapourization. Birch and Simha⁽²⁰⁾ have shown for a number of substances:

$$E_d \approx \frac{1}{3} \Delta E_{vap}$$

where E_d is the energy barrier to diffusion.

The dependence of ΔE_{vap} , for a binary mixture, on the composition of the mixture, may be established by considering the thermodynamic cycle shown below.



It is assumed that the energy of mixing in the gas phase, $\Delta E_m \approx 0$ and that $\Delta E_{mix} \approx K x_1 x_2$.

$$\text{Then } \Delta E_{vap} = x_1 \Delta E_1 + x_2 \Delta E_2 + K x_1 x_2$$

$$= +x_1^2 K + x_1 (K + \Delta E_1 - \Delta E_2) + \Delta E_2$$

where x_i is the molefraction of component i, ΔE_i is the energy of vapourization of component i and K is a constant.

$$\text{If } E_d = \frac{1}{3} \Delta E_{vap}$$

$$\text{then } E_d = \frac{1}{3} [+x_1^2 K + x_1 (K + \Delta E_1 - \Delta E_2) + \Delta E_2] - 2(x)$$

No measurements of the energy barrier to diffusion in

organic solvent binary mixtures of different composition have been reported in the literature. However, Collins and Watts⁽²¹⁾ have measured the energy barrier to viscous flow, which is expected to have the same magnitude as the energy barrier to diffusion, as a function of composition of the benzene - cyclohexane mixture. They obtained a parabolic relationship with a minimum about a molefraction of benzene equal to 0.6, which is predicted for this mixture by equation 2(x). The depth of the minimum is also in good agreement with that predicted by equation 2(x) for this mixture.

CHAPTER III

REVIEW

Effect of Environmental Conditions on Phosphorescence Lifetimes3.1 INTRODUCTION

Phosphorescence is generally only observed in the solid phase. This has often been ascribed to the existence of quenching reactions which become increasingly important as the viscosity of the medium decreases, with a consequent increase in the rate of decay of phosphorescence until eventually, in fluid solutions, the quenching reactions completely dominate the deactivation of the triplet state and no phosphorescence is observed. The viscosity of the medium is closely linked with the temperature. As the temperature increases, so the viscosity decreases.

The temperature dependence of the rate of phosphorescence decay may be conveniently expressed in the form of an Arrhenius plot. See for example, figure 4.8. While this temperature dependence can in some cases be interpreted in terms of quenching reactions, in many other cases it still awaits satisfactory explanation and it is the principal subject of this review.

The effect of other environmental parameters such as pressure and solvent are also mentioned briefly in this review.

3.2 TEMPERATURE DEPENDENCE OF PHOSPHORESCENCE LIFETIMES

A typical Arrhenius plot showing the temperature dependence

of the phosphorescence lifetime of a species in a glassy matrix is shown in figure 4-8. It generally consists of two straight line segments of different slopes. At lower temperatures, (higher viscosities) the Arrhenius plot is virtually flat or shows only a slight negative slope. At higher temperatures, (lower viscosities) the rate constant for the phosphorescence decay starts to increase rapidly with increasing temperature. It is convenient to discuss the work done on the temperature dependence of phosphorescence decay in terms of a "low" viscosity region, defined as the region where the rate constant shows a marked temperature dependence and a "high" viscosity region, defined as the region where the rate constant usually only displays a slight temperature dependence.

(a) "Low" Viscosity Region:

Porter and Windsor⁽²²⁾ studied the effect of dissolved oxygen on the rate of decay of the phosphorescence of anthracene in fluid solution. They concluded from their results that oxygen quenched the phosphorescence of anthracene by a diffusion controlled reaction. Later work⁽²³⁾ on the temperature dependence of the rate of decay of phosphorescence in the presence of oxygen interpreted the sudden increase in the rate constant with increasing temperature as corresponding to the onset of a diffusion controlled quenching reaction with oxygen. A similar interpretation of the behaviour of the low viscosity region of the Arrhenius plot was applied when other quenching species were known to be present^(24, 25).

Very similar Arrhenius plots to those constructed for systems containing oxygen, have been obtained for phosphorescing

molecules in low temperature glasses where care has been taken to eliminate oxygen and other impurities capable of quenching the triplet state. Some workers⁽²⁵⁾ have explained the observed sudden increase in the rate of decay of phosphorescence with increasing temperature in these systems in terms of diffusion controlled reactions with traces of oxygen still remaining in solution.

Assuming that the Stoke-Einstein equation relating the viscosity of the medium to the diffusion coefficient holds for molecular diffusion, other workers⁽²⁶⁾ estimated that concentration of oxygen needed to explain their results was far greater than the concentration of oxygen that could still remain in solution after the solution had been degassed by their methods. The weak point in these arguments is the assumption of the validity of the Stoke-Einstein equation to the diffusion of oxygen. Osbourne and Porter⁽²⁷⁾ studied the temperature dependence of the rate of decay of the phosphorescence of naphthalene in several solvents whose viscosity-temperature dependences had previously been determined. Assuming a diffusion controlled quenching reaction to take place in the presence of oxygen, they found that the rate constant for phosphorescence decay, calculated from the Debye equation for the rate of a diffusion controlled reaction (which is based on the Stoke-Einstein equation), did not agree with their measured values for the rate of the phosphorescence decay. A modified form of the Stoke-Einstein equation was found to give better agreement with experimental results. However, estimates of the concentration of oxygen required to explain the temperature dependence of the phosphorescence lifetime in degassed solutions,

using this modified equation, are still too large to be permitted by the degassing procedures used.

Hilpern, Porter and Stief^(26a) studied the temperature dependence of the phosphorescence decay constant, k, for a number of aromatic hydrocarbons in iso-pentane and propyl-glycol. The viscosities, η , had previously been determined by Stief⁽²⁸⁾ in the temperature range used in this work. $\log_e k$ was plotted against $\log_e(\eta/T)$. These plots consisted of two straight line segments. The slope of the segment in the "low" viscosity region was less than unity. The Debye equation for the rate constant of a diffusion controlled reaction:

$$k = 8RT/3000\eta$$

would have predicted a straight line of unit gradient, provided a diffusion controlled quenching reaction was responsible for the temperature dependence. Despite this, the authors concluded that a diffusion controlled quenching reaction was occurring between the triplet state and some unidentified impurity. The fact that the slope of the Arrhenius plot was less than unity was explained in terms of the existence of some simultaneous unimolecular decay process having a smaller viscosity or temperature dependence than that of a diffusion controlled quenching reaction. Also, it was admitted that the Debye equation was not accurate because the Stoke-Einstein equation is not exactly applicable at the molecular level.

Other data⁽²⁹⁾ are not consistent with a diffusion controlled quenching reaction being responsible for the temperature

effect in degassed solutions composed of highly purified compounds. Therefore, other explanations of the temperature dependence of the phosphorescence lifetime have been sought. Porter and Stief^(29a) studied the temperature dependence of the phosphorescence lifetimes of 9,10-dibromoanthracene in propyl-glycol, 3-methylpentane and isopentane. 9,10-dibromoanthracene was chosen because the heavy atom effect important in this compound would make the unimolecular radiationless decay dominate the deactivation of the triplet state and therefore, the contribution from any diffusion controlled reaction would be negligible. The activation energies derived from the slopes of the Arrhenius plots in the low viscosity region for each solvent were; 16.2, 5.8, and 2.7 Kcals/mole for propyl-glycol, 3-methylpentane and isopentane respectively. It was suggested that Brownian rotational diffusion may have become important as the temperature rose and the solvents' viscosities decreased. If this is so, there could be coupling between the phosphorescing molecule's rotation and its electronic motion, with a consequent increase in the transition probability between the lowest triplet state and the ground singlet state and a concomitant shortening of phosphorescence lifetime.

Leubner and Hodgkins⁽³⁰⁾ examined the temperature dependences of the rates of decay of phosphorescence of benzene and a number of alkyl-benzenes in glassy mixtures of methylcyclohexane and isopentane (4:1 by volume). An activation energy of about 2 Kcals/mole was obtained from the Arrhenius plot for benzene in the low viscosity region. This energy is about that of the CH out-of-plane

bending, methylene rocking and skeletal stretching modes. It was therefore suggested that perhaps these vibrations gave rise to the observed temperature dependence. This is however, not in accordance with the conclusions of Siebrand⁽³¹⁾ which will be dealt with later.

The phosphorescence lifetimes and relative phosphorescence quantum yields have been measured for solutions of palladium (II) mesoporphyrin IX, dimethyl-ester and ρ phenylbenzophenone in methylphthalylethylglycolate as a function of temperature^(29a, 29c). The sudden increase in observed rate constant in the low viscosity region is interpreted as a viscosity effect on the unimolecular radiative and non-radiative processes. The observed rate constant is the sum of these radiative and non-radiative rate constants. Making a number of assumptions, the absolute phosphorescence quantum yields were determined from the measured relative phosphorescence quantum yields. This enabled the radiative and non-radiative rate constants to be separated from the observed rate constant and they were then both plotted separately as a function of temperature. It was found that for both phosphorescing compounds studied, the rate constants for non-radiative decay decreased with increasing viscosity. The radiative rate constant increased for ρ -phenylbenzophenone, but decreased for palladium (II) mesoporphyrin IX, dimethyl-ester with increasing solvent viscosity. It is important to realise that while these authors interpreted their results in terms of changes in solvent viscosity, they could alternatively arise from changes of temperature or some other environmental parameter which depends on temperature.

(b) "High" Viscosity Region:

Some workers⁽³²⁾ have obtained a slight negative gradient in the Arrhenius plots of some phosphorescent species in organic glasses at low temperatures. An activation energy of 0.3 to 0.8 Kcals/mole has been calculated for the process responsible for this, in the work by Porter and Stief^(29d) on the phosphorescence of dibromoanthracene. Porter has proposed a two step, non-radiative deactivation mechanism of the triplet state. This first involves an adiabatic crossing of the triplet state to an isoenergetic level of the ground state which is followed by loss of excess vibrational energy by repeated collisions with solvent molecules. Hilpern, Porter and Stief^(26a) have suggested that a small potential energy barrier may exist to the first process. A molecule in the zeroth vibrational level of the lowest triplet state would have to gain vibrational energy to reach the point from where it could cross to an isoenergetic vibrational level of the ground state. An activation energy of 0.3 to 0.8 Kcals/mole is consistent with this explanation. Other workers^(29a) have observed no temperature dependence of the phosphorescence lifetime in organic glasses in the high viscosity region. Ladner and Becker^(29a) suggest that for palladium (II) mesoporphyrin IX, dimethyl-ester and ρ - phenylbenzophenone in methylphthalylethylglycolate this may be explained in the following way. They believe that the radiative rate constant is very much larger than the non-radiative rate constant and therefore dominates the observed rate constant, which is the sum of the two rate constants. If the radiative rate constant

is temperature independent, then the observed rate constant would show very little temperature dependence even if the non-radiative rate constant is temperature dependent.

There have been very few studies that have measured the rate constant for unimolecular phosphorescence decay in organic glasses over a range of temperature below 77°K. Hodgkins and Woodyard⁽³⁴⁾ investigated a number of benzene derivatives in methylcyclohexane-isopentane (9:1) over the temperature range 3°K to 110°K. They noted that above 80°K, non-radiative processes dominate and emission is small; at about 60°K the emission process becomes increasingly important and finally below about 15°K the rates of phosphorescence decay do not change with temperature. Similar results were obtained by Leubner and Hodgkins⁽³⁰⁾ in their work on benzene and some alkylbenzene compounds. It was suggested that the fact that a temperature dependence for the phosphorescence lifetime of benzene was observed at temperatures of about 20°K and above, may be associated with the small size of the benzene molecule. It was observed that the temperature at which the phosphorescence lifetime started to increase with temperature rose as the size of the phosphorescent molecule increased. The temperature dependence of benzene's phosphorescence lifetime in high viscosity systems will be discussed in more detail later in this review.

Studies⁽³⁵⁾ of phosphorescent molecules embedded in crystals and plastics enable the temperature dependence of their rates of phosphorescence decay to be followed over a wide range of temperature while the matrix remains rigid and viscosity effects

are therefore unimportant. A definite, though not very large temperature dependence has been observed for most aromatic hydrocarbons in these high viscosity matrices. For example, Kellogg and Schwenker^(35a) found that the phosphorescence lifetimes of the compounds they studied, decreased only about twofold as the temperature was increased from 77°K to 300°K. Siebrand^(31, 36) attributed some of this effect to thermally activated quenching. Others^(35a, 35d) do not regard quenching as important because the ratio $\tau_p(77)/\tau_p(298)$ is virtually the same for deuterated and protonated analogues of the same compounds (τ_p refers to phosphorescence lifetimes and the figures in parentheses refer to the temperature (°K) at which they were measured.) These analogues would be expected to be sensitive to the same quenchers, but since the deuterated species has a longer lifetime than the protonated species, it would be expected that its lifetime would be more affected by quenching than its protonated counterpart. Jones and Siegel⁽³⁷⁾ paid careful attention to the possibility of the quenching of phosphorescence by either oxygen or some free radical species produced by photolysis, in their study of solutions of naphthalene, phenanthrene, pyrene, biphenyl and their perdeuterated analogues in polymethylmethacrylate. They concluded that the observed temperature dependences of phosphorescence lifetimes were associated with true unimolecular decay processes. Their results did not permit them to say whether the temperature dependences arose from the radiative or non-radiative decay modes, or from a combination of both, but their results were

consistent with an analysis that assumes that only the non-radiative rate constants are temperature dependent. According to this analysis, a process having an activation energy of about 1.3 Kcals/mole is responsible for the observed temperature effects. This suggests out-of-plane bending modes could be responsible for the effect. Similar conclusions that the triplet state returns to the ground state via a vibrationally excited level have been arrived at by other workers (38, 35d). Baldwin suggests that as the temperature increases, a Boltzmann distribution of energy would predict a significant population of upper vibrational levels of the lowest triplet state. The rate of decay from each vibrational level would be different, due to different Franck-Condon factors and the observed rate of decay could be written:

$$k_{\text{observed}} = \sum_{i=0}^n A_i k_i$$

where k_i is the rate of triplet decay from the i th vibrational level and A_i is the relative population of the i th vibrational level. As the temperature changes, so A_i changes and hence also k_{observed} . Siebrand (31) and Lin and Bersohn (39) have developed theoretical treatments of the effect of temperature on the Franck-Condon overlap integral, which determines the rate of non-radiative decay. This integral is found to depend on the population of the various vibrational states of the lowest triplet state at different temperatures. Siebrand concludes that for most aromatic hydrocarbons, the temperature dependence of the rates of non-radiative decay from the lowest triplet state to the ground singlet state should only be very slight

at temperatures below 300°K, if only intramolecular vibrations are responsible for the temperature effect.

Interesting, anomalously large temperature dependences of phosphorescence lifetime have been observed^(40, 31) for benzene and some alkylbenzene compounds in high viscosity media such as plastics and crystals. This suggests that either some intermolecular effect is intervening in the temperature dependence, or this temperature dependence of the observed rate constant does not arise purely from the non-radiative decay, but from both the radiative and non-radiative decays. In recent papers⁽⁴¹⁾, Rabalais, Maria and McGlynn have suggested that both of these alternatives may be responsible for the large temperature dependence of the phosphorescence lifetimes of the benzene compounds.

A certain amount of evidence exists to support the belief that some sort of solvent interaction with triplet state molecules brings about this anomalously large temperature effect. A number of workers have observed a solvent effect on the phosphorescence lifetime of benzene at 4.2°K. At this temperature, the lifetimes, in seconds, for benzene are given in the parentheses for the following solvents: cyclohexane (11:8)^(40a), borazine (10.2)^(40a), C₆D₆(9.5)^(40a), argon (16)⁽⁴³⁾ and methane (16)⁽⁴³⁾. Work⁽⁴²⁾ done with benzene and various alkylbenzenes in a variety of solvents indicate that the greater the solvent effect, the greater the temperature dependence of the phosphorescence lifetime.

Spectroscopic studies⁽⁴⁴⁾ of benzene in rigid media indicate the benzene molecule undergoes a solvent assisted distortion which

results in two Jahn-Teller states. This Jahn-Teller distortion of the lowest triplet state of benzene would give rise to a low frequency mode corresponding to the interchange between differently distorted hexagons. Excitation of this mode would give rise to an increase in the Franck-Condon overlap integral and therefore an increase in the non-radiative decay rate, since it tends to restore the regular hexagon, which enhances vibrational overlap between the ground and triplet states. Hatch, Erlitz and Nieman^(40c) studied the temperature dependence of the phosphorescence lifetime of mesitylene in B - trimethyl-borazine and while it did display an anomalously large temperature effect at temperatures above 150°K, the rate of decay was independent of temperature below 150°K. The E.S.R. spectrum of this system however, indicates interchange between two Jahn-Teller states at temperature below 150°K. These findings do not support the suggestion that interchange between Jahn-Teller states is responsible for the large temperature effect in benzene compounds.

Melhuish^(38b) has suggested that the temperature dependence he observed for the radiationless decay of the triplet state of benzophenone in PMMA, could be affected by the medium if it could apply some constraint to the triplet benzophenone molecule which is partially removed at some temperature where the medium relaxes. This suggestion was prompted by the fact that a change in phosphorescence lifetime occurs at a temperature where proton resonance studies show a second order phase transition in PMMA.

Recently Jones and Calloway⁽⁴⁵⁾ have reported a large

temperature dependence of the phosphorescence lifetime of naphthalene α_3 in polystyrene (P.S.). They suggested that certain conformations of the solute triplet state which are effective in non-radiative intersystem crossing are constrained by a rigid solvent cage. In P.S., these constraints are relaxed as the temperature increases. They admit that their observed temperature effect in the P.S. system could be due to specific interactions between P.S. rings and the aromatic solute. To test this possibility, they repeated their work using a more rigid stereoisomer of P.S. (isotactic). They found that the temperature variation in phosphorescence lifetime from 77°K to 300°K is about half as large in the more rigid (isotactic) P.S. isomer. Other possible interpretations of their data such as molecular diffusion, impurity effects and triplet-triplet annihilation were ruled out by later experiments⁽⁴⁵⁾.

3.3 PRESSURE DEPENDENCE OF PHOSPHORESCENCE LIFETIME

Baldwin and Offen have published a number of papers which show that the phosphorescence lifetimes of aromatic molecules in a plastic matrix⁽⁴⁶⁾ such as polymethylmethacrylate (P.M.M.A.) and in low temperature organic glasses⁽⁴⁷⁾ are dependent on the pressure applied to the system. It has been found that decreasing the applied pressure diminishes the phosphorescence lifetime and the relationship between the two quantities may be satisfactorily expressed by the equation:

$$\frac{d \log_e \tau_p}{dp} = \frac{\Delta V^*}{RT}$$

where τ_p is the phosphorescence lifetime, P is the pressure, T the absolute temperature, R the gas constant, and ΔV^* is an "activation volume". As yet, the physical interpretation of this volume is in doubt, but it does give a convenient means of summarizing the pressure $\sim \tau_p$ dependence for a given system. It has been tentatively suggested⁽⁴⁸⁾ that this activation volume may correspond to the difference in the volumes occupied by the ground and triplet states. Alternatively, high pressure could lead to compression of solvent cages containing solute molecules. This in turn would lead to distortion of the solute molecule with the consequent effects on the rate of deactivation of the triplet state which have already been suggested in work on the temperature dependence of phosphorescence lifetimes.

3.4 RATIONALE:

The work described in this thesis was directed at the effect of temperature on the phosphorescence lifetime of triplet state aromatic hydrocarbons in organic glassy matrices in the "lower" viscosity region. The viscosities of these organic glasses are intimately linked with the temperature of the glass. The review of previous work has shown that many workers regard the sudden decrease in phosphorescence lifetime with increasing temperature as being associated with the concomitant decrease in viscosity of the medium. However, in many cases, the increase in temperature, or some temperature dependent environmental parameter, could equally

well have been responsible for the observed decrease in phosphorescence lifetime. No adequate attempt has been made to separate temperature and viscosity effects on the phosphorescence lifetime of solutions of triplet state species in organic glasses.

In solutions containing oxygen, it is accepted that a diffusion controlled reaction between oxygen and the triplet state is responsible for the observed temperature effect in the "low" viscosity region. However, in rigorously degassed solutions, made up from carefully purified components, the only evidence against a diffusion controlled quenching reaction between the triplet state and traces of oxygen or impurities, is the unreasonably large quantities of those quenching species, as estimated by the Debye equation, required to produce the observed temperature effect. These estimated quantities of quench could be in error because the Debye equation is based on the Stoke-Einstein equation, whose validity is doubtful at the molecular level.

(i) It was decided to first study the temperature dependence of the phosphorescence lifetime of naphthalene in a series of 3-methylpentane - methylcyclohexane glass mixtures of different compositions in the presence of oxygen. In chapter II it was theoretically established that the energy barrier to translational diffusion varied with the composition of a binary mixture. Since it is commonly believed that the activation energy derived from the slope of the "low" viscosity region of the Arrhenius plot for the solutions described above, corresponds to the energy barrier to translational diffusion of oxygen, the aim of the first part of

The project was to provide an experimental check of the theoretical result derived in chapter II.

(ii) Once the dependence of the energy barrier to translational diffusion on the composition of β -methylpentane-methylcyclohexene mixtures at low temperature had been experimentally established, the next step was to study the temperature dependence of the phosphorescence lifetime of naphthalene in these mixtures, in the absence of oxygen. If the activation energies derived from the Arrhenius plots in the "low" viscosity region did not follow the expected dependence on composition for energy barriers to translational diffusion, then the possibility of a diffusion controlled quenching reaction being responsible for the observed temperature effect in these systems could be ruled out.

(iii) Porter and Stief⁽²⁹⁾ suggested that the temperature effect could arise from Brownian rotational diffusion of the triplet state molecules. To test this possibility, the third part of the project was an attempt to separate temperature effects from viscosity effects. This was done by studying the temperature dependence of the phosphorescence lifetimes of a group of similar molecules expected to exhibit the same diffusional characteristics in the same solvent at the same temperature. The molecules studied were some mono-methyl-substituted 1,2-benzanthracenes which were dissolved in degassed β -methylpentane glasses. These molecules were known to have different phosphorescence lifetimes in the same glass at low temperature⁽⁴⁹⁾. This suggests that the intrinsic radiative decay rates, the non-radiative decay rates, or both, are different in these compounds.

If rotational diffusion was responsible for the observed temperature effect in these systems, the activation energies derived from the slopes of the Arrhenius plots should be the same. If however, the temperature effect arises from some other factor which is different in these molecules (and is perhaps responsible for the different phosphorescence lifetimes), the observed activation energies will be different.

(iv) A good deal of work has been done in an effort to correlate a phenomenon known as the photodynamic action of a compound with its potency as a skin carcinogen. In many cases impressive correlations have been found⁽⁵⁰⁾. Photodynamic action is the light mediated killing of cells or inactivation of enzymes by chemicals in the presence of oxygen. It is often regarded as a sensitized photo-oxidation process. One reaction often proposed in the mechanism for photodynamic action is:



where 3S refers to the triplet state of the species responsible for photodynamic action.

Badger⁽⁶¹⁾ has found a correlation to exist between the rate of addition of O_4 to some polycyclic hydrocarbons and their potencies as carcinogens.

The existence of these correlations make it tempting to suggest that a correlation exists between the rate of a reaction of the type 3(i) and carcinogenic potency. The observation that the carcinogenic mono-methyl substituted 1,2-benzanthracenes

exhibit shorter phosphorescence lifetimes than the non-carcinogenic methyl derivatives of 1,2-benzanthracene⁽⁴⁹⁾ could also be an indication of the importance of a reaction of the type 3(i) in determining carcinogenic potency. This is because if the rate of reaction 3(i) is diffusion controlled and the diffusional characteristics of the methyl 1,2-benzanthracenes are identical, the rates of oxygen quenching (reaction 3(i)) should be the same for all the benzanthracenes. However, if the reaction of the non-carcinogenic methyl 1,2-benzanthracenes with oxygen had an activation energy greater than the energy barrier to the diffusion of oxygen, then the rate of this reaction would be slower than the rate of the reaction of the carcinogenic compounds with oxygen. This would correspond to the observation of shorter phosphorescence lifetimes for the carcinogenic benzanthracenes if some oxygen was present in solution in the work described in reference 49.

To see if there was any difference in the activation energies for the reactions of the carcinogenic and non-carcinogenic methyl 1,2-benzanthracenes with oxygen, the slopes of the "low" viscosity segments of the Arrhenius plots constructed from the rates of decay of the triplet states of some carcinogenic and non-carcinogenic benzanthracenes in the presence of oxygen, in 3-methylpentane were measured.

CHAPTER IV

EXPERIMENTAL

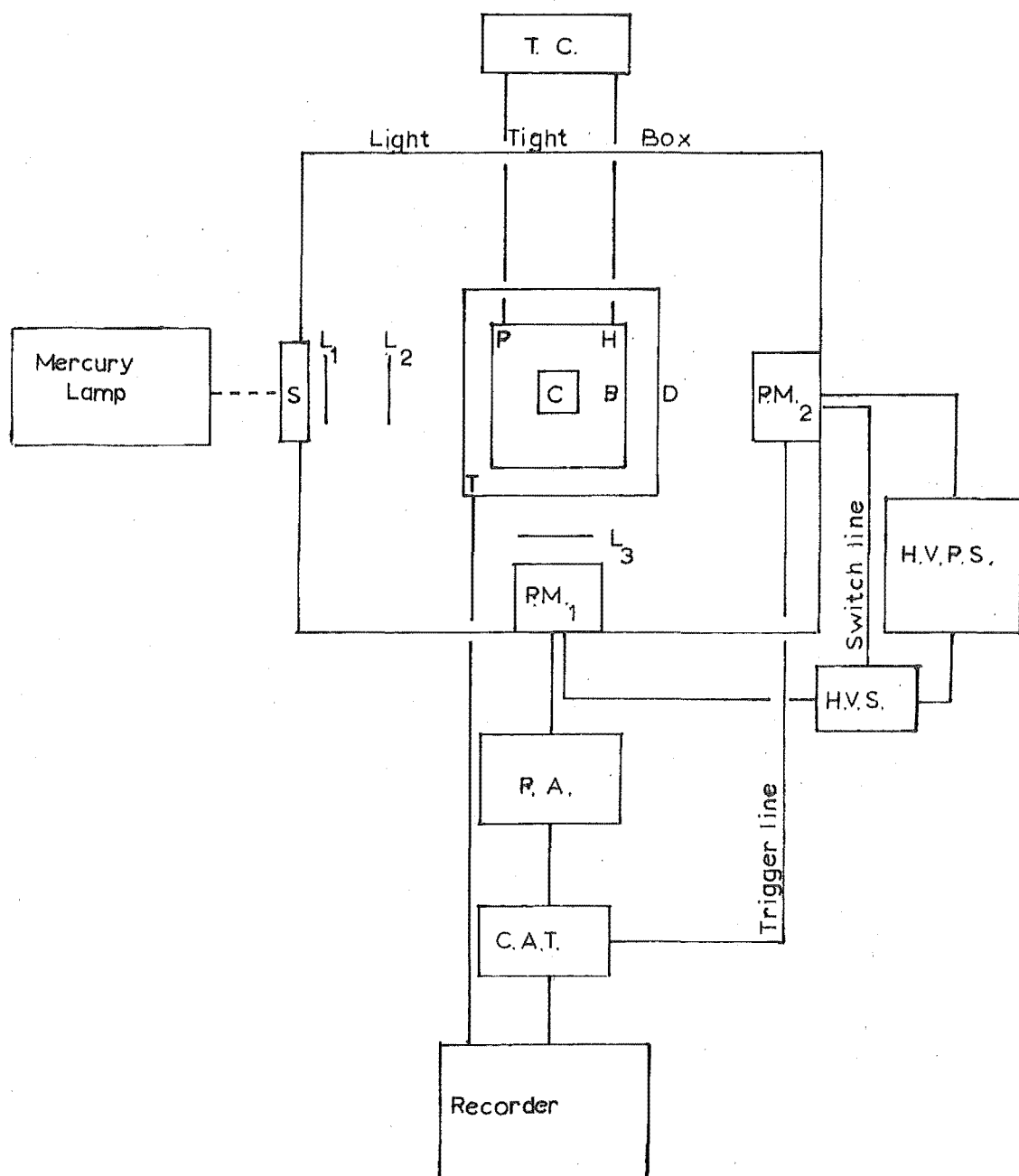
4.1 INTRODUCTION

The principal elements of the apparatus, developed to record the rate of decay of phosphorescence at measured low temperatures are shown in the schematic diagram 4.1.

Light from a medium pressure Phillips, type 57201E, mercury lamp was focused on a glass which had been obtained by cooling a solution of a potentially phosphorescent molecule in a suitable organic solvent contained in a quartz cell. The cooling was achieved by housing the cell in a copper block whose lower end dipped into liquid air contained in an unsilvered pyrex dewar. The emission from the cell was focused on the photocathode of the photomultiplier, P.M.₁, situated at right angles to the irradiating beam. When the irradiating beam was shut off by the camera shutter another photomultiplier, P.M.₂, actuated a switching circuit, which switched P.M.₁, on. The luminescence decay from the cell was then detected by P.M.₁, the signal amplified and fed to a Varian G-102B time averaging computer. The signal was stored in the time averaging computer and then read out at a suitably slow rate onto a Hitachi Model QPD53 recorder. The temperature of the copper block was determined by measuring the voltage of a chromel-constantan thermocouple attached to the copper block. The temperature of contents of the cell was assumed to be that of the copper block near the cell.

DIAGRAM 4.1

Block Diagram of Apparatus



S Camera shutter
L Lens
C Cell
P Resistance thermometer

H Heater
B Copper block
D Dewar
PM Photomultiplier

T Thermocouple
RA. Preamp.
H.V.S. Voltage switch
T.C. Temp. controller
HVPS. High voltage power supply

In the first two parts of the project two series of solutions of naphthalene in mixed 3 methylpentane - methylcyclohexane solvents of different compositions were prepared. The solutions of one series were all saturated with oxygen while the solutions of the other series were thoroughly degassed to remove oxygen. It was found impractical to work with solutions of mole-fraction greater than 0.7 in methylcyclohexane (MCH) because the glasses formed on cooling solutions of high MCH concentration to liquid air temperature, cracked badly, breaking the quartz cell.

In the second two parts of the project, both oxygenated and deoxygenated solutions of the 5, 10, 8 and 3 methyl mono-substituted 1,2 benzanthracene compounds all in 3 methylpentane (3MP) solvent were prepared.

Arrhenius plots (plots of $\log k$ against the reciprocal of the absolute temperature, T) were constructed for each solution by determining the rate constants, k , for the disappearance of the triplet state from the decays of phosphorescence recorded at about eleven or twelve temperatures in the range from about 80°K to 115°K . Before each phosphorescence decay was recorded the solution was kept at each temperature for about ten minutes to ensure that the solution had come to thermal equilibrium with the copper block.

4.2 PREPARATION OF CELLS

All the solutions were contained in quartz cells made from 9 m.m. o.d. quartz tubing. Quartz was used instead of pyrex

because quartz was found to give considerably less emission after irradiation with light from the mercury lamp. Emission from the walls of the cell and the dewar were found to be important when studying the phosphorescence decay from the methyl substituted 1,2-benzanthracenes solutions. This was because, although the emission from the glass walls decayed more rapidly than that from the 1,2-benzanthracenes solutions, it still made a significant contribution to the observed emission in the earlier part of the phosphorescence decay, if the phosphorescence intensity was low. This set a lower limit to the minimum usable concentration of the 1,2-benzanthracenes solutions. In order to make the emission from the glass walls negligible by comparison with the emission from the solution, a concentration of about 10^{-4} molar was necessary. The measured phosphorescence lifetimes were independent of concentration provided the solutions were not too concentrated. A too concentrated solution could lead to the formation of micro-crystals of the solute. The emission then recorded from the solution would be the sum of two emissions of different lifetime, viz., that from the solute in solution and that from the crystalline state.⁽⁵¹⁾ Further, concentrated solutions enhance the possibility of triplet - triplet quenching and delayed fluorescence. This would again result in modifications to the observed decay of the triplet state.

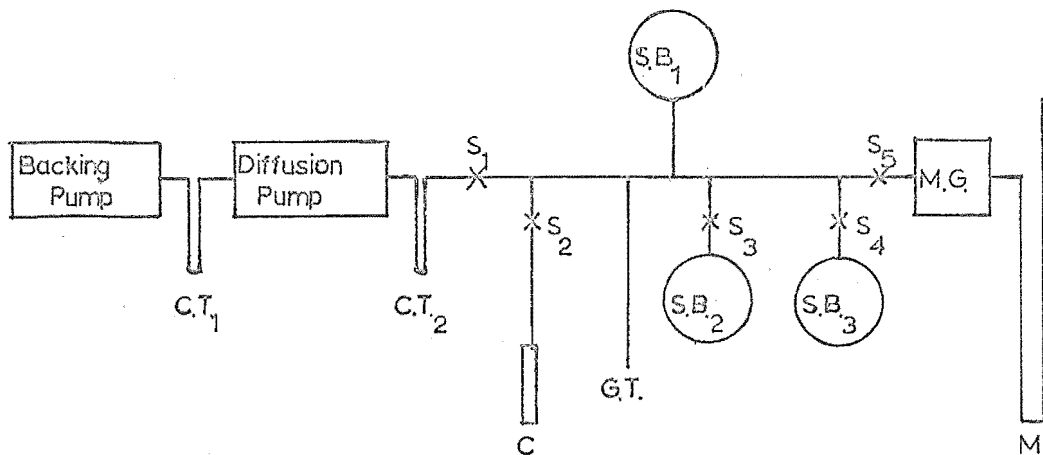
The quartz cell was sealed onto the vacuum line shown in diagram 4.2.

The following methods were used to prepare the solutions.
Naphthalene Solutions;

To prepare naphthalene solutions a small quantity of

DIAGRAM 4.2

Schematic Diagram of Vacuum Line

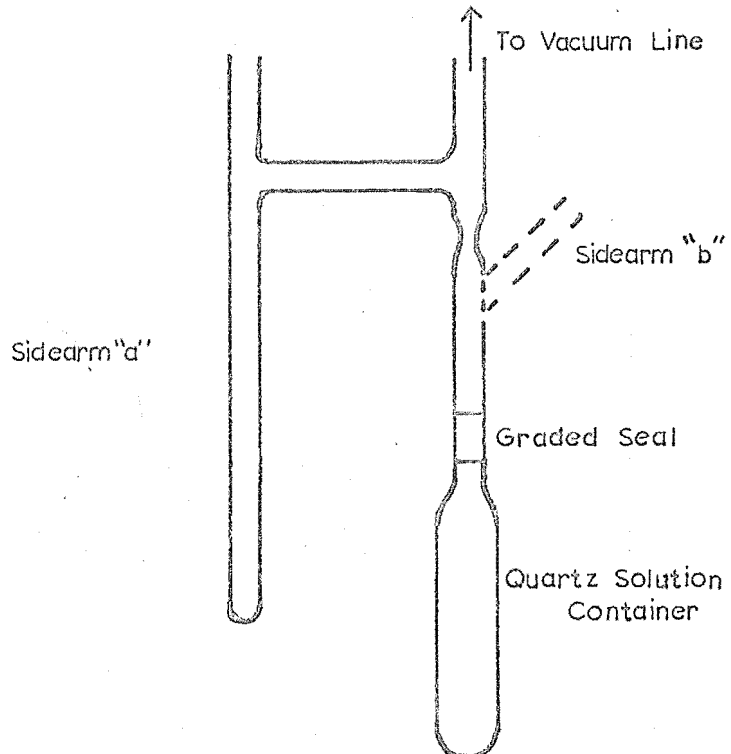


C.T. Cold Trap
 S. Greaseless Stopcock
 C. Cell
 G.T. Graduated Tube

S.B. Storage Bulb
 M.G. McLeod Gauge
 M. Manometer

DIAGRAM 4.3

Diagram of Cell



naphthalene (about 10^{-3} grams) was placed in the sidearm "a" (see diagram 4-3). The top of this sidearm was sealed off and stopcock, S_2 , was opened for a few seconds to degas the cell and sidearm. The stopcock was then shut and the naphthalene was sublimed into the cell by putting a cold trap of liquid air around the cell and applying a little gentle heat to the naphthalene. A quantity of 3MP and a quantity of MCHI were in turn distilled over into the graduated tube "G.T." from their respective storage bulbs. The mixed solvent was then distilled over into the cell. The volumes of the solutions were about 3 to 4 mls. The concentration of the solution was therefore about 10^{-3} M. Use of the graduated tube gave an approximate indication of the composition of the mixed solvent. A more exact determination of the composition of the solvent was made after data for an Arrhenius plot for the solution had been obtained. A sample of the solution was injected into a Varian Model 1200 gas chromatograph using an SE-30 column at 80°C . An integrator measured the areas under the peaks in the gas chromatogram due to 3MP and to MCHI. From the areas under the peaks, the mole fraction of MCHI in each mixture was determined. This assumes that the area under each peak is proportional to the number of moles of the corresponding compound and the proportionality constant is the same for both compounds. The proportionality constants are 1.08 and 1.10 for MCHI and 3MP respectively⁽⁵²⁾.

Mono-substituted methyl 1,2 benzanthracene solutions:

In the preparation of these solutions a small quantity of

the solute on a glass rod was introduced into the cell via sidearm "b". This sidearm was sealed off and stopcock S_2 opened to degas the cell. About 3 to 4 mls of 3MP were then distilled into the cell. The concentration of the solution so formed was about 10^{-5} to 10^{-4} M.

All the solutions to be saturated with oxygen were completed by introducing oxygen at 8 to 10 torr pressure into the cell and then sealing off the cell by heating the constriction with a glass-blowing torch.

The deoxygenated solutions were completed by four cycles of: freezing the solution, degassing to a pressure of less than 10^{-5} torr, thawing, distilling into sidearm "a" and then back into the cell. The cell was then sealed off at the constriction.

4.3. IMPURITIES

In chapter I it was pointed out that impurities can have a significant effect on the measured rate constant for the decay of phosphorescence. In fact the removal of the last traces of some impurities was the principal experimental difficulty encountered in this project. This difficulty is accentuated by the fact that the nature of the objectionable impurities cannot be predicted with certainty and there is no general method for their detection at very low levels, apart from the effect they have on the lifetime of the phosphorescence or on the Arrhenius plot. The only way of testing the effectiveness of a purification technique was to use it to purify a sample of compound, dissolve the "purified" sample in a

glass matrix, and construct an Arrhenius plot from the measured phosphorescence lifetimes of the compound in the glass matrix at a number of temperatures. Then repurify the "pure" compound using the same purification technique and construct another Arrhenius plot from data obtained from this new sample dissolved in the same glass matrix as before. If the slopes of the corresponding parts of the two Arrhenius plots are the same, then the impurities capable of influencing the rate of decay of phosphorescence have been reduced to the lowest level that the purification technique is capable of.

Since oxygen is known to be a very effective quenching species⁽⁵³⁾ and was present in the oxygenated solutions at a far greater concentration than any other impurity likely to be present, it was presumed that it would dominate the quenching reactions in these solutions. Therefore the presence of traces of other impurities are not as important in these solutions as they are in deoxygenated solutions.

The most important impurities to be eliminated are those that are capable of accepting triplet state energy from the compound being studied. Such impurities can introduce errors at concentrations below 10^{-9} molar⁽⁵⁴⁾. This problem is greatest when the compound under investigation has a relatively high triplet state energy.

4. CHOICE OF PHOSPHORESCENT MATERIALS

The height of the triplet state energy therefore obviously influences the choice of the phosphorescent compound to be studied. However factors such as phosphorescent quantum yield, stability,

solubility and ease of purification are also important factors in the choice.

Although naphthalene has a relatively high triplet state energy of 2.63eV (by comparison anthracene is 1.84eV) it is readily purified by zone refining and is fairly soluble in the solvents used in this work. It also has a comparatively long phosphorescence lifetime which means that its recorded decay is not affected by much shorter lived background emission from glass elements of the optical system.

The methyl derivatives of 1,2-benzanthracene have a much lower triplet state energy (about 2.05eV) than naphthalene. However, they have a much lower solubility and about five times as fast a phosphorescence decay as naphthalene. Further, their purification is more difficult because their high melting points (over 200°C), and the small quantities available made zone-refining impractical. Some are known to be skin carcinogens and must therefore be handled carefully.

The reason for studying these benzanthracene compounds is discussed in chapter III.

4.5 PURIFICATION

(a) Solvents:

The solvents, 3MP and MCH, were Phillips "Pure grade". They were both purified by stirring with concentrated sulphuric acid for about fifty hours, washing with distilled water, and drying over anhydrous calcium chloride. The solvents were then

vacuum distilled into their storage bulbs where they were kept under vacuum over fresh sodium mirrors. The 3MP used for preparing solutions of the methyl substituted 1,2 benzanthracenes was scrubbed, washed and dried as before and then fractionated using a reflux ratio of about 8 to 1. The middle 50% was collected and then distilled into the storage bulb. No difference was found between results obtained from benzanthracene solutions using fractionated 3MP and those obtained using unfractionated 3MP.

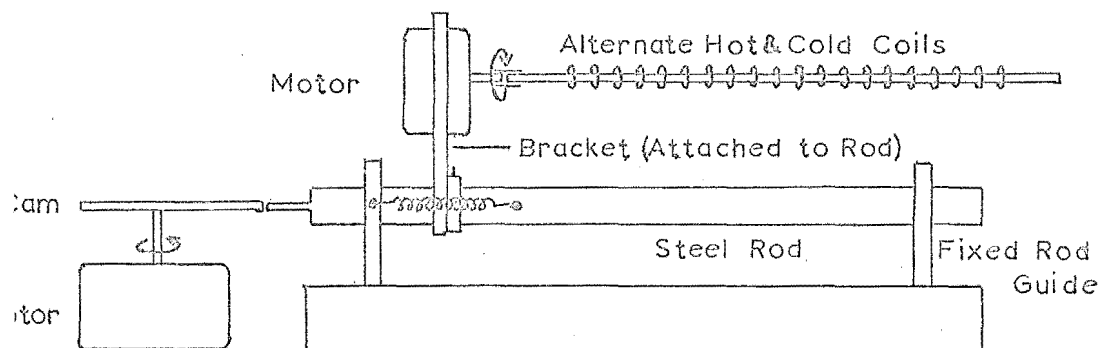
(b) Naphthalene:

The naphthalene was zone-refined using a micro-multipass zone refiner built for this project. This zone refiner is shown in diagram 4.4. It consists of a 1 m.m. diameter capillary tube about 8 inches long which fits through a series of alternately hot and cold loops placed $\frac{1}{2}$ cm. apart. These form a series of molten and solid zones of naphthalene contained in the capillary tube. This tube was rotated at a rate of 4 revs/min. to keep the molten zone stirred and the solid-molten interface normal to the glass tube. At the same time the tube was driven forward through the loops at a rate of 4 cm./hours. After the tube had been moved forward 1 cm. it was quickly returned to its starting position and the process repeated. After about twenty of these cycles a large crystal of naphthalene was seen to have formed in one end of the tube. If the refining was continued too long, the tube shattered, probably because of volume changes in the naphthalene ingot on melting and freezing. The tube was loaded with naphthalene by quickly sucking molten naphthalene up into it. Difficulty was experienced in

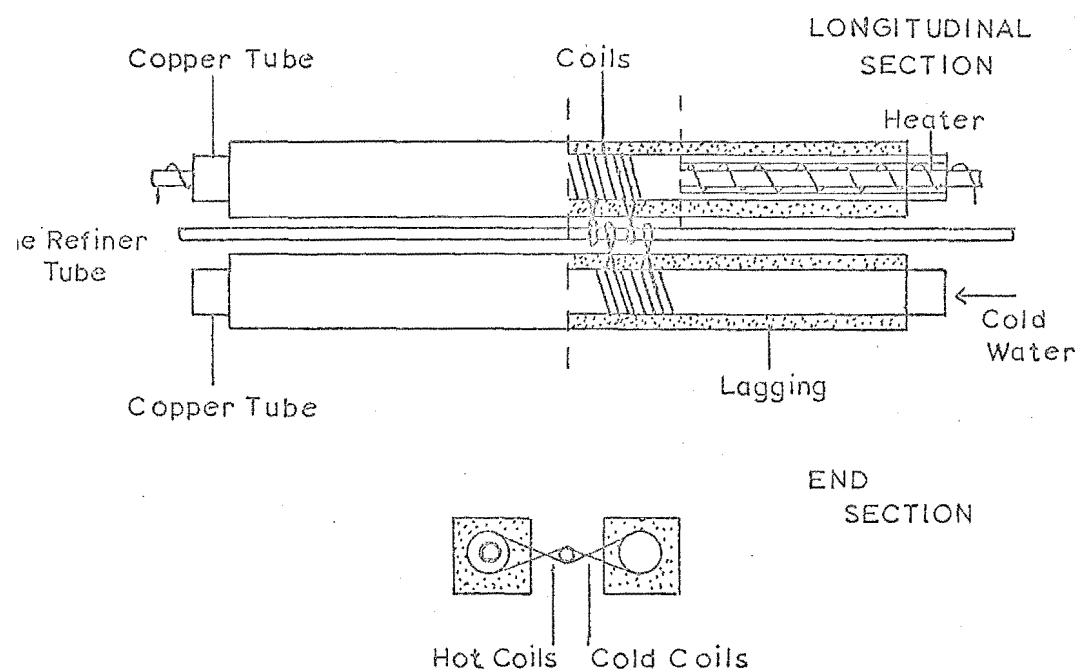
DIAGRAM 4.4

Zone Refiner

Drive Assembly



Coil Assembly



removing air-locks from the naphthalene ingot. Even so, when a red dye was added to the naphthalene to check the performance of the zone-refiner it was found that all the red dye was shifted to one end of the tube after a few cycles.

A short discussion of the theory of zone-refining is given in Appendix I.

(c) Mono methyl substituted 1,2-Benzanthracenes:

The methyl substituted 1,2-benzanthracenes were kindly donated by Dr. M. S. Newman, Ohio State University and were purified by a temperature gradient sublimation method. Originally the method described by Melhuish⁽⁵⁵⁾ was employed. This involves establishing a temperature gradient along a glass tube which contains the compound to be purified at the hottest end. Oxygen free nitrogen is passed along the tube from the hot to the cold end and the components of the material being purified crystallize out in different regions along the length of the tube. When 1,2-benzanthracene and 9,10-dimethyl 1,2-benzanthracene were treated in this fashion and then dissolved in 3MP glasses, they gave non-exponential phosphorescence decays. For some time these non-exponential decays were thought to arise from the presence of micro-crystals of solute in the solutions. A variety of solvents were employed to avoid the possibility of crystal formation. Those tried were iso-pentane (iP) and a variety of mixtures of iP, 3MP and MCH. The phosphorescence decays were still non-exponential so it was then suspected that impurities were responsible for the non-

exponential decays. A mass spectral analysis of a sample believed to be purified 1,2-benzanthracene showed the presence of higher molecular weight impurities. These may have been produced by traces of oxygen present in the nitrogen used in the purification.

The purification method finally adopted was suggested by W. Metcalf⁽⁵⁶⁾. It was much the same as that used before, except instead of elution with nitrogen, the tube containing the material to be purified was attached to the vacuum line, degassed, and then sealed off. A temperature gradient was established along the tube and the system was left overnight to allow the purification to take place. Two bands were formed when mono-methyl derivatives of 1,2-benzanthracene were purified in this way. Mass-spectral analysis of samples taken from both bands showed that both had the molecular weight of a methyl 1,2-benzanthracene with no detectable higher molecular weight impurities. These bands may be different crystalline forms of the same compound. Solutions of samples taken from both bands were prepared by dissolving them in 3MP and Arrhenius plots were constructed from data obtained from both solutions. More solutions were prepared using samples of solute taken from both bands resulting from the repurification of samples that had already been subjected to this method of purification. This process was repeated until reproducible slopes were obtained from the Arrhenius plots.

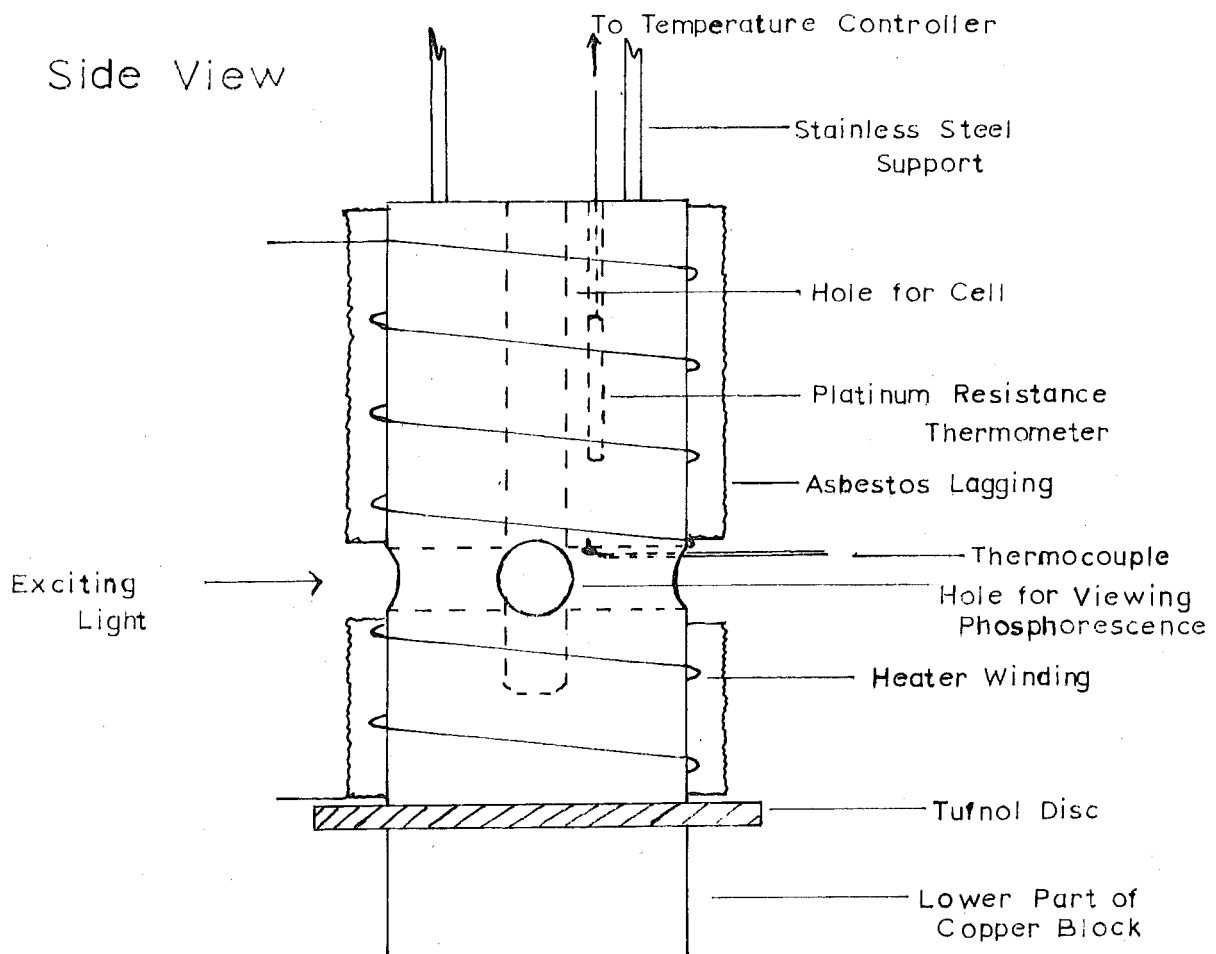
4.6 TEMPERATURE CONTROL AND MEASUREMENT

The quartz cell containing the solution to be studied

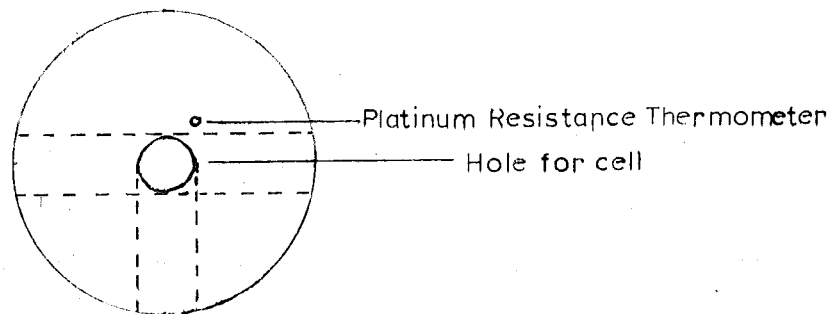
was inserted in the copper block shown in diagram 4.5. Temperature control at any temperature up to about 50 degrees above that of liquid air could be achieved by adjusting the current flowing through the heater winding around the top section of the copper block. This heating compensates for the loss of heat that takes place through the insulation to the lower end of the block which is surrounded by liquid air. The circuit of the temperature controller is shown in Appendix II. A platinum resistance thermometer embedded in the copper block was used as one of the arms in a bridge circuit. Any change in temperature was sensed as a resistance change in the bridge circuit. When the bridge became unbalanced by a change in temperature it either switched a transistor on or off allowing more or less current to flow through the heater winding, depending on whether the temperature had gone up or down. To achieve a suitable rate of heat loss from the copper block it was found necessary to lag the heater winding with asbestos tape. It was also found necessary to surround the whole copper block with a copper shroud that was maintained near the temperature of liquid air by dipping the lower end of the shroud into liquid air. The temperature of the cell was measured by a chromel-constantan thermocouple attached to the copper block near the cell. The voltage of the thermocouple was measured with a Tinsley Type 3397B potentiometer and recorded on a Hitachi Model QPD53 recorder. The chart recorder displayed any fluctuations or drift in temperature. The copper block and hence the solution in the quartz cell was maintained at a given temperature for at least ten minutes before the decay

DIAGRAM 4.5

Copper Block



Top View



of the phosphorescence from the solution was recorded at that temperature. The temperature control was better than $\pm 0.05^{\circ}\text{C}$.

4.7 RECORDING OF PHOSPHORESCENCE

The phosphorescence from the solution was focused on the photocathode of an IP28 photomultiplier tube. In order to protect this photomultiplier tube while irradiating the solution with light from the mercury lamp the full voltage was not applied to the photomultiplier. This was achieved in the following way. Light from the mercury lamp fell on the photocathode of P.M.₂ which switched on a transistor connected across some of the dynode resistors of P.M.₁. The voltage developed across the remainder of the dynode chain was considerably less than that developed across the complete dynode chain which was in effect when the irradiating light was switched off P.M.₂. The circuit of this protection system is shown in Appendix II.

The signal from the photomultiplier tube, P.M.₁, was amplified by a preamplifier shown in Appendix II. The phosphorescence decays studied were all too fast to read out directly onto the chart recorder available (maximum speed of 240 m.m./min.).

At the beginning of the project, the amplified signal was fed to the vertical plates of an oscilloscope and the trace of the signal was photographed. The photograph negatives were then "measured-up" using a travelling microscope. This method of recording and measuring decays was time consuming and tedious

particularly in the preliminary trial and error work involved in setting up the system. The method that was finally developed to record the phosphorescence decays employed the Varian C-1024 time averaging computer (CAT). The signal was fed into the CAT at a rate of perhaps 1024 channels in 5 seconds and later read out to the Hitachi recorder at a rate of 1024 channels in 100 seconds. Using these rates of reading into and out of the CAT, a twenty fold expansion in the time scale was achieved. The CAT's "sweep" was triggered by a voltage pulse produced from a voltage drop at a point in the dynode resistor chain of P_M_2 which occurred when the irradiating light was switched off P_M_2 . It was found there was only about a 10 millisecond delay from the time the irradiating light was switched off, to the time the signal received by P_M_1 was being stored in the CAT. In most cases a good deal of noise appeared on the recorded signal. Before "measuring-up" the decays, a smooth curve was drawn through the middle of the noise which was superimposed on the decay. Two further smooth curves were drawn through the upper and lower extremities of this noise. The interval between these latter two curves, at any given time, gave an estimate of the maximum error in the measurement of intensity at that time. See diagram I-6.

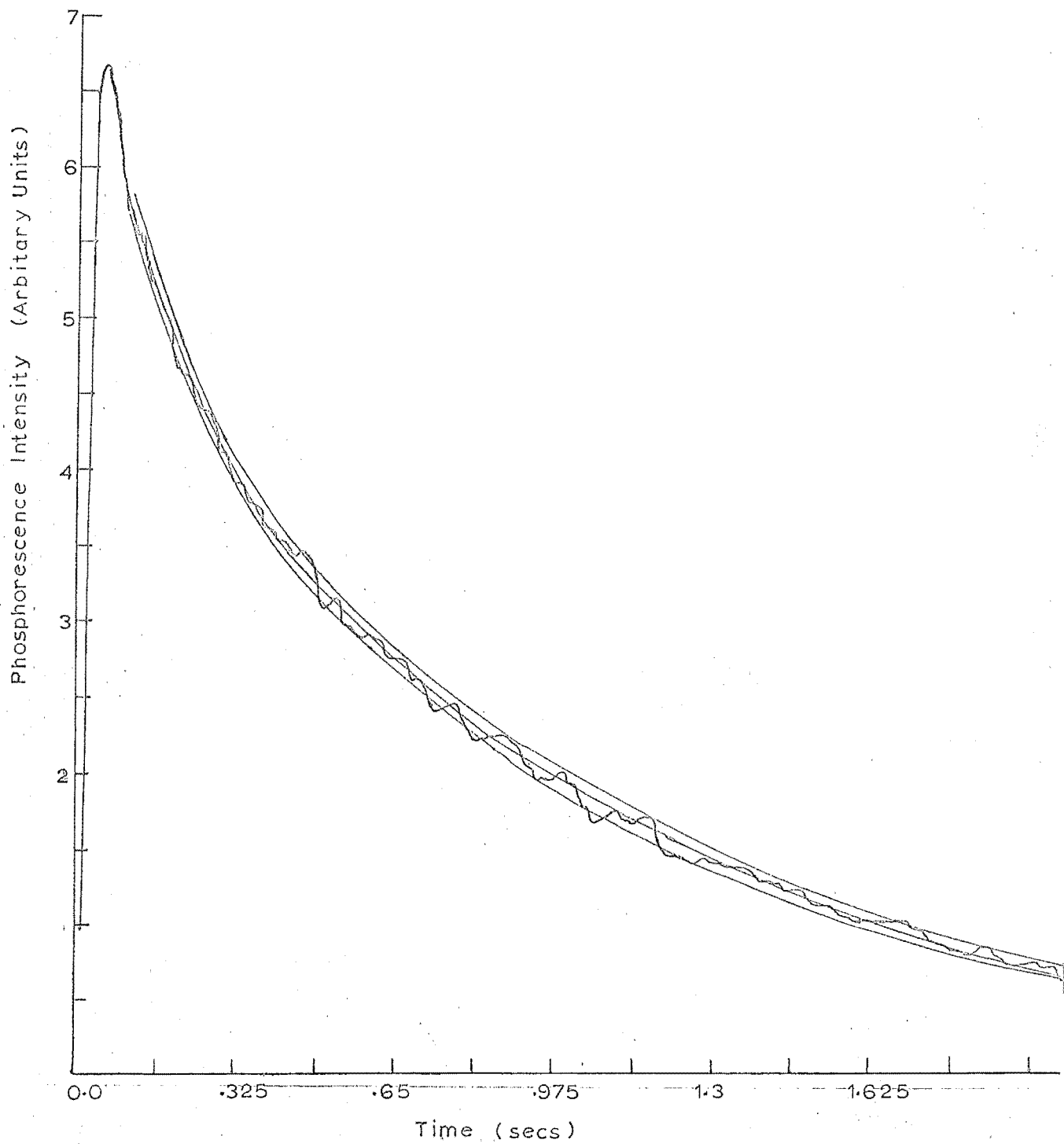
4.8 ANALYSIS OF DATA

In order to calculate the rate constant, k , of a phosphorescence decay, about twenty pairs of intensity, I , and

Typical Phosphorescence Decay

Solution 1.3

Temperature 96.2°K



time, t , values were measured from the recorded decay. The maximum error in measuring the intensity was estimated in the way outlined above and the error in the time was assumed to be negligible by comparison with that in the intensity. This data was fed into the I.B.M. 360/44 computer at the University of Canterbury and by use of a least squares program, values of A and k were computed which gave the least squares fit of the data to the equation:

$$I = Ae^{-kt}$$

together with estimated errors in the parameters. The program used was a modified version of ORCLS⁽⁵⁷⁾. It is described and listed in Appendix III.

Before feeding the data measured from the recorded decays into the computer they were given a preliminary check to ensure they were exponential by plotting $\log I$ against t .

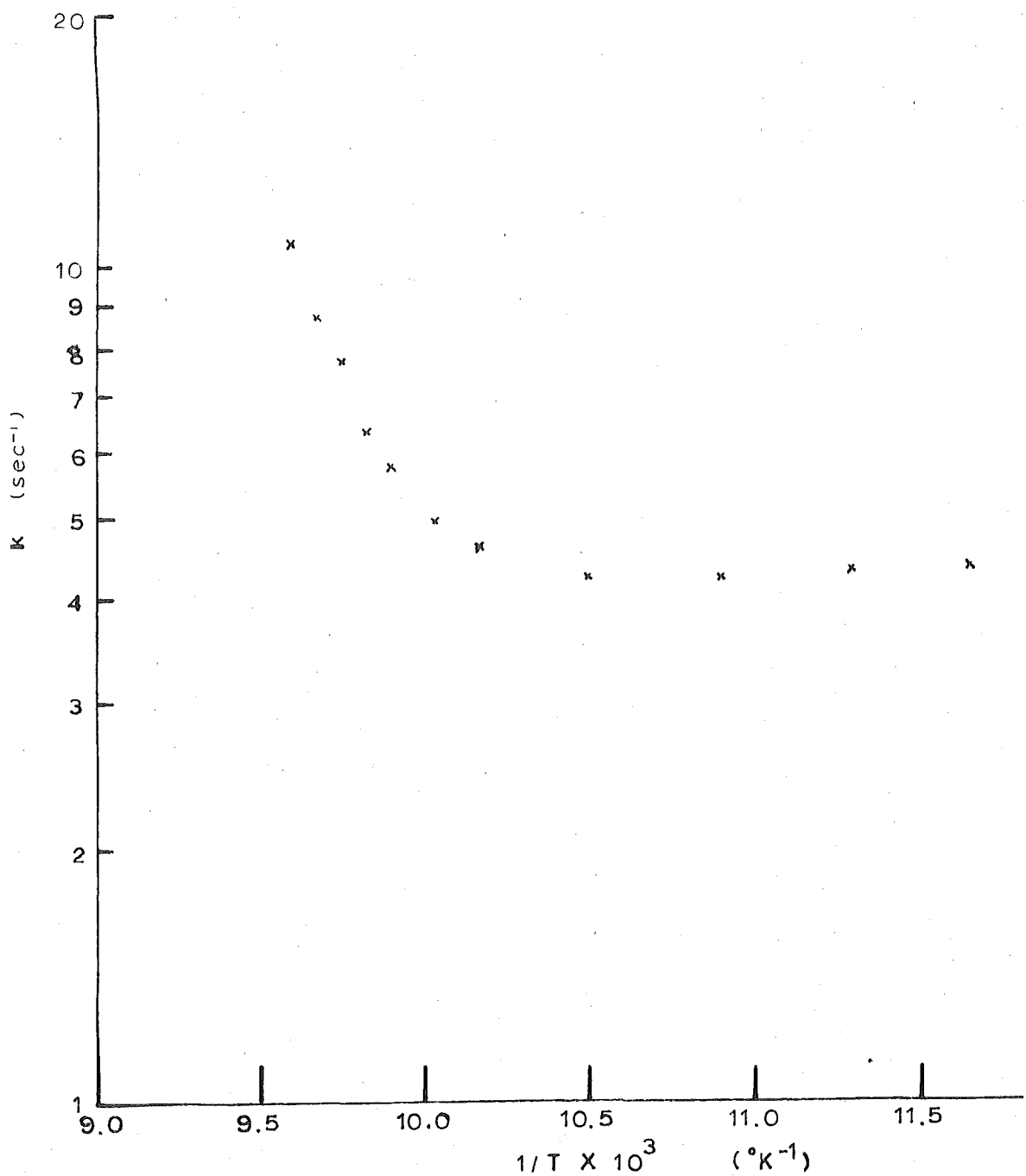
The values of rate constant determined at different temperatures were plotted as an Arrhenius plot. An example of the type of plot obtained is shown in Figure 4.7. The few points found to lie well off the best line fitted (by eye) through the points of the Arrhenius plot were discarded in the later analysis of data.

The low temperature portion of the Arrhenius plots of data obtained from deoxygenated solutions were almost flat. i.e. There was almost no change in rate constant with change in temperature. It was therefore decided to fit the rate constants at different temperatures obtained from deoxygenated solutions to

DIAGRAM 4.7

Typical Arrhenius Plot

Solution 2.5



an equation of the form:

$$k = Be^{-b/T} + D \quad 4(i)$$

where B and D are constants. b is also a constant and is equal to E/R , where E is the magnitude of the energy barrier to some process whereby a triplet state molecule can return to its ground state. R is the gas constant.

In this least squares fit, all rate constants were given the same weight. The reason for using this weighting scheme will be explained in the section discussing errors. The absolute temperature, T, was assumed to have negligible error.

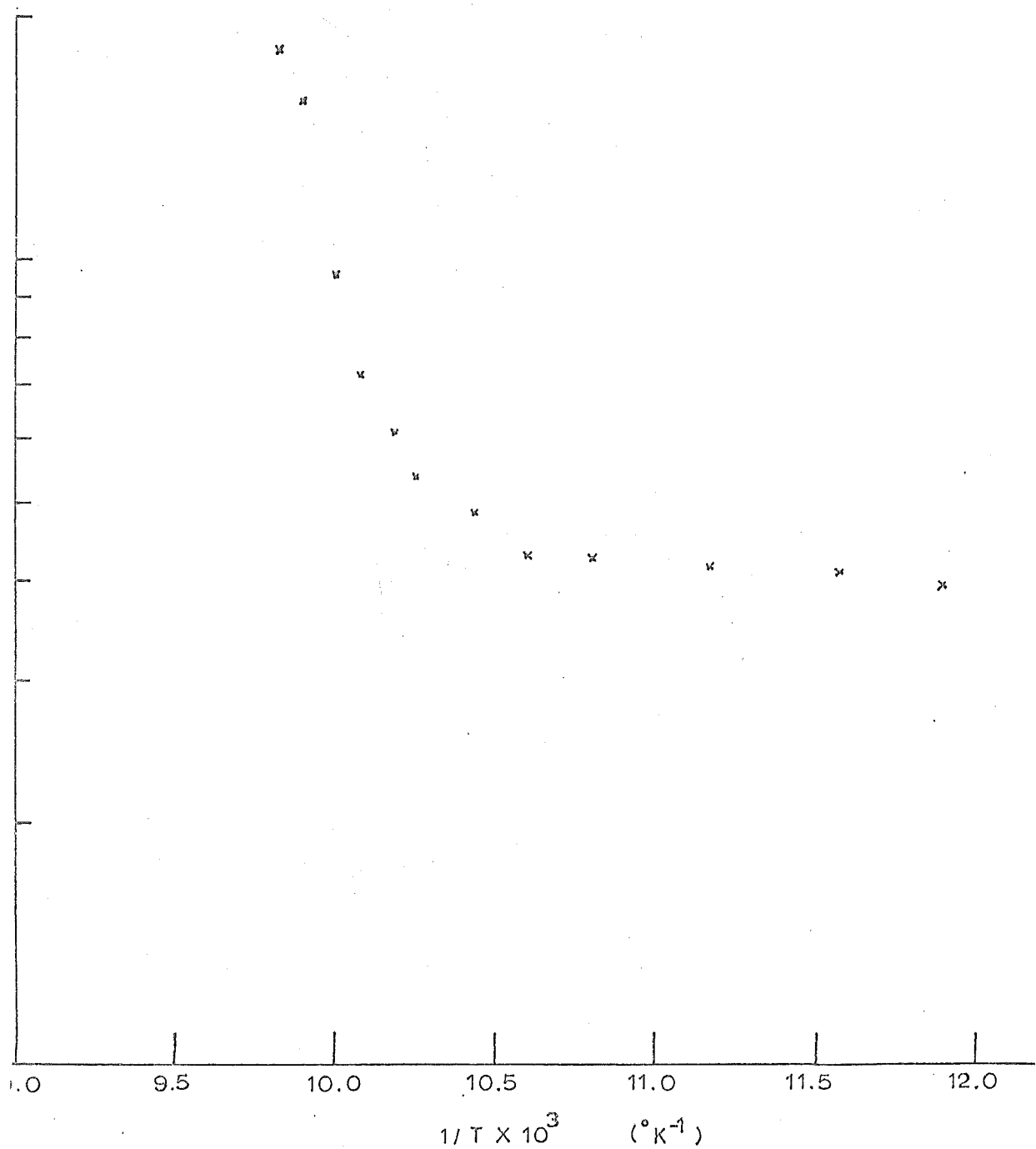
Figure 4.8 shows a typical Arrhenius plot derived from data obtained from a solution containing oxygen. By comparison with Figure 4.7 which is an Arrhenius plot typical of those derived for deoxygenated solutions it can be seen that the onset of the rapid increase in rate constant with increasing temperature occurs at lower temperatures in the oxygenated solutions than in the deoxygenated solutions. This means that there are fewer points in the low temperature portion of the Arrhenius plot in oxygenated solutions, which often made it difficult to decide whether there was a significant slope in this section of the plot. So although an equation having the form of equation 4(i) may be a good theoretical description of the temperature dependence of the rate constant, often, in practice, an equation of the form:

$$k = Be^{-b/T} + De^{-d/T} \quad 4(ii)$$

gave a better description of the data obtained from solutions

DIAGRAM 4.8

Typical Arrhenius Plot
Solution 1.8



containing oxygen. Attempts to fit this data to equation 4(i) were therefore unsuccessful. Even when trial parameters for equation 4(i) were found which the least squares process did refine, the estimate of the value of the parameter, D, so obtained often appeared to be in error. This was presumably because of the lack of data in the low temperature region where equation 4(i) is sensitive to parameter D. While an inaccurate value of D has little effect on the values of the rate constants measured at high temperatures it does have a significant effect on the rate constants measured at low temperatures, and since all points in the Arrhenius plot were given equal weight it could lead to an inaccurate estimate of the parameter, b.

Attempts to fit the rate constant-temperature data to equation 4(ii) were also unsuccessful. It was found that the computer could not invert the matrix of the normal equations. This was because some of the elements of this matrix are derived from parameters B and d in equation 4(ii) which have considerably different magnitudes (B of the order of 10^{20} and d of the order of 10^{-7}). Matrix inversion using a computer is a notoriously difficult operation when there is a large difference in the magnitude of some of the elements. To overcome this difficulty an attempt was made to fit the temperature-rate constant data to an equation which is equivalent to equation 4(ii), but of the form:

$$k = e^{c+b/T} + De^{-d/T} \quad (B = e^c)$$

This eliminated the difficulty of matrix inversion, but further problems then arose. It is explained in Appendix III that trial values of the parameters must be chosen and then the changes required in these parameters to give a least squares fit of the data are calculated. In fitting to a non-linear function, the calculated changes in the parameters are only approximations to the changes actually required. Because of poor estimates of trial parameters, insufficient data and insufficient precision of the available data, the required changes in some of the parameters were wildly overestimated causing the computation to stop after a few cycles, because the parameters had become negative.

It was found that the rate constant-temperature data for the solutions containing oxygen could only be handled successfully in the following way. Rate constants in the low temperature region of the Arrhenius plot before the onset of the rapid increase in rate constant with increasing temperature were fitted to an exponential:

$$k = D e^{-d/T}$$

Rate constants in the region of rapid increase in rate constant were then corrected in the following way.

$$T_k_{\text{corrected}} = T_k_{\text{exp}} - D e^{-d/T}$$

where $T_k_{\text{corrected}}$ is the corrected rate constant at temperature, T , and T_k_{exp} is the experimentally determined value of the rate constant at temperature, T . Values of $T_k_{\text{corrected}}$ at different temperatures were then fitted by the least squares process to the equation:

$$\log_e k_{\text{corrected}}^T = \log_e B - b/T$$

Parameter b in this equation has the same significance as it has in equation 4(1).

4.9 ERRORS

Although errors were estimated for the rate constants derived from a least squares fit of phosphorescence intensity - time data, their significance in the subsequent fitting of rate constants determined at different temperatures to a function of temperature is doubtful. This is because the error estimated for a rate constant at a given temperature was based on the phosphorescence decay resulting from only one irradiation of the solution. The error arises from the noise on the recorded phosphorescence decay for that "observation" and does not take account of other sources of fluctuation in the value obtained for the rate constant that may occur from one "observation" to another. These sources of fluctuation could include a difference in the base line for the decay, fluctuation in temperature, or change in environment of the phosphorescing species. To enable a proper statistical analysis of the errors, a number of "observations" at each temperature should have been made. However, this was impractical for a number of reasons. At low temperatures where diffusion processes are slow, a sufficient time would have to be allowed between "observations" to ensure that the phosphorescing system had returned to a random distribution of molecules as had existed before the first "observation".

The maintenance of a constant temperature for the time then required for, say, ten "observations" at each temperature was well beyond the capabilities of the temperature controller. Also, the measurement and processing of data to construct an Arrhenius plot for a solution where only one "observation" was made at each temperature was a lengthy process and the time required if more than one "observation" had been made at each temperature would have been prohibitive.

Having no reliable estimate for the error in each rate constant they were all given the same weight in fitting them to equations of the type:

$$k = B e^{-b/T} + D$$

$$\text{or} \quad k = B e^{-b/T}$$

This weighting scheme may be shown to be justified in the following way:

In the Arrhenius plots obtained in this project most of the points lie close to continuous smooth curves and there was no greater scatter of results in any region of the plots than in any other region. This suggests that the errors in k are similar for all regions of an Arrhenius plot. Hence an equal weighting scheme is reasonable for fitting rate constant-temperature data to an equation of the type:

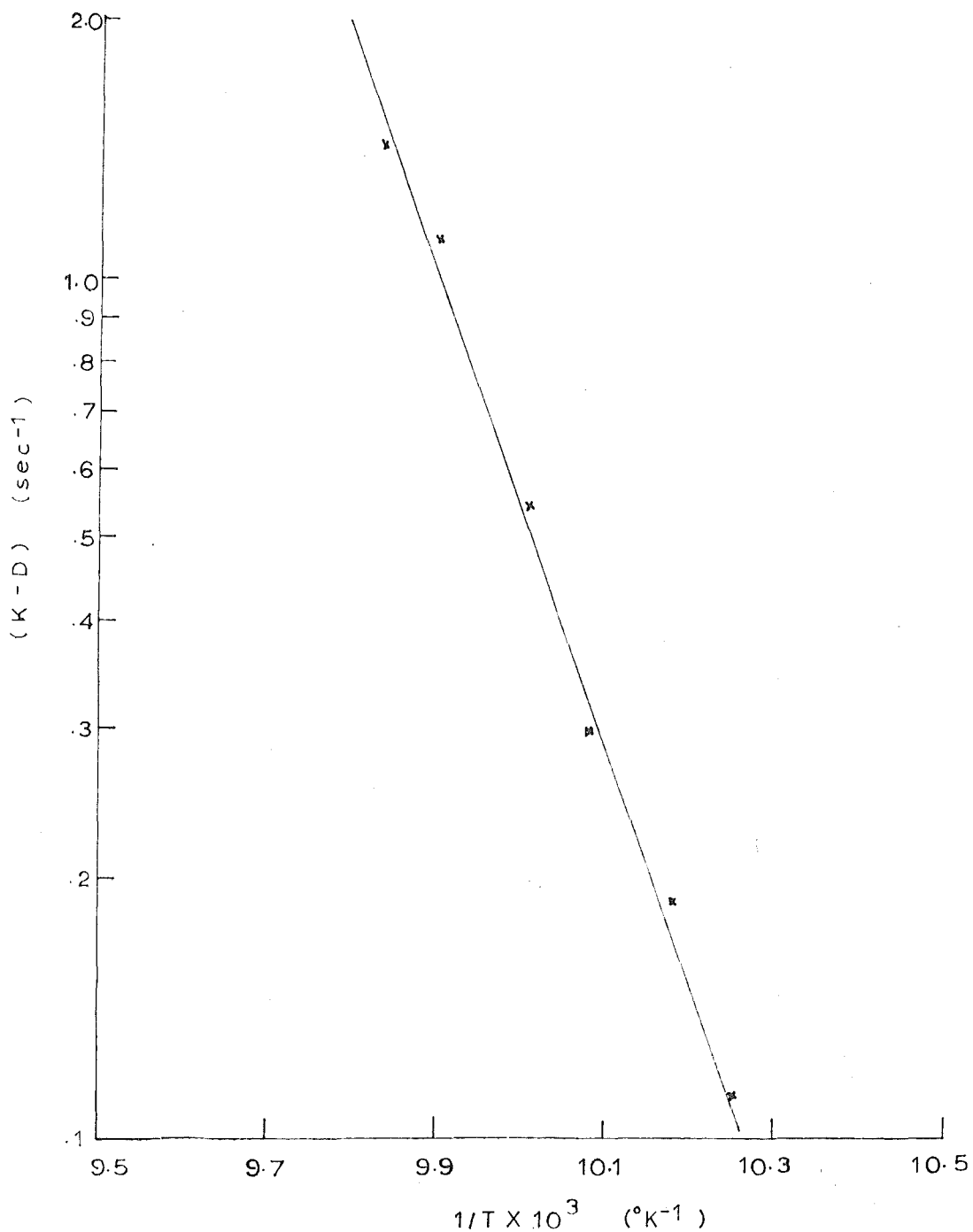
$$k = B e^{-b/T} + D$$

Similarly, if a plot of $(k-D)$ against the reciprocal of the absolute temperature, T_p , is made (see for example, figure 4-9), most of the

DIAGRAM 4.9

Typical Plot of (K-D) vs. 1/T

Solution 1.8



points lie close to a straight line and there is no greater scatter of results in any region of the $(k \cdot D)$ against $1/T$ plot than in any other regions. Hence by the same reasoning used above, an equal weighting scheme was assumed to be reasonable in fitting values of T_k _{corrected} to an equation of the type:

$$T_k_{\text{corrected}} = B e^{-b/T}$$

In an Arrhenius plot, the estimated error in the slope of the line is inversely proportional to the product of the range of temperature over which measurements are made and the square root of the number of measurements. Therefore, in order to obtain greater precision in the estimate of the slope of the line, it is more profitable to double the range of temperature over which measurements are made rather than double the number of measurements within a range. However in the systems studied in this project the range of temperature over which rate constants could be measured was limited. No rate constants could be measured below the temperature of liquid air because this was the minimum temperature attainable by the temperature controller described earlier in this chapter. As the temperature increases, non-radiative mechanisms for deactivating the triplet state become more important with a consequent lowering of phosphorescence intensity, until, at temperatures about 120°K, the signal to noise ratio becomes too low to make meaningful measurements.

CHAPTER V

Results and Discussion

A typical example of the determination of the rate constant for a phosphorescence decay is shown for solution 1.3 at a temperature of 96.2°K.

The recorded phosphorescence decay is shown in diagram 4.6 and computer output after the fifth and final cycle of the least squares fit is given below.

NAPHTHALENE&3MP&MCNCO2 SOLN1.3 TEMPERATURE 96.2

PARAMETERS AFTER LEAST SQUARES CYCLE 5

OLD	CHANGE	NEW	ERROR
1 0.5297E 01	0.3677E-05	0.5297D 01	0.4052E-01
2 0.9829E 00	0.7711E-06	0.9829D 00	0.7923E-02

ESTIMATED AGREEMENT FACTORS BASED ON PARAMETERS AFTER CYCLE 5

SUM(W*(O-C)**2) IS 0.2640 01

SQRTF(SUM(W*(O-C)**2)/(NO-NV)) IS 0.3729

NAPHTHALENE&3MP&MCNCO2 SOLN1.3 TEMPERATURE 96.2

CALCULATED Y BASED ON PARAMETERS BEFORE CYCLE 6

Y(OBS)	Y(CALC)	OBS-CALC	SIG(0) (O-C)/SIG(0)	X(I)
1.3000	1.2894	0.0106	0.0600	0.1774
1.3900	1.3710	0.0190	0.0600	0.3159
1.1600	1.1403	0.0197	0.0600	0.3286
1.0100	1.0084	0.0016	0.0600	0.0259
1.0900	1.0723	0.0177	0.0600	0.2943
1.2300	1.2125	0.0175	0.0600	0.2912
1.4700	1.4579	0.0121	0.0600	0.2014
1.5500	1.5503	-0.0003	0.0600	-0.0048
1.6400	1.6485	-0.0085	0.0600	-0.1419
1.7400	1.7530	-0.0130	0.0700	-0.1852
1.8400	1.8640	-0.0240	0.0700	-0.3433
2.0800	2.1077	-0.0277	0.0800	-0.3465
2.2100	2.2413	-0.0313	0.0800	-0.3909
2.3700	2.3833	-0.0133	0.0800	-0.1659
2.5000	2.5343	-0.0343	0.0800	-0.4285
2.6600	2.6948	-0.0348	0.1000	-0.3485
2.8300	2.8656	-0.0356	0.1000	-0.3559
3.0300	3.0472	-0.0172	0.1000	-0.1715
3.2300	3.2402	-0.0102	0.1000	-0.1022
3.4800	3.4456	0.0345	0.1000	0.3448
3.7700	3.6638	0.1062	0.1000	1.0617
				0.3750

AGREEMENT FACTORS BASED ON PARAMETERS BEFORE CYCLE 6

SUM(W*(O-C)**2) IS 0.2640 01

SQRTF(SUM(W*(O-C)**2)/(NO-NV)) IS 0.3729

Section 1

Results:

The rate constants which were evaluated from phosphorescence intensity decay curves at different temperatures are given below in tabular form for solutions of naphthalene in 3 methylpentane (3MP) - methylcyclohexane (MCH) mixtures of different compositions in the presence of oxygen at a pressure of about 5 to 10 mm.

Solution 1+1 Naphthalene + 3MP + O₂

Voltage of Thermocouple (mV)	Temperature T(°K)	10^3 $\frac{1}{T}$	Rate Constant k(sec ⁻¹)
8.4	86.4	11.574	0.4969
8.575	80.3	12.453	0.4400
8.55	81.3	12.300	0.4503
8.495	83.2	12.019	0.4764
8.45	84.8	11.792	0.4612
8.355	87.9	11.376	0.6257
8.585	80.0	12.500	0.4549
8.29	90.1	11.098	1.826
8.308	89.5	11.173	1.054

Solution 1.2 Naphthalene + 3MP + NaOH + O₂

Voltage of Thermocouple (mV)	Temperature T(⁰ K)	10^3 T	Rate Constant k(sec ⁻¹)
8.505	83.0	12.048	0.4607
8.395	86.7	11.534	0.5317
8.295	90.0	11.111	0.5206
8.18	94.1	10.626	0.4949
7.995	100.5	9.950	0.9661
7.965	101.7	9.832	1.149
8.125	96.0	10.416	0.4953
8.045	99.0	10.101	0.7509
8.01	100.0	10.000	0.8513

Solution 1.3 Naphthalene + 3MP + NaOH + O₂

Voltage of Thermocouple (mV)	Temperature T(⁰ K)	10^3 T	Rate Constant k(sec ⁻¹)
8.50	83.1	12.033	0.4703
8.39	86.8	11.520	0.4753
8.31	89.5	11.173	0.4699
8.24	91.9	10.976	0.4663
8.155	95.0	10.526	0.4830
7.95	102.0	9.803	1.072
7.91	103.2	9.689	1.325
7.88	104.3	9.587	1.827
8.12	96.2	10.395	0.4997
8.025	99.6	10.040	0.6986
8.0	100.3	9.970	0.8219

Solution 1.4 Naphthalene + 3MP + MgI + O₂

Voltage of Thermocouple (mV)	Temperature T(°K)	10^3 T	Rate Constant k(sec ⁻¹)
8.455	84.7	11.81	0.4122
8.355	87.9	11.38	0.4051
8.28	90.5	11.05	0.4443
8.19	93.7	10.67	0.4606
8.10	97.0	10.31	0.4934
8.03	99.4	10.06	0.6457
7.975	101.2	9.881	1.281
7.925	102.7	9.737	2.673
8.13	95.8	10.44	0.4700
8.065	98.2	10.18	0.5531
8.01	100.0	10.00	0.9474

Solution 1.5 Naphthalene + 3MP + MgI + O₂

Voltage of Thermocouple (mV)	Temperature T(°K)	10^3 T	Rate Constant k(sec ⁻¹)
8.51	82.8	12.08	0.4020
8.43	85.4	11.71	0.4280
8.35	88.1	11.35	0.4581
8.26	91.3	10.95	0.4341
8.175	94.2	10.62	0.4310
8.095	97.1	10.30	0.4563
8.015	99.9	10.01	0.4576
7.93	102.6	9.746	0.4822
7.86	105.0	9.523	0.5079
7.81	106.4	9.398	0.5294
7.765	107.8	9.276	0.7047
7.705	109.8	9.107	0.8847
7.84	105.5	9.478	0.5250

Solution 1.6 Naphthalene + BIP + MCII + O₂

Voltage of Thermocouple (mV)	Temperature T(⁰ K)	10^3 T	Rate Constant k(sec ⁻¹)
8.49	83.9	12.121	0.4117
8.28	90.5	11.160	0.4307
8.15	95.1	10.670	0.5096
8.025	99.6	10.235	0.9020
8.085	97.5	10.395	0.6480
8.06	98.3	10.341	0.7578
7.995	100.7	10.131	1.210
7.95	102.0	9.980	1.312

Solution 1.7 Naphthalene + BIP + MCII + O₂

Voltage of Thermocouple (mV)	Temperature T(⁰ K)	10^3 T	Rate Constant k(sec ⁻¹)
8.50	83.1	12.034	0.4009
8.415	86.0	11.628	0.4253
8.225	92.5	10.811	0.6420
8.185	93.9	10.650	1.241
8.39	86.9	11.507	0.4272
8.29	86.9	11.507	0.4272
8.29	90.2	11.087	0.5325
8.155	95.0	10.526	1.358
8.255	91.5	10.929	0.5769
8.205	93.2	10.730	0.8644

Solution 1.8 Naphthalene + 3MP + MCII + O₂

Voltage of Thermocouple (mV)	Temperature T(°K)	10^3 $\frac{1}{T}$	Rate Constant k(sec ⁻¹)
8.46	84.4	11.848	0.3913
8.40	86.4	11.574	0.4063
8.31	89.5	11.173	0.4166
8.225	92.5	10.811	0.4252
8.13	95.8	10.438	0.4811
8.175	94.2	10.616	0.4247
8.085	97.5	10.256	0.5359
8.035	99.2	10.081	0.7138
8.065	98.2	10.183	0.6025
8.015	99.9	10.010	0.9571
7.982	101.0	9.901	1.521
7.96	101.8	9.823	1.803

Solution 1.9 Naphthalene + 3MP + MCII + O₂

Voltage of Thermocouple (mV)	Temperature T(°K)	10^3 $\frac{1}{T}$	Rate Constant k(sec ⁻¹)
8.51	82.7	12.092	0.4155
8.395	86.7	11.534	0.3989
8.28	90.4	11.062	0.4254
8.175	94.2	10.616	0.4333
8.125	96.0	10.417	0.6320
8.075	97.8	10.225	0.8508
8.03	99.4	10.060	1.379
8.225	92.5	10.811	0.4532
8.145	95.3	10.493	0.5373
8.09	97.2	10.288	0.8205
8.055	98.7	10.132	0.8873

The measurements of composition for each solution are given below.

Solution 1.1

Molefraction of MCH = 0.0

Solution 1.2

Molefraction of MCH = 0.55

Solution 1.3

Molefraction of MCH = 0.58

Solution 1.4

Molefractions in MCH = 0.79, 0.85, 0.81, 0.81, 0.83, 0.86, 0.84,
0.82, 0.84.

Average molefraction in MCH = 0.82

Standard deviation ≈ 0.021

Solution 1.5

Measurements of molefraction in MCH = 0.31, 0.36, 0.34, 0.34, 0.32,
0.38, 0.33.

Average molefraction in MCH = 0.34

Standard deviation ≈ 0.024

Solution 1.6

Measurements of molefraction in MCH = 0.62, 0.63, 0.62, 0.61, 0.63,
0.61, 0.62, 0.63.

Average molefraction in MCH = 0.62

Standard deviation ≈ 0.008

Solution 1.7

Measurements of molefraction in MCH = 0.26, 0.26, 0.31, 0.33, 0.33,
0.32.

Average molefraction in MCH = 0.30

Standard deviation ≈ 0.030

Solution 1.9

Measurements of molefraction MCH = 0.66, 0.63, 0.64, 0.64, 0.65,
0.65, 0.65, 0.64, 0.64, 0.65,
0.64, 0.63

Average molefraction MCH = 0.64

Standard deviation = 0.009

Solution 1.8

Molefraction MCH = 0.68

Listed below are the activation energies, E, obtained by a least squares fit of corrected rate constant - temperature data to an equation of the type:

$$\log_e k_{\text{corrected}} = B - E/RT$$

where B is a constant, R is the gas constant, T is the absolute temperature, and $k_{\text{corrected}}$ is a rate constant for the decay of phosphorescence corrected in the way described in chapter IV.

Solution	Average molefraction MCH	E/R	E(Kcals/mole)
1.1	0.0	8.04 ± 0.43	16.00 ± 0.86
1.2	0.55	3.63 ± 0.27	7.21 ± 0.34
1.3	0.58	3.60 ± 0.14	7.15 ± 0.28
1.4	0.82 ± 0.02	8.22 ± 0.88	16.36 ± 0.76
1.5	0.34 ± 0.02	5.78 ± 0.66	11.48 ± 1.32
1.6	0.62 ± 0.01	3.71 ± 0.28	7.38 ± 0.56
1.7	0.30 ± 0.03	5.79 ± 0.76	11.52 ± 1.52
1.8	0.68	6.21 ± 0.46	12.36 ± 0.92
1.9	0.64	4.53 ± 0.17	8.66 ± 0.34

These results are plotted in graph 5.1.

Section 1Discussion

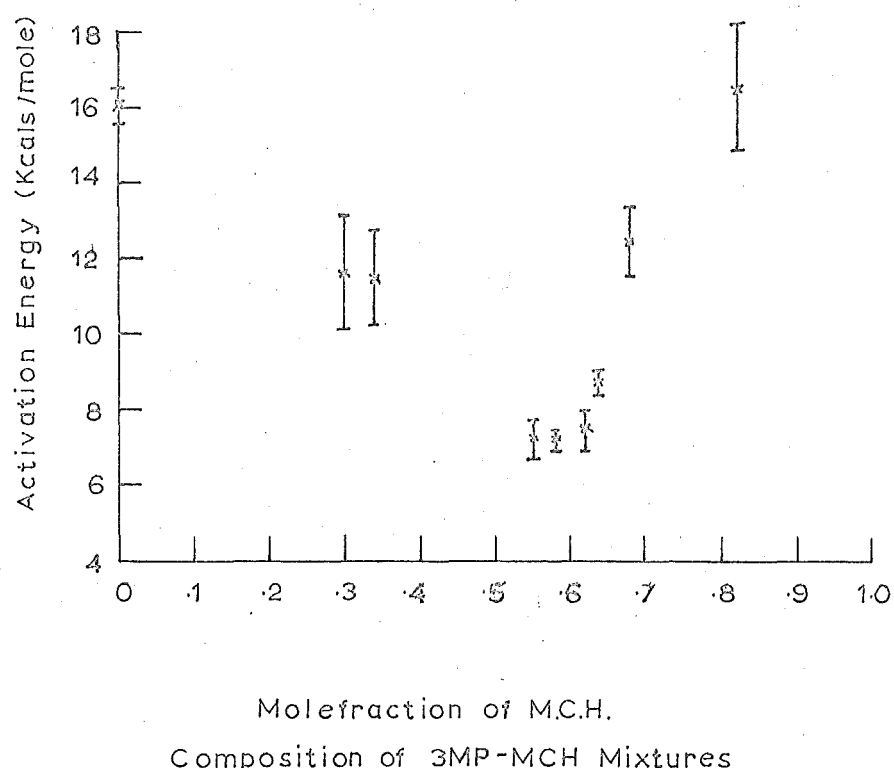
Both models for diffusion in binary mixtures presented in sections 2.4 and 2.5 predict a parabolic relationship between the energy barrier to translational diffusion in a binary mixture and the composition of the mixture. The first approach, being in terms of molecular interaction energies, lends itself to refinement and improvement. However, the second semi-empirical method gives a result in terms of directly measurable thermodynamic properties of the mixture and its components. It is therefore more amenable to comparison with experimental results than the first approach.

In this section of the project, the activation energies determined from the Arrhenius plots were energy barriers to the translational diffusion of oxygen in 3MP-MCH mixtures. The activation energy-composition relationship is shown in figure 5.1. There is a distinct minimum at a molefraction between 0.5 and 0.6 in MCH. In terms of equation 2(X), this is consistent with the fact that the heats of mixing of 3MP-MCH mixtures show a maximum at about the same composition at 20°C. (53) Heats of mixing and of vapourization are temperature dependent. While the heats of vapourization of 3MP and MCH could be estimated at about 100°K where the measurements in this project were done, no data exists to estimate the heats of mixing of 3MP-MCH mixtures at 100°K. It is therefore not possible to predict, using equation 2(X), the depth of the minimum in the energy barrier-composition relationship.

FIGURE 5·1

Activation Energy - Composition

Naphthalene & Oxygen in 3MP - MCH



Willard⁽⁵⁹⁾ has measured the viscosity of a number of 3MP-MCH glass mixtures of different composition as a function of temperature by measuring the rate of extrusion of a plug of the organic glass from the end of a tube to which high pressures of helium gas were applied. Although no values of data were given in the paper,⁽⁵⁹⁾ a plot of $\log_{10}\eta$ against $1/T$ for each mixture was given. (η is the viscosity of the mixture in poise and T is the absolute temperature). These plots were straight lines, of slope E_v/R where E_v is the energy barrier to viscous flow, and R is the gas constant. The relationship between E_v and composition of the mixture derived from the data obtained by Willard is shown in figure 5.2.

Comparison of figures 5.1 and 5.2 indicates that no simple relationship exists between E_v and the energy barrier to the translational diffusion of oxygen in these systems.

If $D = D_0 \exp(-E_D/RT)$ the reciprocal temperature dependence of $\log_e D$ is $-E_D/R$. Hence the Stoke-Einstein equation:

$$\eta = 6\pi Dr/RT$$

would predict the reciprocal temperature dependence of $\log_e \eta$ as:

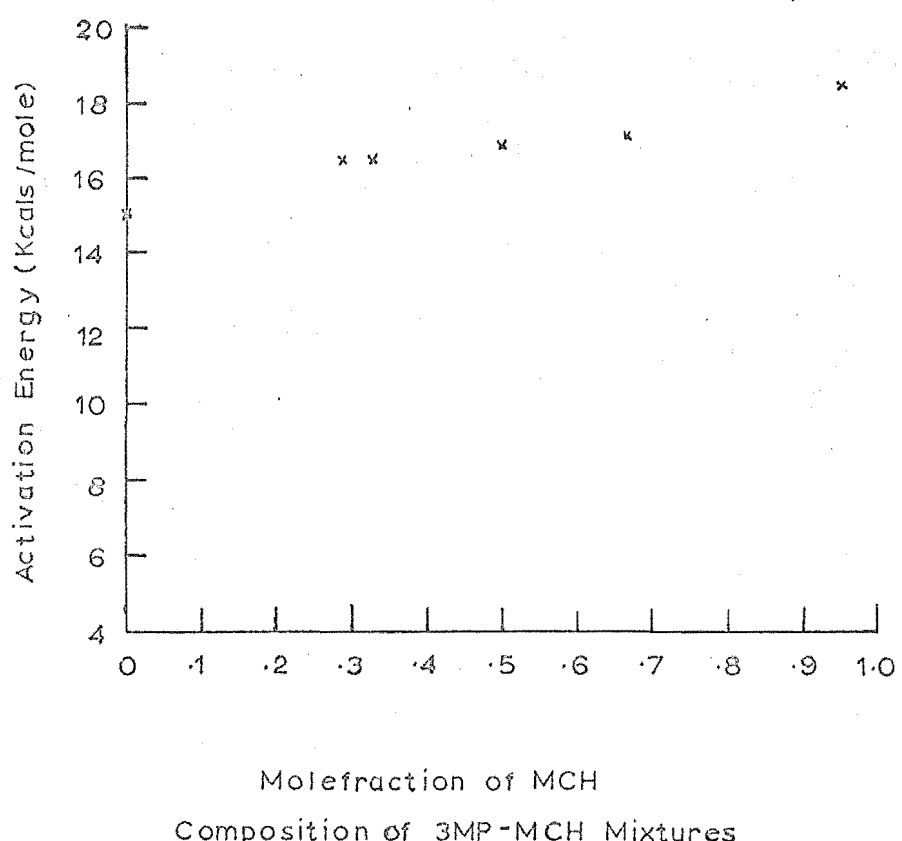
$$E_D/R + 1/T \approx E_v/R$$

i.e. The Stoke-Einstein equation predicts the reciprocal temperature dependences of $\log_e \eta$ and $\log_e D$ have the same magnitude, or $E_v = -E_D$. Therefore this work has demonstrated that the Stoke-Einstein equation is not a valid relationship between the diffusion coefficient of oxygen in 3MP-MCH mixtures and the macroscopic viscosity of these

FIGURE 5·2

Activation Energy - Composition

Energy of Viscous Flow in 3MP - MCH



mixtures.

A number of other workers have reported the failure of the Stoke-Einstein equation in predicting the molecular diffusion coefficients from macroscopic viscosities, particularly in the case of the diffusion of oxygen⁽⁶²⁾.

This invalidates arguments against a diffusion controlled quenching reaction of oxygen with phosphorescing molecules occurring in degassed solutions, which are based on the Debye equation. This is because the estimates of the concentration of oxygen necessary to account for the observed rates of decay in degassed solutions are based on the diffusion coefficient for oxygen derived from the macroscopic viscosity of the medium by the Stoke-Einstein equation.

Section 2

Results

The rate constants together with estimated errors which were evaluated from phosphorescence intensity decay curves at different temperatures are given below in tabular form for solutions of naphthalene in 3methylpentane-methylcyclohexane mixtures of different compositions in the absence of oxygen.

Solution 2.1 Naphthalene + 3MP

Voltage of Thermocouple (mV)	Temperature $T(^{\circ}\text{K})$	10^3 T	Rate Constant $k(\text{sec}^{-1})$	Error
8.525	82.1	12.180	0.4558	0.006
8.295	90.0	11.111	0.4382	0.003
8.21	93.0	10.753	0.4560	0.003
8.09	97.25	10.283	0.5195	0.002
8.005	100.1	9.990	0.9082	0.043
7.98	101.1	9.891	1.176	0.003
7.942	102.2	9.785	1.557	0.010
7.913	103.05	9.704	1.959	0.010
8.355	87.9	11.377	0.4443	0.002
8.15	95.2	10.504	0.4485	0.002

Solution 2.2 Naphthalene + 3MP + MCII

Voltage of Thermocouple (mV)	Temperature $T(^{\circ}\text{K})$	10^3 $\frac{1}{T}$	Rate Constant $k(\text{sec}^{-1})$	Error
8.49	83.4	11.990	0.4152	0.002
8.415	86.0	11.627	0.4106	0.004
8.33	88.8	11.261	0.4133	0.002
8.16	94.8	10.548	0.4034	0.005
8.11	96.9	10.351	0.4535	0.002
8.045	99.0	10.101	0.4987	0.002
7.99	100.7	9.930	0.6190	0.003
7.90	103.7	9.643	1.145	0.017
7.965	101.7	9.832	0.7156	0.007
7.915	103.0	9.708	0.9428	0.020
7.87	104.7	9.551	1.476	0.012

Solution 2.3 Naphthalene + 3MP + MCII

Voltage of Thermocouple (mV)	Temperature $T(^{\circ}\text{K})$	10^3 $\frac{1}{T}$	Rate Constant $k(\text{sec}^{-1})$	Error
8.505	83.0	12.048	0.4207	0.002
8.32	89.1	11.223	0.4053	0.004
8.21	93.0	10.752	0.4192	0.002
8.135	95.7	10.515	0.4412	0.002
8.055	98.7	10.131	0.5166	0.003
8.02	99.8	10.020	0.6133	0.002
7.995	100.7	9.930	0.7450	0.006
7.97	101.5	9.852	0.8355	0.005
7.935	102.4	9.765	1.073	0.004
7.90	103.7	9.643	1.463	0.011
8.40	86.4	11.574	0.4268	0.002

Solution 2.4 Naphthalene + 3MP + MCl

Voltage of Thermocouple (mV)	Temperature T($^{\circ}$ K)	10^3 T	Rate Constant k(sec^{-1})	Error
8.49	83.5	11.976	0.4147	0.002
8.40	86.3	11.587	0.4030	0.002
8.295	90.0	11.111	0.3954	0.001
8.215	92.8	10.775	0.4014	0.002
8.105	96.8	10.330	0.4133	0.002
8.03	99.3	10.060	0.4063	0.002
7.975	101.2	9.881	0.4032	0.003
7.93	102.6	9.746	0.4664	0.003
7.885	104.1	9.606	0.5216	0.003
7.825	106.0	9.433	0.6309	0.003
7.802	106.8	9.363	0.7747	0.003
7.78	107.4	9.310	0.9032	0.009

Solution 2.5 Naphthalene + 3MP + MCl

Voltage of Thermocouple (mV)	Temperature T($^{\circ}$ K)	10^3 T	Rate Constant k(sec^{-1})	Error
8.525	82.2	12.165	0.4198	0.002
8.42	85.8	11.665	0.4368	0.003
8.335	88.6	11.286	0.4310	0.003
8.25	91.7	10.905	0.4217	0.002
8.145	95.3	10.493	0.4216	0.002
8.06	98.4	10.162	0.4594	0.002
8.02	99.7	10.030	0.4942	0.002
7.977	101.2	9.881	0.5711	0.002
7.96	101.8	9.823	0.6327	0.003
7.93	102.6	9.746	0.7714	0.003
7.907	103.4	9.671	0.8659	0.006
7.885	104.2	9.596	1.069	0.011

Solution 2.6 Naphthalene + 3MP + NaCl

Voltage of Thermocouple (mV)	Temperature $T(^{\circ}\text{K})$	10^3 $\frac{1}{T}$	Rate Constant $k(\text{sec}^{-1})$	Error
8.525	82.2	12.165	0.4205	0.002
8.455	84.7	11.806	0.4193	0.002
8.345	88.3	11.325	0.4181	0.002
8.22	92.7	10.787	0.4211	0.002
8.14	95.5	10.471	0.4214	0.004
8.065	98.2	10.183	0.4262	0.003
8.015	99.9	10.010	0.4948	0.003
7.96	101.8	9.823	0.5661	0.002
7.915	103.0	9.709	0.6617	0.003
7.865	104.8	9.542	0.8854	0.004
7.83	105.8	9.452	1.197	0.010
7.935	102.4	9.766	0.6222	0.004
7.887	104.1	9.606	0.7362	0.003

Solution 2.7 Naphthalene + 3MP + NaCl

Voltage of Thermocouple (mV)	Temperature $T(^{\circ}\text{K})$	10^3 $\frac{1}{T}$	Rate Constant $k(\text{sec}^{-1})$	Error
8.495	83.3	12.005	0.4007	0.002
8.425	85.6	11.682	0.4049	0.007
8.34	88.4	11.312	0.4394	0.002
8.252	91.3	10.953	0.4479	0.006
8.165	94.7	10.560	0.4041	0.003
8.065	98.2	10.183	0.4081	0.001
7.985	101.0	9.901	0.4426	0.002
7.905	103.4	9.671	0.4879	0.003
7.86	105.0	9.524	0.5836	0.004
7.832	105.8	9.452	0.6041	0.003
7.80	106.8	9.363	0.7414	0.006
7.77	107.7	9.285	0.9033	0.005

Measurements of composition in molefraction of MCH
are given below for each solution.

Solution 2.1

Molefraction MCH ≈ 0.0

Solution 2.2

Measurements of molefraction MCH $\approx 0.12, 0.16, 0.18, 0.19, 0.18,$
 $0.17, 0.21, 0.24, 0.22, 0.21.$

Average molefraction MCH ≈ 0.19

Standard deviation ≈ 0.033

Solution 2.3

Measurements of molefraction MCH $\approx 0.25, 0.21, 0.25, 0.21, 0.22,$

Average molefraction MCH ≈ 0.23

Standard deviation ≈ 0.017

Solution 2.4

Measurements of molefraction MCH $\approx 0.71, 0.72$

Average molefraction MCH ≈ 0.72

Standard deviation ≈ 0.01

Solution 2.5

Average molefraction MCH ≈ 0.40

Solution 2.6

Average molefraction MCH ≈ 0.66

Solution 2.7

Average molefraction MCH ≈ 0.54

Listed below are the activation energies, E, derived by a least squares fit of rate constant - temperature data for each solution to an equation of the type:

$$k = \exp(B - E/RT) + D$$

where B, E and D are constants; k is the rate constant, T is the absolute temperature and R is the gas constant.

Note: In the least squares fit all rate constants were given equal weight.

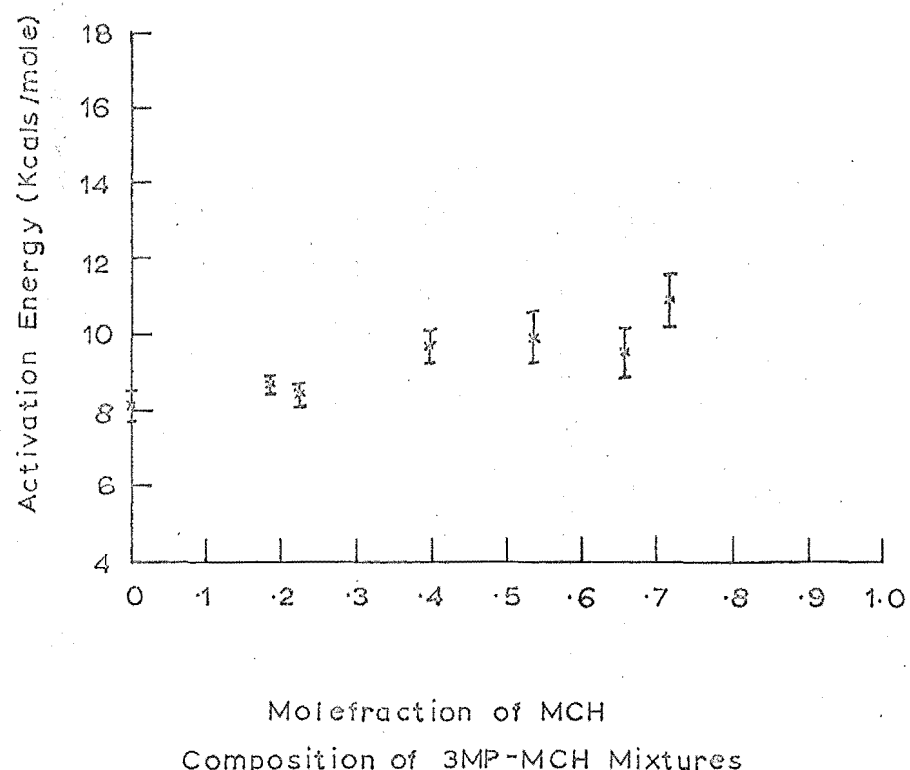
Solution	Average Molefraction MCH	E/R	E (Kcals/mole)
2.1	0.0	4.11 ± 0.19	8.17 ± 0.38
2.2	0.19 ± 0.03	4.37 ± 0.10	8.69 ± 0.20
2.3	0.23 ± 0.02	4.25 ± 0.15	8.46 ± 0.30
2.4	0.72 ± 0.01	5.45 ± 0.35	10.85 ± 0.70
2.5	0.40	4.86 ± 0.22	9.67 ± 0.44
2.6	0.66	4.77 ± 0.32	9.49 ± 0.64
2.7	0.54	4.98 ± 0.34	9.90 ± 0.68

These results are plotted in graph 5.3.

FIGURE 5.3

Activation Energy - Composition

Naphthalene in 3MP - MCH



Section 2Discussion

The energy barriers to the deactivation of the triplet state in deoxygenated solutions in the "low" viscosity region of the β MP-MCH glassy mixtures show only a slight, almost linear, upward trend as the molefraction of MCH increases. (See graph 5.3). Graph 5.3 does not bear any similarity to graph 5.1 in section 1 which is the relationship obtained when oxygen is present in the solutions. | Therefore, the energy barriers to triplet state deactivation in these degassed solutions do not arise from the translational diffusion of traces of oxygen remaining in the solutions.

Figures 2⁽⁷⁾ and 1

Further, comparison of graphs 5.4 and 5.3 shows that the energy barriers derived in this section of the project in the regions of high and low molefraction of MCH are lower than those for the diffusion of oxygen in the corresponding composition regions. If the translational diffusion of some quenching impurity other than oxygen was responsible for the observed energy barriers, it would be expected to always exhibit a greater energy barrier to diffusion than does oxygen. This is because any other quenching species likely to be present in the solutions would be larger than oxygen and therefore experience a greater energy barrier to diffusion.

We have
This section of the project has therefore demonstrated that the observed activation energies to the degradation of the triplet state in the degassed solutions studied are not energy

81₁₆

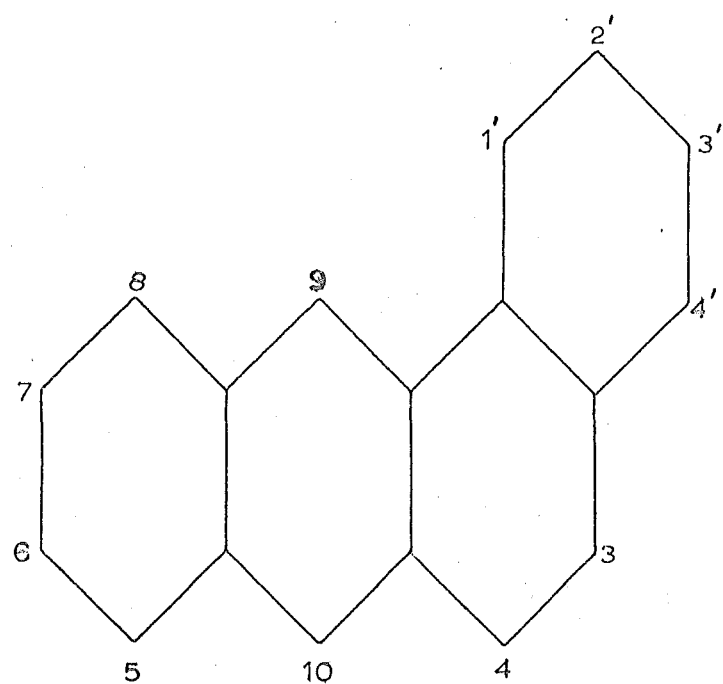
barriers to diffusion encountered in diffusion controlled
quenching reactions, as has been suggested by some workers (25, 26). /

Further discussion of the results in this section of
the work will be left until after the results have been given for
degassed solutions of some mono-methyl substituted 1,2 benzanthracones
in ZMP.

DIAGRAM 5.4

Numbering Scheme

Methyl Substituted 1,2-Benzanthracenes



Section 3Results

The rate constants together with estimated errors which were evaluated from phosphorescence intensity decay curves at different temperatures are given below in tabular form for degassed solutions of four mono-methyl substituted 1,2-benzanthracenes in 3methylpentane glasses. The naming scheme for these compounds is shown in diagram 5.4.

Solution 3.1

10-Methyl 1,2-benzanthracene + 3MP: The solute used in this solution was taken from the first band resulting from a vacuum sublimation of the crude 10-methyl 1,2-benzanthracene (see experimental section).

Voltage of Thermocouple (mV)	Temperature $T(^{\circ}\text{K})$	10^3 T	Rate Constant $k(\text{sec}^{-1})$	Error
8.505	83.0	12.048	4.194	0.024
8.40	86.35	11.581	4.303	0.022
8.30	89.85	11.130	4.235	0.020
8.15	91.6	10.917	4.471	0.049
7.985	101.0	9.901	4.644	0.032
7.90	103.65	9.648	5.480	0.063
7.875	104.5	9.569	5.779	0.032
7.845	105.35	9.497	6.221	0.031
7.805	106.7	9.372	7.315	0.112
7.76	108.0	9.259	8.831	0.096
7.73	109.0	9.174	9.458	0.087

Solution 3.2

10-Methyl 1,2-benzenthrene + BIP: The solute used in this solution was taken from the first band resulting from the vacuum sublimation of a sample of the material used for the solute in solution 1.

Voltage of Thermocouple (mV)	Temperature $T(^{\circ}\text{K})$	10^3 T	Rate Constant $k(\text{sec}^{-1})$	Error
8.51	82.8	12.077	4.299	0.022
8.435	85.2	11.737	4.244	0.013
8.15	95.2	10.504	4.386	0.027
9.035	99.3	10.070	4.357	0.023
7.930	102.65	9.742	4.547	0.027
7.835	105.75	9.456	4.923	0.010
7.785	107.25	9.324	5.057	0.055
7.68	110.35	9.062	5.95	0.037
7.635	111.70	8.953	6.923	0.075
7.60	112.60	8.881	7.073	0.014
7.545	114.2	8.757	8.272	0.10

Solution 3.3

10-Methyl 1,2-benzanthracene + SMP: The solute used in this solution was taken from the second band resulting from the vacuum sublimation of a sample of the material used for the solute in solution 1.

Voltage of Thermocouple (mV)	Temperature $T(^{\circ}\text{K})$	10^3 T	Rate Constant $k(\text{sec}^{-1})$	Error
8.495	83.25	12.012	4.286	0.017
8.41	86.05	11.621	4.347	0.070
8.275	90.75	11.019	4.232	0.065
8.135	95.75	10.444	4.527	0.038
8.005	100.1	9.990	4.487	0.019
7.91	103.25	9.685	5.122	0.056
7.858	105.1	9.515	5.733	0.027
7.81	106.45	9.394	6.196	0.043
7.76	108.0	9.259	7.251	0.019
7.727	109.05	9.170	7.689	0.090
7.705	109.8	9.107	8.665	0.062

Solution 3_{el}

5-Methyl 1,2-benzanthracene + 3MP: The solute used in this solution was taken from the first band resulting from the vacuum sublimation of the crude 5-methyl 1,2-benzanthracene.

Voltage of Thermocouple (mV)	Temperature $T(^{\circ}\text{K})$	$\frac{10^3}{T}$	Rate Constant $k (\text{sec}^{-1})$	Error
8.495	83.3	12.005	2.963	0.018
8.36	87.75	11.396	2.988	0.017
8.255	91.4	10.944	2.926	0.011
8.045	99.0	10.101	2.952	0.012
7.925	102.7	9.737	2.124	0.020
7.86	105.0	9.524	3.330	0.015
7.805	106.7	9.372	3.647	0.030
7.765	108.15	9.246	4.061	0.020
7.71	109.7	9.116	4.606	0.044
7.665	110.88	9.021	5.694	0.044
7.615	112.15	8.917	6.192	0.042
7.56	113.8	8.787	7.849	0.060

Solution 3,5

5-Methyl 4,2-benzanthracene + SHP: The solute used in this solution was taken from the first band resulting from the vacuum sublimation of a sample of the material used for the solute in solution 4.

Voltage of Thermocouple (mV)	Temperature $T(^{\circ}\text{K})$	10^3 T	Rate Constant $k(\text{sec}^{-1})$	Error
8.50	83.1	12.034	3.004	0.019
8.422	85.7	11.669	2.983	0.016
8.285	90.3	11.074	3.034	0.015
8.150	95.2	10.504	2.901	0.017
8.025	99.7	10.030	3.093	0.016
7.93	102.6	9.747	3.205	0.020
7.868	104.75	9.533	3.433	0.018
7.845	105.35	9.461	3.558	0.025
7.810	106.4	9.398	3.691	0.011
7.745	108.45	9.221	4.433	0.029
7.715	109.45	9.137	5.339	0.031
7.625	111.95	8.935	7.362	0.016

Solution 3.6

5-Methyl 1,2-benzanthracene + 3MP: The solute used in this solution was taken from the second band resulting from vacuum sublimation of a sample of the material used for the solute in solution 4.

Voltage of Thermocouple (mV)	Temperature $T(^{\circ}\text{K})$	$\frac{10^3}{T}$	Rate Constant $k(\text{sec}^{-1})$	Error
8.48	83.8	11.933	2.847	0.013
8.255	91.3	10.953	3.007	0.016
8.145	95.25	10.499	3.121	0.009
8.065	98.2	10.183	2.989	0.013
7.915	103.0	9.709	3.136	0.012
7.855	105.1	9.515	3.182	0.015
7.795	107.0	9.346	3.505	0.035
7.70	109.9	9.099	4.131	0.027
7.655	111.1	9.001	4.338	0.031
7.617	112.1	8.921	5.261	0.036
7.575	113.3	8.826	5.773	0.029

Solution 3.7

3-Methyl 1,2-benzanthracene: The solute used in this solution was taken from the first band resulting from the vacuum sublimation of the crude 3-methyl 1,2-benzanthracene.

Thermocouple (mV)	Voltage of Thermocouple	Temperature $T(^{\circ}\text{K})$	$\frac{10^3}{T}$	Rate Constant $k(\text{sec}^{-1})$	Error
8.455		84.7	11.806	2.703	0.013
8.325		89.0	11.236	2.737	0.010
8.235		92.15	10.852	2.770	0.013
8.115		96.35	10.379	2.846	0.025
8.03		99.4	10.060	2.816	0.009
7.897		103.75	9.639	3.024	0.021
7.85		105.25	9.501	3.175	0.024
7.82		106.2	9.416	3.645	0.012
7.77		107.7	9.285	4.147	0.031
7.73		109.0	9.174	4.637	0.025
7.69		110.2	9.074	5.747	0.042
7.65		111.25	8.989	7.028	0.017

Solution 3.8

3-Methyl 1,2-benzanthracene: The solute used in this solution was taken from the second band resulting from the vacuum sublimation of the crude 3-methyl 1,2-benzanthracene.

Voltage of Thermocouple (mV)	Temperature $T(^{\circ}\text{K})$	10^3 T	Rate Constant $k(\text{sec}^{-1})$	Error
8.495	83.3	12.005	2.578	0.019
8.375	87.2	11.468	2.790	0.017
8.26	91.2	10.965	2.772	0.027
8.16	94.9	10.537	2.705	0.041
8.025	99.65	10.035	2.845	0.019
7.885	104.1	9.606	3.053	0.058
7.82	106.2	9.416	3.129	0.024
7.77	107.7	9.285	3.268	0.022
7.715	109.45	9.137	3.711	0.018
7.64	111.50	8.969	4.043	0.022
7.58	113.2	8.834	5.569	0.067
7.55	114.1	8.764	6.248	0.044

Solution 3.9

3-Methyl 1,2-benzanthracene + 3MP: The solute used in this solution was taken from the second band resulting from the vacuum sublimation of a sample' of the material used for the solute in solution 7.

Voltage of Thermocouple (mV)	Temperature $T(^{\circ}\text{K})$	10^3 T	Rate Constant $k(\text{sec}^{-1})$	Error
8.452	84.7	11.806	2.667	0.009
8.38	87.15	11.474	2.667	0.008
8.285	90.25	11.080	2.780	0.012
8.03	99.4	10.060	2.665	0.019
7.925	102.7	9.737	2.851	0.020
7.89	104.0	9.615	3.001	0.011
7.83	105.9	9.443	3.203	0.014
7.78	107.3	9.320	3.658	0.021
7.74	108.7	9.200	3.936	0.047
7.705	109.8	9.107	4.540	0.040
7.66	111.0	9.009	5.399	0.048
8.16	94.9	10.537	2.766	0.013

Solution 3.10

8-Methyl 1,2-benzanthracene + ZMP: The solute used in this solution was taken from the first band resulting from the vacuum sublimation of the crude 8-methyl 1,2-benzanthracene.

Voltage of Thermocouple (mV)	Temperature $T(^{\circ}\text{K})$	10^3 T	Rate Constant $k(\text{sec}^{-1})$	Error
8.45	84.7	11.806	3.506	0.025
8.375	87.2	11.468	3.616	0.018
8.29	90.1	11.099	3.530	0.021
8.205	93.1	10.741	3.600	0.015
8.157	95.0	10.526	3.594	0.020
7.905	103.35	9.676	3.749	0.032
7.84	105.6	9.470	4.518	0.034
7.805	106.7	9.372	4.964	0.035
7.77	107.7	9.285	5.733	0.039
7.745	108.5	9.217	5.957	0.036
7.70	109.8	9.103	7.782	0.074

Solution 3.11

8-Methyl 1,2-benzanthracene + 3MP: The solute used in this solution was taken from the first band resulting from the vacuum sublimation of a sample of the material used for the solute in solution 10.

Thermocouple (mV)	Voltage of Thermocouple	Temperature $T(^{\circ}\text{K})$	10^3 T	Rate Constant $k(\text{sec}^{-1})$	Error
8.502		83.0	12.048	2.821	0.014
8.385		87.0	11.494	2.787	0.016
8.26		91.3	10.953	2.729	0.014
8.16		94.85	10.543	2.801	0.017
8.06		98.45	10.157	2.824	0.014
7.95		102.0	9.804	2.872	0.012
7.95		102.00	9.804	2.868	0.018
7.78		107.35	9.315	3.063	0.025
7.74		108.7	9.200	3.461	0.023
7.69		110.20	9.074	3.666	0.021
7.65		111.25	9.989	4.284	0.032
7.65		111.25	9.989	4.410	0.091
7.605		112.45	8.893	4.690	0.027

Listed below are the activation energies, E, derived by a least squares fit rate constant - temperature data for each solution to an equation of the type:

$$k = \exp(B - E/RT) + D$$

where B and D are constants, R is the gas constant and T is the absolute temperature.

Note: All rate constants were given equal weight in the least squares fitting process.

1,2-Benzanthracene Derivative	Solution	E/R	Activation Energy (Kcals/mole)
10-methyl	3.1	3.03 ± 0.21	6.04 ± 0.42
"	3.2	2.79 ± 0.21	5.55 ± 0.42
"	3.3	2.80 ± 0.12	5.57 ± 0.24
5-methyl	3.4	3.27 ± 0.06	6.52 ± 0.12
"	3.5	3.62 ± 0.16	7.20 ± 0.32
"	3.6	3.38 ± 0.35	6.73 ± 0.70
3-methyl	3.7	4.05 ± 0.15	8.07 ± 0.30
"	3.8	3.85 ± 0.36	7.67 ± 0.72
"	3.9	3.75 ± 0.20	7.46 ± 0.40
8-methyl	3.10	3.65 ± 0.45	7.26 ± 0.90
"	3.11	3.85 ± 0.37	7.65 ± 0.74

Section 3Discussion

The activation energies derived from the slopes of the Arrhenius plots in the "low" viscosity region are not the same for all the mono-methyl substituted 1,2-benzanthracenes studied. Therefore, if all the compounds studied are assumed to exhibit the same rotational diffusion characteristics, the activation energies derived from their Arrhenius plots in the "low" viscosity region can not be associated with the rotation of the triplet state molecules as suggested by Porter and Stief^(29d).

The activation energies obtained for the compounds studied increase in the order 10 methyl < 5 methyl < 3 methyl \approx 8 methyl derivatives. Despite the fact that only a few members of the mono-methyl substituted 1,2-benzanthracene group of compounds were studied, it is interesting to note that the "limiting" phosphorescence lifetimes (i.e. those measured in the temperature region where lifetime is independent of temperature) also increase in the order 10 methyl (.22) < 5 methyl (.33) < 3 methyl (.37) \approx 8 methyl (.38). The numbers in parentheses are approximate values of "limiting" phosphorescence lifetimes of the derivatives in seconds. Also, the two carcinogenic members of the group of compounds studied exhibit lower activation energies to degradation of the triplet state in the higher temperature region of the Arrhenius plots than the other two compounds studied.

While it would be speculative to suggest at this stage that correlations exist between the magnitude of the activation energies to triplet state decay, carcinogenic potency and "limiting" phosphorescence lifetimes, the results do indicate that more members of the mono-methyl substituted 1,2-benzanthracenes should be studied to see if any such correlations do exist. It would not be unreasonable to expect a relationship to exist between the "limiting" phosphorescence lifetime and the height of the energy barrier to the deactivation of the triplet state. The "limiting" lifetime is the reciprocal of the sum of the internal radiative and non-radiative rate constants for the decay of the triplet state. Therefore, since in the absence of quenching species the process responsible the activation energies measured in the "low" viscosity regions of these systems presumably involves internal radiative or non-radiative degradation mechanisms, the lower the activation energy, the faster the "limiting" phosphorescence decay (or shorter "limiting" lifetime).

While the results from sections 2 and 3 of this project do not show what processes are responsible for the observed temperature dependence of the phosphorescence lifetimes in the degassed solutions studied, two possibilities are ruled out: viz.

- (i) Diffusion controlled quenching reactions.
- (ii) Increased probability of intersystem crossing caused by coupling between the orbital motion of the electrons in the phosphorescing

molecule and Brownian rotation of the molecule.

Whatever the process is, that is responsible for the temperature dependence of the phosphorescence lifetimes, it shows a slight dependence on the nature of the solvent. From graph 5.3 it can be seen that as the amount of MCH in the 3MP-MCH mixtures increases, the activation energy of the process increases. This effect may arise from a distortion of the phosphorescing molecule which is assisted by MCH solvent molecules. The results of section 3 indicate that, not only is the process solvent dependent, but it also depends on the nature of the phosphorescing molecule. The different activation energies measured for the four mono-methyl substituted 1,2-benzanthracene compounds studied could mean that the effects of the solvent on the process responsible for the temperature dependence of the phosphorescence lifetime are not the same for each of the phosphorescing species. Alternatively, the observed differences in activation energy could arise from differences in some truly intramolecular factor in the phosphorescing molecule, such as the Franck-Condon overlap integral.

Section 4

Results

The rate constants of phosphorescence decay together with estimated errors which were evaluated from the phosphorescence decay curves at different temperatures are tabulated below for solutions of the 4'-methyl, 10 -methyl and 3 -methyl substituted 1,2 -benzanthracenes, all containing oxygen, in 3 -methylpentane glasses. All the solutes were purified by one temperature gradient vacuum sublimation which was described in the experimental section.

Solution 1

4'-methyl 1,2 -benzanthracene + 3MP

Voltage of Thermocouple (mV)	Temperature $T(^{\circ}\text{K})$	10^3 T	Rate Constant $k(\text{sec}^{-1})$	Error
8.54	81.5	12.270	3.294	0.016
8.505	82.95	12.055	3.307	0.022
8.45	84.75	11.799	3.471	0.026
8.322	89.0	11.236	3.628	0.019
8.27	90.85	11.007	4.091	0.025
8.205	93.15	10.735	5.230	0.046
8.16	94.8	10.549	7.216	0.068
8.135	95.75	10.444	9.628	0.079
8.385	87.0	11.494	3.451	0.018

Solution 2: 10-methyl 1,2-benzanthracene + 3MP

Voltage of Thermocouple (mV)	Temperature $T(^{\circ}\text{K})$	$\frac{10^3}{T}$	Rate Constant $k(\text{sec}^{-1})$	Error
8.425	85.65	11.675	4.386	0.026
8.395	86.7	11.534	4.432	0.041
8.365	87.65	11.409	4.475	0.027
8.322	89.0	11.236	4.429	0.041
8.275	90.7	11.025	4.840	0.052
8.24	92.0	10.870	5.587	0.035
8.195	93.55	10.689	6.847	0.036
8.162	94.8	10.549	8.880	0.054
8.135	95.7	10.449	11.160	0.115
8.450	84.8	11.792	4.305	0.088
8.38	87.2	11.468	4.455	0.036

Solution 3: 3-Methyl 1,2-benzanthracene + 3 MP

Voltage of Thermocouple (mV)	Temperature $T(^{\circ}\text{K})$	$\frac{10^3}{T}$	Rate Constant $k(\text{sec}^{-1})$	Error
8.43	85.3	11.723	2.655	0.017
8.40	86.3	11.587	2.627	0.020
8.355	87.9	11.377	2.696	0.012
8.305	89.75	10.142	2.864	0.014
8.255	91.3	10.953	3.449	0.021
8.217	92.7	10.787	3.966	0.048
8.175	94.2	10.616	5.240	0.049
8.135	95.75	10.444	8.134	0.110
8.51	82.75	12.085	2.619	0.021
8.47	84.15	11.884	2.580	0.011
8.157	95.0	10.526	7.082	0.069

Listed below are the activation energies, E, obtained by a least squares fit of corrected rate constants - temperature data to an equation of the type:

$$\log_e k_{\text{corrected}} = A - E/RT$$

where A is a constant, R is the gas constant, T is the absolute temperature, and $k_{\text{corrected}}$ is a rate constant for the rate of phosphorescence decay corrected in the way described in chapter IV.

Solution	1,2-Benzanthracene Derivative	E/R	Activation Energy (Kcals/mole)
1	4'-methyl	4.51 ± 0.16	8.99 ± 0.32
2	10-methyl	4.15 ± 0.47	8.26 ± 0.94
3	3-methyl	4.78 ± 0.37	9.50 ± 0.74

Section 4Discussion

The activation energies for the degradation of the triplet states of the three compounds studied are the same within experimental error, though these errors are fairly large in two of the solutions. In chapter III, it was pointed out that there is evidence to suggest that the activation energies for the reaction of oxygen with the carcinogenic polycyclic hydrocarbons such as 10-methyl 1,2-benzanthracene and for the non-carcinogenic methyl derivatives of 1,2-benzanthracene would be different. The fact that no significant difference was found in the measured activated energies for the degradation of the triplet state to the ground state means the energy barriers to diffusion are greater than the activation energies of reaction with oxygen at the viscosities encountered in β MP glass. However, any attempt to determine the activation energies of the reaction of oxygen with these compounds in a medium of lower viscosity would probably be unsuccessful because of the increased importance of other quenching and deactivation processes important in solutions of low viscosity.

The measured activation energies being the same, is consistent with them arising from the diffusion of oxygen in a diffusion controlled reaction involving the triplet state and oxygen. It is usually believed that the diffusivity of oxygen is larger than that of the triplet state molecules, to the extent that it alone determines the energy barrier to diffusion encountered in reactions

between oxygen and the triplet state. Therefore, on the basis of the equation derived in chapter II part 3, it would be expected that the activation energies derived from the 1,2-benzanthracene solutions (about 8.9 Kcals/mole) and from the naphthalene solution (about 13.8 Kcals/mole) should be the same. The observed difference can be rationalized in terms of a more sophisticated theory of diffusion in a one component condensed phase than the one outlined in chapter II part 3. This treatment is due to McLaughlin⁽⁶⁰⁾.

The successful movement of a molecule from one equilibrium position to the next depends not only on the molecule having sufficient energy to overcome the energy barrier, E_j , but also on the existence of a hole at the next equilibrium position in the medium, large enough to accommodate the diffusing molecule. The probability, P , of such a vacancy existing is given by:

$$P \approx \exp(-w'/kT)$$

where w' is the work done due to the disruption of local intermolecular forces in the formation of a hole. This probability in molar quantities is:

$$P' \approx \exp(-E_h/RT)$$

Therefore the empirical transmission coefficient, K , appearing in equation 2(vi) to allow for the possibility of a molecule, although having reached the "activated state" between the equilibrium positions, returning to its original position, may be replaced by P' .

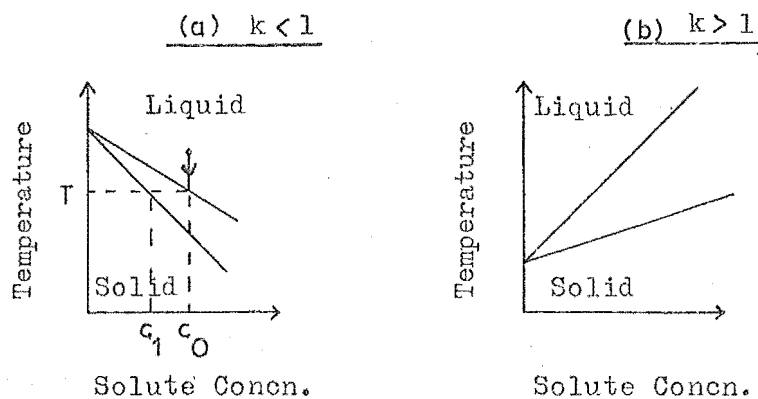
i.e. equation 2(vi) becomes:

$$D = (kT/2\pi\mu)^{1/2} (d^2/v_f^{1/3}) \exp[-(E_h + E_j)/RT]$$

It is now assumed that the measured energy barrier to diffusion corresponds to an oxygen molecule penetrating the shroud of solvent molecules immediately surrounding the triplet state solute molecule. While E_j would be independent of the nature of the triplet state molecules, E_h will depend on their interactions with solvent molecules. If these interactions were less in the 1,2-benzanthracene solutions than in the naphthalene solutions, then E_h and hence the measured activation energies, ($E_h + E_j$), would also be less.

APPENDIX IZone Refining

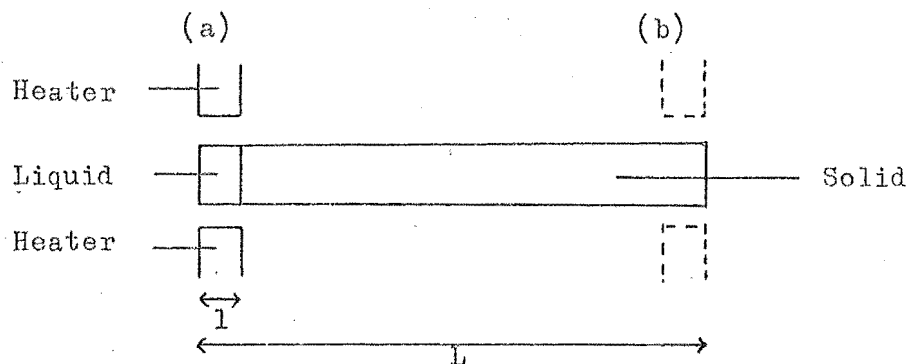
In order to understand how zone-refining works, first consider what happens when a solution is cooled. The possible types of phase diagrams for solutions in the dilute region are shown below.



If the original concentration of the solution is c_0 and the temperature is lowered to T , the first solid formed will have a concentration $c_1 = kc_0$. If the solution has a phase diagram like (a) then the first solid frozen out will be more pure than the original solution. At the same time the concentration of impurity in the remaining liquid solution increases and so the concentration of the impurity in the solid formed on further lowering of the temperature increases.

Consider now, a solution of a compound and an impurity having a phase diagram of type (a). Let the concentration of the impurity in the compound be c_0 and the solution be in the form of

an ingot of length, L .

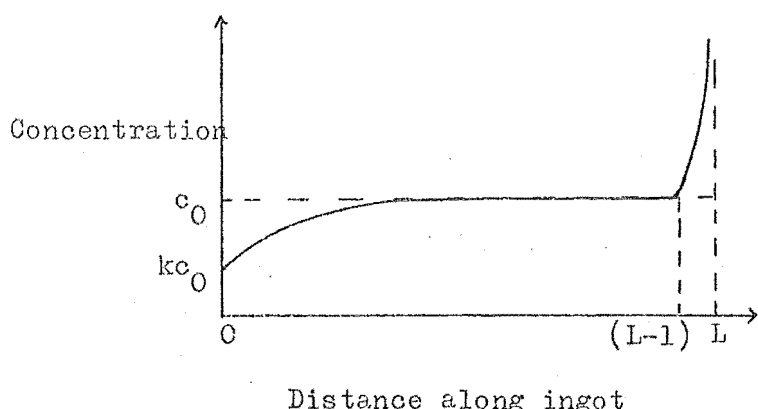


If a heater in position "a" produces a molten zone of length, l , at the left hand end of the sample, the concentration of the molten zone is the same as the rest of the sample, c_0 . If the heater is now moved slowly from left to right, the solid forming at the left hand side of the heater at the extreme left hand end of the sample will have an impurity concentration equal to $kc_0 (< c_0)$. The concentration of impurity in the molten zone will now be greater than c_0 . Therefore, as the molten zone advances through the sample the concentration of the solid forming on the left hand side of the heater becomes increasingly more concentrated in the impurity until a concentration of c_0/k in the molten zone is reached, at which point the solidifying material attains a concentration of $kc_0/k = c_0$. At this stage the concentration of the solidifying material remains constant until the heater has travelled a distance of $(L - l)$ (position "b"). Then the concentration of the solidifying material rises sharply over the remaining length of the sample.

108.

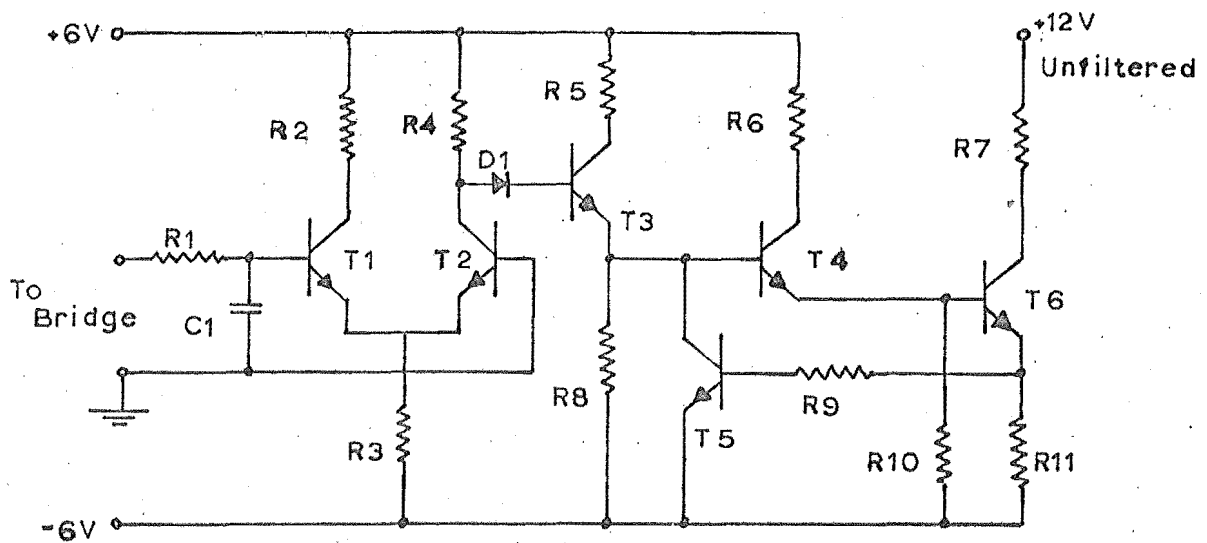
Figure I.1 represents the distribution of the impurity along the length of the sample after one "pass" of the molten zone through the sample. The more times the process described above is repeated, the less impurity remains at the left-hand end of the sample. To speed up the purification, several molten zones can be passed through the sample at once; one behind the other. This technique is employed in the zone-refiner described in the experimental section.

FIGURE I.1



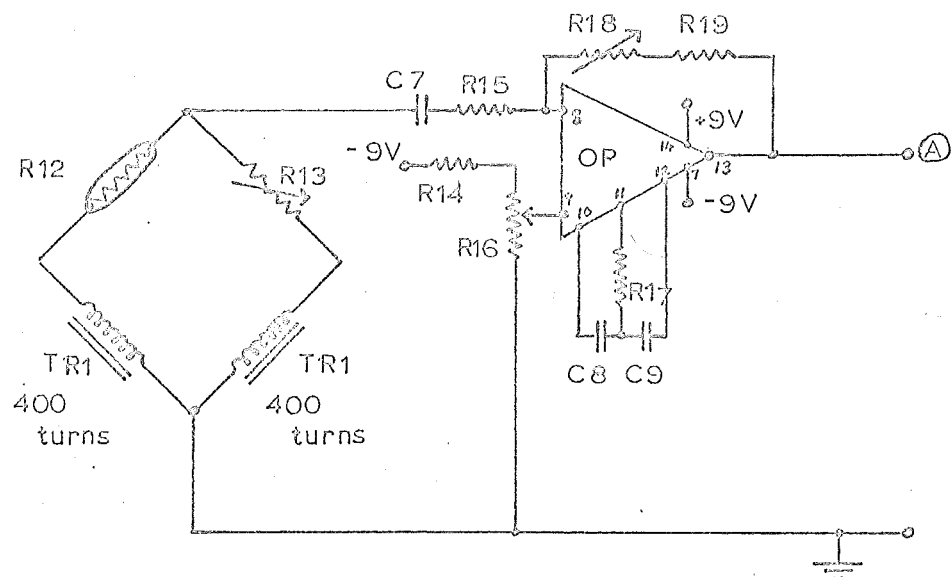
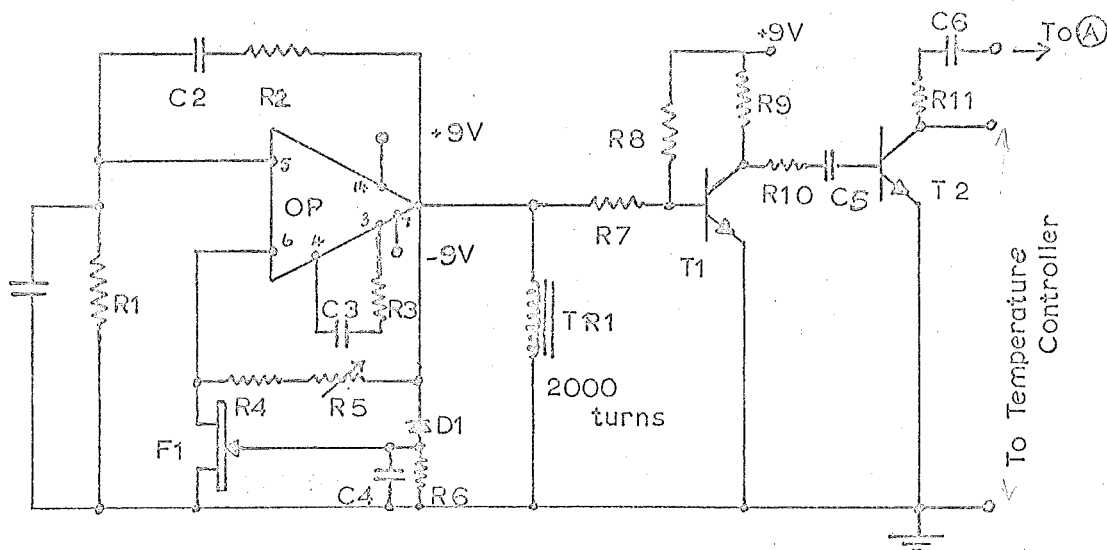
APPENDIX II

Temperature Controller



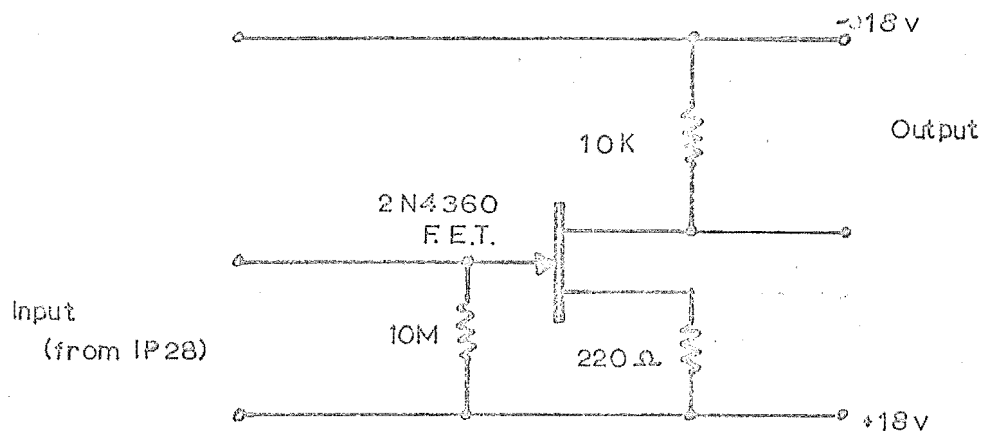
R1	3K3	R10	470 Ω	T6	2N3054
R2	1K	R11	.075 Ω		
R3	2K7	C1	.47 μ F		
R4	3K3	D1	Si Diode		
R5	220 Ω	T1	BC107		
R6	18 Ω	T2	BC107		
R7	4 Ω Heater	T3	BC107		
R8	820 Ω	T4	40317		
R9	75 Ω	T5	BC107		

Bridge & Amplifier Circuit

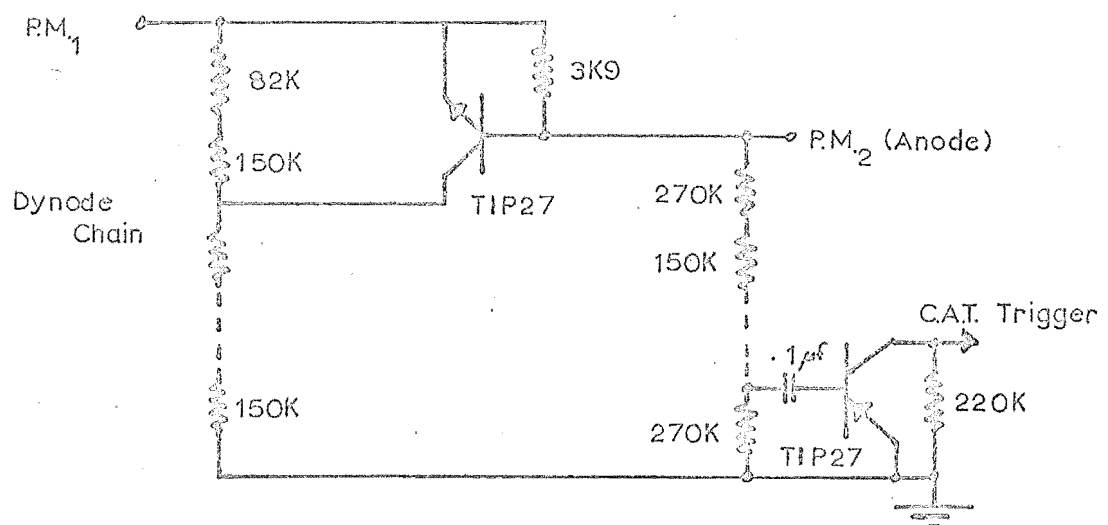


R1	5K6	R11	1K5	C1	15K	T1	BC107
R2	5K6	R12	Pt. Thermom.	C2	15K	T2	BC107
R3	33 Ω	R13	Resistance Box	C3	.005	TR1	HTC5300
R4	470 Ω	R14	5K6	C4	10K	D1	OA91
R5	1K	R16	5K	C5	.05	OP	μA739C
R6	120K	R17	150 Ω	C6	390K		
R7	470 Ω	R18	200K	C7	.1		
R8	15K	R19	1K5	C8	.001		
R9	10K	R15	1K5	C9	.001		
R10	5K6			F1	2N5457		

Preamplifier



Photomultiplier Switch Circuit & C.A.T. Trigger



APPENDIX IIILeast Squares fitting of Data to a Function

This appendix is intended to give a brief outline of the least squares fitting method and a description of the ORGLS program. A fuller description of this program is given in reference⁵⁷.

Suppose that two variables, x and y , are believed to be related by an equation of the form:

$$y = f(p_1, p_2, \dots, p_n, x) \quad (i)$$

where p_1, \dots, p_n are parameters.

If a number of pairs of measurements of the variables x and y are made, the least squares fitting method provides a means of obtaining the values of p_1, \dots, p_n which give the "best" fit of the measured variables to equation (i). The term "best" will be defined later.

The least squares fitting method will be described in terms of fitting data to a simple linear equation followed by an outline of how this method can be extended to the fitting of data to non-linear equations.

Consider a linear equation having two parameters, a and b .

$$\text{e.g.} \quad y = ax + b \quad (ii)$$

where x and y are measured variables having values x_i and y_i .

Assume that y_i is subject to error, e_i which belongs to a population whose variance is J_i , and that x_i is without error.

Also assume that a number of pairs of measurements, x_i , y_i , have been made. It is now required to calculate the values of the parameters a and b that give the "best" fit of the measured data to equation (ii). Let these values of the parameters be \hat{a} and \hat{b} . \hat{y}_i and \hat{x}_i are the values of y_i and x_i which satisfy the equation

$$\hat{y}_i = \hat{a} \hat{x}_i + \hat{b}_i$$

The "residuals" d_i in y_i are defined as:

$$d_i = \hat{y}_i - y_i$$

x_i is assumed to be without error, so the residual in x_i is zero.

Each y_i , x_i pair is weighted by the reciprocal of the variance in the measurement of y_i

$$\text{i.e. } w_i = \frac{1}{J_i^2}$$

The "best" values of the parameters are taken to be those that lead to the minimum value of the weighted sum of the squares of the residuals.

The weighted sum of the squares of the residuals is:

$$\sum_i w_i d_i^2 = \sum_i w_i (y_i - \hat{a} \hat{x}_i - \hat{b})^2$$

This quantity is minimized by partially differentiating with respect to \hat{a} , then with respect to \hat{b} , and equating both results to zero. This gives two equations known as the normal equations. (If the equation that data was to be fitted to was linear in n parameters, n normal equations would result). Solution of these simultaneous

equations results in an estimate of the values of the parameters that give the "best" or least squares fit of the data supplied.

These parameters will have an associated error. The standard deviation, s_p , of the error in parameter, p , is given by:

$$s_p = (\partial p / \partial y_i) \sum_{i=1}^k d_i^2 / (k-1)$$

where k is the number of pairs of x, y measurements.

The least squares method requires that the parameters to be determined are linear function of the measured variables. Although in many cases this requirement is not met, the least squares method can still be applied by making some approximations. The non-linear equation may be linearized by expanding the equation as a Taylor series around approximate, or trial, values of the parameters. These values are written; \hat{p}_i .

If the observational equation is of the form:

$$y = f(p_1, \dots, p_n, x)$$

$$\text{then } y = \sum_i^n \frac{\partial y}{\partial p_i} (p_i - \hat{p}_i) x + \text{higher order terms}$$

$$\therefore y \approx \sum_i^n \frac{\partial y}{\partial p_i} \Delta p_i x \quad (\text{iii})$$

if the values, \hat{p}_i , are close to the true values (i.e. Δp_i small); because then the terms of higher order may, to a first approximation, be neglected. Strictly, the partial derivatives in equation (iii) should be taken at the true values of p_i . Little error will result however, if they are taken at the neighbouring values \hat{p}_i . These

partial derivatives are known numbers and therefore equation (iii) is linear in the corrections, Δp_i . The least squares method described before, can now be applied to estimate the "best" values for these corrections. Once obtained, these corrections can then be applied to the old values of $^0 p_i$ to obtain better values of $^0 p_i$ and the procedure can then be repeated. If the original values of $^0 p_i$ were reasonably near the true values, after a few cycles of this procedure, a "best" value of each parameter will be converged on.

The ORGLS program is designed to fit data to any function, using the least squares method. The program may be divided into five subroutines. The first contains the function to which data is to be fitted. If required, it also contains the equations for the algebraic evaluation of the partial derivatives with respect to each parameter. Alternatively the derivatives which are needed in the normal equations may be evolved numerically. The next subroutine contains the bulk of the least squares computation and includes the setting up of the normal equations which are written in matrix form and solved by calling a matrix inversion subroutine, evaluating the inverse and multiplying the product of the original matrix and parameter vector by it. The other two subroutines enabling preliminary processing of data and testing of calculated parameters were not used.

In most cases five cycles were sufficient for the parameters to converge on their final values.

A modified version of the ORGLS program used in this project is listed below.

```

C      GENERAL LEAST-SQUARES (L11) FORTRAN MATRIX INVERSION
C      MODIFIED OR GLS (GENERAL LEAST-SQUARES)
C
C      DOUBLE PRECISION A(1700),X(1700),U(1700),V(1700),W(1700),
C      DIMENSIONS FOR NV(NMAX)=100, UP(NMAX)=200, UG(NMAX)=1000, UK(PFK)=5
C      DIMENSION TITLE(18), X(1700), Y(1700), SIGY(1200), X(1700)
C      DIMENSION DP(200), SQRTG(2), V(50), UG(200), UV(50), UD(200)
C      DIMENSION DIAIG(100), P(50), RUM(50)
C
C      COMMON AR,V,UD,UV,DP,YC,P,X
C      COMMON NC,NV,NK,ED,INIP,LT,UP,ISENT,IND,NP,NCY,IC
C      COMMON SORTH, DPK,PSAVE,YD,JR,ISENT,LT,ED,POLO
C      COMMON SIGP,LSTOP,NT,NPC
C      COMMON TITLE, D,SIGY,Y,KEY, SOSTR, DD,PLAU,PD,RUM
C
C      FORMAT STATEMENTS
C      51 FORMAT(18A4)
C      52 FORMAT(1H11RA4)
C      53 FORMAT(24I3)
C      54 FORMAT(32HNUMBER OF CYCLES IN THIS JOB IS 12/37HNUMBER OF PARAMETERS
C      TERS TO BE VARIED IS 15/57HNUMBER OF INDEPENDENT VARIABLES PER OBS)
C      55 FORMAT(1H21)
C      56 FORMAT(31HDERIVATIVES PROGRAMMED BY US-RI)
C      59 FORMAT(57HNUMERICAL DERIVATIVES UNLESS PARAMETER INCREMENT IS ZERO)
C      101
C      61 FORMAT(31HWEIGHTS TO BE SUPPLIED BY USER)
C      62 FORMAT(14HOUNT HEIGHTS TO BE SET BY PROGRAM)
C      63 FORMAT(36HPARAMETERS TO BE READ AS INPUT DATA)
C      64 FORMAT(34HPARAMETERS TO BE TAKEN FROM CYCLE 16H OF PREVIOUS JOB)
C      11
C      66 FORMAT(13,7X/(6012,5,RY))
C      67 FORMAT(29HNUMBER OF PARAMETERS READ IS 13)
C      68 FORMAT(11,0,4,10,4,10,4,61)
C      69 FORMAT(31HNUMBER OF OBSERVATIONS READ IS 14)
C      70 FORMAT(17211)
C      71 FORMAT(HE9.4)
C      72 FORMAT(46HCALCULATED Y BASED ON PARAMETERS BEFORE CYCLE 12)
C      73 FORMAT(59H0 Y(OBS) Y(CALC) ORS-CALC SIG(0) (0-C)/SIG(0)
C      11/1H )
C      79 FORMAT(1H 11F0.4)
C      80 FORMAT(1H0AGREEMENT FACTORS BASED ON PARAMETERS BEFORE CYCLE 12/ 0
C      120RSQW((0-C)*12) IS 11.4/35HSQRTF(SUM((0-C)*12)/(10-C)*11)) EGSLSX
C      2 10,41
C      81 FORMAT(60H0ESTIMATED AGREEMENT FACTORS BASED ON PARAMETERS AFTER CYCLE
C      1CYCLE 12/20HSQSUMW((0-C)*12) IS 11.3/35HSQRTF(SUM((0-C)*12)/(10-C)*11)) HGSLSX
C      2-RV11 IS 110,4)
C      83 FORMAT(16H MATRIX HAS A ZERO DIAGONAL ELEMENT CORRESPONDING TO PARAMETER
C      14H OF THOSE VARIED)
C      85 FORMAT(40H SINGULARITY RETURN FROM MATRIX INVERTER)
C      86 FORMAT(37HPARAMETERS AFTER LEAST SQUARES CYCLE 12/5PHD
C      1      CHANGE   IN-W   ERR/R/11 ) OLD ALW 47
C      88 FORMAT(1H 13,E10.4,10X, 10,4) ALW 48
C      89 FORMAT(1H 13,415X,E10.4) ALW 49
C      90 FORMAT(66HOSUBROUTINE TST INDICATES THAT JOB IS TO BE TERMINATED
C      1FOR REASON 12)
C      92 FORMAT(11H0INPUT DATA/4 100 1      P(1)      K(1)      DP(1)/ALW 51
C      11H )
C      93 FORMAT(1H 13,5X,D10.4,5X,14,3X,D11,3) ALW 53
C      94 FORMAT(1H0CORRECTED PARAMETERS NOT TO BE SAVED FOR LATER USE) ALW 54
C      95 FORMAT(1H0CORRECTED PARAMETERS TO BE RETENTION ON PRIVATE TAPE) ALW 55
C      96 FORMAT(1H0CORRECTED PARAMETERS TO BE RETENTION FOR CARD OUTPUT) ALW 57
C      97 FORMAT(19H0CORRELATION MATRIX) ALW 58
C      98 FORMAT(1H013110F-9.4/(1H 3X,10F0,4)) ALW 59
C      99 FORMAT(1H013110F-9.4/(1H 3X,10F0,4)) ALW 60
C
C      INTEGER RDR, PTR, PCH
C      GER=0
C      NCH=7
C      RDR=5
C      PTR=6
C
C      READ TITLE AND CONTROL CARD
C      READ(RDR,51)TITLE(1),I=1,10
C      WRITE(PTR,52)TITLE(1),I=1,10
C      READ(RDR,53)NC, NV, ND, INP, PTR, PCH
C      WRITE(PTR,54)NC, NV, ND
C      IF(I10)206,206,206
C
C      204  WRITE(PTR,58)
C      GO TO 207
C
C      206  WRITE(PTR,59)
C
C      207  IF(I1210,208,210
C
C      208  WRITE(PTR,61)
C      GO TO 211
C
C      210  WRITE(PTR,62)
C
C      211  IF(I1212,212,214
C
C      212  WRITE(PTR,63)
C      GO TO 215
C
C      214  WRITE(PTR,64)IP
C
C      215  IF(IP-11216,218,221
C
C      216  WRITE(PTR,64)
C      GO TO 301
C
C      218  WRITE(PTR,65)
C      GO TO 301
C
C      221  WRITE(PTR,66)
C
C      READ TRIAL PARAMETERS
C      301  IF(IP)401,401,501
C
C      ORGLS 61
C      ORGLS 62
C      ORGLS 63
C      ORGLS 64
C      ORGLS 65
C      ORGLS 66
C      ORGLS 67
C      ORGLS 68
C      ORGLS 69
C      ORGLS 70
C      ORGLS 71
C      ORGLS 72
C      ORGLS 73
C      ORGLS 74
C      ORGLS 75
C      ORGLS 76
C      ORGLS 77
C      ORGLS 78
C      ORGLS 79
C      ORGLS 80
C      ORGLS 81
C      ORGLS 82
C      ORGLS 83
C      ORGLS 84
C      ORGLS 85
C      ORGLS 86
C      ORGLS 87
C      ORGLS 88
C      ORGLS 89
C      ORGLS 90
C      ORGLS 91
C      ORGLS 92
C      ORGLS 93
C      ORGLS 94
C      ORGLS 95
C      ORGLS 96
C      ORGLS 97
C      ORGLS 98
C      ORGLS 99
C      ORGLS 100

```

```

C      401 READ(RDR,66NP),P(1),I=1,NP)          ORGLS101
C      GO TO 601                                ORGLS102
C      501 DO 503 J=1,IP                         ORGLS103
C      503 CONTINUE                               ORGLS104
C      601 WRITE(PTR,67)NP                         ORGLS107
C      IF(IGER.NE.0) GO TO 1621                  ORGLS108
C      READ OBSERVATIONS TO SENTINEL           ORGLS109
C      J=0                                     ORGLS110
C      801 J=J+1
C      READ(RDR,68)(SENT,YD(J),SIGYD(J),X(J),J),I=1,NX)
C      IF(SENT.EQ.801) J=101
C
C      1101 NO=J+1
C      WRITE(PTR,69)NO
C      READ KEY INTEGERS AND PARAMETER INCREMENTS IF SPECIFIED
C      IF(NV>1601,1601,1301)
C
C      1301 READ(RDR,70)(K(I),I=1,NP)           ORGLS121
C      6601 IF(ID11501,1611,1501)                 ORGLS122
C
C      1501 READ(RDR,71)(DP(I),I=1,NP)           ORGLS123
C      GO TO 1621                                GLSX 126
C
C      1601 DO 1602 I=1,IP                      ORGLS124
C      1602 K(I)=0                                GLSX 125
C
C      1611 DO 1612 I=1,IP                      ORGLS126
C      1612 DP(I)=0.0                             GLSX 127
C
C      INITIALIZE PROBLEM AND ENTER SUBROUTINE PRELM IF PROVIDED
C      1621 NH=(INV*(NVEL))/2                     ORGLS128
C      SOSIG(1)=0.0                               GLSX 128
C      CALL PRELM
C
C      PUT OUT TRIAL PARAMETERS, KEY INTEGERS, AND PARAMETER INCREMENTS
C      WRITE(PTR,92)
C      DO 1653 I=1,NP
C
C      1653 WRITE(PTR,93)I,P(I),K(I),DP(I)        ORGLS129
C
C      START LOOP TO PERFORM NV CYCLES AND ONE FINAL CALCULATION OF Y
C      NCY=NCE
C      DO 8501 IC=1,NCY
C
C      CLEAR ARRAYS AH AND V EXCEPT ON LAST CYCLE
C      IF(IC-NCY)>851,2001,2001
C
C      1851 DO 1852 I=1,NH                      ORGLS130
C      1852 AH(I)=0.0                            ORGLS131
C
C      DO 1902 I=1,NV
C
C      1902 V(I)=0.0                            ORGLS132
C
C      INITIALIZE FOR CYCLE IC AND PUT OUT CAPTION FOR LIST OF Y(CALC)
C      2001 SOSIG(2)=SOSIG(1)                      ORGLS133
C      SIG=0.0                                  ORGLS134
C      WRITE(PTR,52)(TITLE(I),I=1,IP)            ORGLS135
C      WRITE(PTR,72)IC                           ORGLS136
C      WRITE(PTR,73)                            ORGLS137
C
C      START LOOP THROUGH NO OBSERVATIONS
C      2201 DO 5101 I=1,NO
C
C      ENTER USERS SUBROUTINE TO COMPUTE Y(CALC) AND DERIVATIVES
C      CALL CALCX(L,1),YC,P,DC
C
C      OBTAIN HEIGHT AND CALCULATE QUANTITIES FROM Y(OBS)-Y(CALC)
C      IF(IW12601,2501,2-01)
C
C      2501 SORTH=1.0/SIGY(I)                   ORGLS138
C      GO TO 2701
C
C      2601 SIGYD(I)=1.0
C      SORTH=1.0
C
C      2701 DY=Y(I)-YC
C      HDY=SORTH*DY
C      SIG=SIG*HDY*DY
C
C      PUT OUT Y(CALC) AND OTHER INFORMATION FOR ONE OBSERVATION
C      WRITE(PTR,79)Y(I),YC,DY,SIGYD(I),HDY,(X(J),J=1,NX)
C
C      BY-PASS DERIVATIVE AND MATRIX SET-UP ON FINAL CALC OF Y
C      IF(IC-NCY)>3001,5101,5101
C
C      START LOOP TO STORE AN ARRAY OF NV DERIVATIVES
C      3001 J=1
C      DO 4101 K=1,NP
C
C      IF(K<(K))4101,4101,5201
C
C      3201 IF(IW13401,3301,3401)
C
C      OBTAIN DERIVATIVE FROM THOSE PROGRAMMED BY USR
C      3301 DV(J)=SORTH*DC(K)
C      GO TO 4001
C
C

```

```

C          OBTAIN DERIVATIVE NUMERICALLY UNLESS PARAMETER
C          INCREMENT IS ZERO
3401      DPK=DP(K)
          1F(DPK>33601,3301,3601)

C          PSAVE=P(K)
          P(K)=PSAVE+DPK
          CALL CALC(X(1,1),YD,P,001)
          DV(J)=SQRTH*(YD-YC)/DPK
          P(K)=PSAVE

C          J=J+1
C          CONTINUE
C          END LOOP TO OBTAIN DERIVATIVES

C          START LOOP TO STORE MATRIX AND VECTOR.
C          1604 OR GLS STORAGE SCHEME IS REVERSE OF 7090 OR GLS
C          JK=1
C          DO 5001 J=1,NV

C          TEMP=DP(V,J)
          IF(TEMP>4501,4401,4501)

C          BY-PASS IF DERIVATIVE IS ZERO
          JK=JK+N1-J
          GO TO 5001

C          DO 4801 K=J,NV
          AM(J,K)=AM(J,K)+TEMP*DV(K)
          JK=JK+1
          CONTINUE

C          V(J)=V(J)+TEMP*HDY
          CONTINUE
          END LOOP TO STORE MATRIX AND VECTOR

C          5001      CONTINUE
C          END LOOP THROUGH NO OBSERVATIONS

C          COMPUTE AND PUT OUT AGREEMENT FACTORS
          SOSIG(1)=DSQRT(SIG/FLOAT(14C-IV))
          WRITE(PTR,B01C,SIG,SOSIG(1))

C          BY-PASS MATRIX INVERSION AND PARAMETER OUTPUT ON FINAL CYCLE
          IF(LC-NV>15401,4701,4701)

C          START LOOP TO TEST FOR ZERO DIAGONAL ELEMENT
          5401      ISING=0
          I1=1
          I10=NV
          DO 5801 I=1,NV
          IF(AM(I,I)>5701,5601,5701)

C          5601      ISING=1
          WRITE(PTR,B31I)

C          5701      I1=I1+10
          I10=I10-1
          CONTINUE
          END LOOP TO TEST FOR ZERO DIAGONAL ELEMENT

C          TERMINATE JOB IF ZERO DIAGONAL ELEMENT HAS BEEN FOUND
          IF(I1>110301,6001,110301)

C          ENTER SUBROUTINE TO REPLACE MATRIX WITH INVERSE
          CALL MATINV(AM,NV,ISING)
          IF(I1>116201,6101,6201)

C          TERMINATE JOB IF SINGULAR MATRIX WAS FOUND
          WRITE(PTR,B51)
          GO TO 10301

C          START LOOP FOR MATRIX VECTOR MULTIPLICATION FOR
          C          PARAMETER CHANGES
          6301      DO 7201 I=1,NV
          C          PD1=0.0
          C          IJ=1
          C          IJD=IV-1
          DO 7001 J=1,NV
          C          PD1=PD1+AM(IJ)*V(J)
          C          IFL(I-1)=6701,6001,6201

C          6701      IJ=IJ+1D0
          C          IJ=IJ-1
          GO TO 7001

C          SAVE DIAGONAL ELEMENTS OF INVERSE MATRIX
          6801      DIAG(I)=AM(I,I)
          C          IJ=IJ+1
          C          CONTINUE

C          6901      IJ=IJ+1
          C          CONTINUE

C          7001      PD1=PD1+PD1
          SIG=SIG-PD1*V(I)
          C          CONTINUE
          END LOOP FOR MATRIX VECTOR MULTIPLICATION

C          RECOMPUTE AGREEMENT FACTOR USING PREVIOUS SIG
          3655      SOSIG(1)=DSQRT(SIG/FLOAT(14C-IV))

C          PUT OUT CAUTION FOR LIST OF CORRECTED PARAMETERS
          WRITE(PTR,B51)
          WRITE(PTR,B51)
          WRITE(PTR,B51)
          C          START LOOP TO PRINT AND PUT OUT PARAMETER

```

```

C
      J=1
      DO 9001 I=1,NP
C
      IF(KI(I,I)=763) GO TO 7701
C
      7601      WRITE(PTR+P01,I,P01),P01
      GO TO 9001
C
      7701      P01=PO1+P02
      P01=PO1+PO2*PD(J)
C
      8111      STOP=SQRT(DIA(I,J)*SQSIG(I))
      WRITE(PTR+P01,I,P01,I,P01),STOP
      J=J+1
C
      8001      CONTINUE
      END LOOP TO CORRECT AND PUT OUT PARAMETERS
C
      PUT OUT ESTIMATED AGREEMENT FACTORS
      WRITE(PTR+P01,I,SIG,SQSIG(I))
C
      ENTER USERS SUBROUTINE TO TEST AND MODIFY PARAMETERS
      OR END JOB
C
      8112      ISTOP=0
      CALL TEST
C
      WRITE CORRECTED PARAMETERS ON AUXILIARY TAPE IF
      DESIRED
      IF(IT-1) 8501,8204,P204
C
      8204      NT=7
C
      8205      NPCD=DR((LNP-1)/NCD)
      WRITE(PCH,66)NP,(P01),I=NPCD
      GO TO 8501
      8401      WRITE(PTR,901)STOP
      GO TO 8701
C
      8501      CONTINUE
      END LOOP THROUGH NC CYCLES AND FINAL CALL OF Y
C
      TERMINATE JOB
      8701  IF(YG(I)0501,10501,BR01
C
      CALCULATE AND PUT OUT CORRELATION MATRIX
      8801      WRITE(PTR,52)(TITLE(I),I=1,L)
      WRITE(PTR,97)
      DO 9101 I=1,NV
C
      DIAG(I)=1.0/SQRT(DIAG(I))
      CONTINUE
C
      J=1
      DO 10201 I=1,NV
C
      DO 9601 J=1,NV
C
      RDW(J)=0.0
      CONTINUE
C
      DO 10001 J=1,NV
C
      RDW(J)=AM(I,J)*DIAG(I)*DIAG(J)
      IJ=IJ+1
      10001  CONTINUE
C
      WRITE(PTR,98)I,(RDW(J),J=1,NV)
      10201  CONTINUE
C
      10301  CONTINUE
C
      10501  GER=GER+1
      GO TO 301
      END
C
      DUMMY SUBROUTINE PRELIM
      SUBROUTINE PRELIM
      RETURN
      END
C
      DUMMY SUBROUTINE TEST
      SUBROUTINE TEST
      RETURN
      END
      SUBROUTINE MATINV(AM,N,IFAIL)
      REAL#R AM(700),SUMA,TERM,DEPM
C
C      ***** SEGMENT 1 OF CHOLESKY INVERSION *****
C      ***** FACTOR MATRIX L= LOWER TRIANGLE X TRANSPOSE *****
      K=1
      IF(N-1)10,8,7
      8 AM(1,1)=0/AM(1)
      GO TO 204
C
      ***** LOOP N OF A(L,M) *****
      9 DO 7 M=1,N
      IMAX=M-1
      ***** L TOP L OF A(L,M) *****
      DO 6 L=M,N
      SUMA=0.0
      KLI=L
      KMI=M
      IF(IHAX123,23,1)
      ***** SUM OVER I=1,M-1 A(L,I)*A(M,I) *****
      1 DO 2 I=1,IMAX
      SUMA=SUMA+AM(KLI)*AM(IKMI)
      PRINT3645; AM(KLI),AM(KMI)
      J=N-I
      KLI=KLI+J
      2 KMI=KMI+J
      3

```

```

C      6666666666 TERM=A(L,M)-SUMA 6666666666
C      23 TERM=AH(K)+SUMA
C      24 IF(L-M)3,3,5
C      3 3(ITERN10,10,4
C      4 4(ITERN10)=SUBT(ITERN) 6666666666
C      5 5(ITERN)=DSORT(ITERN)
C      6 AH(K)=DENOM
C      7 GOTO 6
C      10 HAILE=K
C      11 DO 70 300
C      300 6666666666 A(L,M)=TERM/A(H,M) 6666666666
C      5 AH(K)=TERM/DENOM
C      6 KHK61
C      7 CONTINUE
C
C      6666666666 SEGMENT 2 OF CHOLESKI INVERSION 6666666666
C      6666666666 INVERSION OF TRIANGULAR MATRIX6666666666
C      100 AH(1)=1.0/AH(1)
C      100 K0M61
C
C      6666666666 STEP L OF B(L,M) 6666666666
C      DO 104 L=2,N
C      KDM=K0M61-L62
C
C      6666666666 RECIPROCAL OF DIAGONAL TERM 6666666666
C      TERM = 1.0/AH(KDH)
C      AH(KDH)=TERM
C      KDH=0
C      KLI=L
C      IMAX=L-1
C
C      6666666666 STEP M OF B(L,M) 6666666666
C      DO 103 M=1,IMAX
C      KMKL1
C
C      6666666666 SUM TERMS 6666666666
C      SUMA=0.0
C      DO 102 I=N,IMAX
C      110 KHK61
C      SUMA=SUMA-AH(KLI)*AH(I)
C      102 KLI=KLI+LN-1
C
C      6666666666 MULT SUM * RECIP OF DIAGONAL 6666666666
C      AH(K)=SUMA+TERM
C      J=N-M
C      KLI=KJ
C      103 KHI=KHI+J
C      104 CONTINUE
C
C      6666666666 SEGMENT 3 OF CHOLESKI INVERSION 6666666666
C      6666666666 PREMULTIPLY LOWER TRIANGLE BY TRANSPOSE6666666666
C
C      200 K1
C      DO 203 M=1,N
C      KLI=K
C      DO 202 L=M,N
C      KHI=K
C      IMAX=N-L61
C      SUMA=0.0
C      DO 201 I=1,IMAX
C      SUMA=SUMA+AH(KLI)*AP(KHI)
C      KLI=KLI+1
C      201 KHI=KHI+1
C      AH(K)=SUMA
C      202 KKI=K
C      203 CONTINUE
C      204 HAILE=0
C      300 RETURN
C      END

```

REFERENCES

1. Schmidt, Ann. Physik, 58, 103, (1896).
- 2a. S. Vavilov and V. Levschin, Z. Physik, 35, 930, (1926).
- 2b. A. Schischolovski and S. Vavilov, Phys. Z. Sowjet, 5, 379, (1934).
- 3a. e.g. G. Lewis and M. Kasha, J.A.C.S., 66, 2100, (1934).
- 3b. A. Terenin, Acta Physicochem. URSS., 18, 210, (1943).
A. Terenin, Zh. Fiz. Khim., 18, 1, (1944).
- 4a. J. D. Wineforder and P. A. St. John, Anal. Chem., 35, 2211, (1945)
- 4b. F. Smith, J. Smith and S. McGlynn, Rev. Sci. Instr., 33, 1367, (1962).
5. e.g. G. Oster, N. Geacintov and T. Cassen, Acta Phys. Polon., 26, 489, (1964).
6. e.g. W. H. Melhuish and R. Hardwick, Trans. Faraday Soc., 58, 1908, (1962).
- 7a. e.g. K. Benz and H. Wolf, Z. Naturforsch, 19A, 181, (1964).
- 7b. J. Olness and H. Spomer, J. Chem. Phys., 38, 1779, (1963).
8. H. Linschitz, C. Steel, J. Bell, J. Phys. Chem., 66, 2574, (1962)
9. S. K. Lower and M. A. El Sayed, Chem. Revs., 66, 228, (1966).
- 10a. C. A. Parker, "Advances in Photochemistry", Vol. 2, pp305, Interscience 1964.
- 10b. C. A. Parker, "Photoluminescence of Solutions", Elsevier 1968.
11. A. Terenin and V. Ermolaev, Trans. Faraday Soc., 52, 1042, (1956).
- 12a. G. A. Robinson and R. Frosch, J. Chem. Phys., 37, 1962, (1962).

- 12b. G. A. Robinson and R. Frosch, J. Chem. Phys., 38, 1187, (1963).
- 12c. G. A. Robinson and R. Frosch, J. Mol. Spectry., 6, 58, (1961).
- 13a. W. Siebrand, J. Chem. Phys., 44, 4055, (1966).
- 13b. W. Siebrand, J. Chem. Phys., 46, 440, (1967).
14. S. H. Lin, J. Chem. Phys., 44, 3759, (1966).
- 15a. G. R. Hunt, E. F. McCoy and I. G. Ross, Aust. J. Chem., 15, 591, (1962).
- 15b. E. F. McCoy, and I. G. Ross, Aust. J. Chem., 15, 573, (1962).
- 15c. J. P. Byrne, E. F. McCoy and I. G. Ross, Aust. J. Chem., 18, 1589, (1965).
16. S. Chandrasekhar, Revs. Modern Phys., 15, 1, (1943).
- 17a. T. R. Waite, Phys. Rev., 107, 463, (1957).
- 17b. T. R. Waite, J. Chem. Phys., 28, 103, (1958).
- 17c. T. R. Waite, J. Chem. Phys., 32, 21, (1960).
18. F. C. Collins and G. E. Kimball, J. Colloid Sci., 4, 425, (1949).
19. S. Glasstone, K. J. Laidler and H. Eyring, "Theory Of Rate Processes", McGraw-Hill.
20. F. Erich and R. Simha, J. Chem. Phys., 7, 116, (1939).
21. D. A. Collins and H. Watts, Aust. J. Chem. 17, 516, (1964).
22. G. Porter and M. W. Windsor, Disc. Faraday Soc., 17, 178, (1954).
23. A. D. Osbourne and G. Porter, Proc. Royal Soc., 284, 9, (1965).
24. G. Porter and M. R. Wright, Disc. Faraday Soc., 27, 18, (1959).
- 25a. T. H. Jones and R. Livingston, Trans. Faraday Soc., 60, 2168, (1964).
- 25b. R. Livingston and W. R. Ware, J. Chem. Phys., 39, 2593, (1963).

- 25c. G. Jackson and R. Livingstone, J. Chem. Phys., 35, 2182, (1961).
- 26a. J. Hilpern, G. Porter and L. Stief, Proc. Royal Soc., 277, 437, (1964).
- 26b. B. Stevens and M.S. Walker, Proc. Royal Soc., 281, 420, (1964).
27. A. D. Osbourne and G. Porter, Proc. Royal Soc., 284, 9, (1965).
28. J. Hilpern, G. Porter and L. Stief, Proc. Royal Soc. 277, 442, (1964).
- 29a. S. J. Ladner and R. S. Becker, J. Chem. Phys., 43, 3344, (1965).
- 29b. G. Porter and M. R. Wright, Disc. Faraday Soc., 27, 96, (1959).
- 29c. S. J. Ladner and R. S. Becker, J.A.C.S., 86, 4205, (1964).
- 29d. G. Porter and L.J. Stief, Nature, 195, 991, (1962).
30. I. H. Leubner and J. E. Hodgkins, J. Phys. Chem., 73, 2545, (1969).
31. W. Siebrand, J. Chem. Phys., 47, 2411, (1967).
32. G. Porter and L. J. Stief, Bull. Soc. Chim. Belges, 71, 641, (1962).
also references 25a. and 29d.
33. G. Porter, Disc. Faraday Soc., 27, 95, (1959).
34. J. E. Hodgkins and J. D. Woodyard, J.A.C.S., 89, 710, (1967).
35. e.g. (a) R. E. Kellogg and R. P. Schwenker, J. Chem. Phys., 41, 2860, (1964).
(b) N. Trublin, R. Santos and M. Ptak, Compt. Rend., 260, 1134, (1965).
(c) R. E. Kellogg and N. C. Wyeth, J. Chem. Phys., 45, 3156, (1966).
(d) B. A. Baldwin, J. Chem. Phys., 50, 1039, (1969).

36. W. Siebrand, J. Chem. Phys., 50, 1040, (1969).
37. P. F. Jones and S. Siegel, J. Chem. Phys., 50, 1134, (1969).
- 38a. Gurney and Mott, Trans. Faraday Soc., 35, 69, (1939).
- 38b. W. H. Melhuish, Trans. Faraday Soc., 62, 3384, (1966).
39. S. H. Lin and R. Bersohn, J. Chem. Phys., 48, 2732, (1962).
- 40a. G. F. Hatch, M. D. Erlitz and G. C. Nieman, J. Chem. Phys., 49, 3723, (1968).
- 40b. M. D. Erlitz and G. C. Nieman, J. Chem. Phys., 50, 1479, (1969).
- 40c. G. F. Hatch, M. D. Erlitz and G. C. Nieman, "Intern. Conf. Molec. Lumin.", E. C. Lim. 1964. PP. 21.
- 41a. J. W. Rabalias, H. J. Maria and S. P. McGlynn, J. Chem. Phys., 51, 2259, (1969).
- 41b. J. W. Rabalias, H. J. Maria and S. P. McGlynn, Chem. Phys. Letters, 3, 59, (1969).
42. G. F. Hatch, M. D. Erlitz and G. C. Nieman, "Intern. Conf. Molec. Lumin.", E. C. Lim. 1964, pp. 23.
43. M. R. Wright, R. P. Frosch and G. W. Robinson, J. Chem. Phys., 33, 934, (1960).
- 44a. J. H. van der Waals, A. M. D. Berghius and M. S. de Groot, Mol. Phys., 13, 301, (1967).
- 44b. M. S. de Groot, I.A.M. Hesselmann and J. H. van der Waals, Mol. Phys., 10, 91, (1965).
- 44c. G. C. Nieman and D. S. Tinti, J. Chem. Phys., 46, 1432, (1967).
45. P. F. Jones and A. R. Calloway, J. Chem. Phys., 51, 1661, (1969).

- 46a. B. A. Baldwin and H. W. Offen, J. Chem. Phys., 46, 4509, (1967)
- 46b. B. A. Baldwin and H. W. Offen, J. Chem. Phys., 49, 2937, (1968)
47. H. W. Offen and D. F. Hein, "Intern. Conf. Molec. Lumin.",
E. C. Lim. 1964, pp. 1.
48. B. A. Baldwin and H. W. Offen, J. Chem. Phys., 48, 5358, (1968)
49. Y. Hirshberg, Anal. Chem., 28, 1954, (1956)
- 50a. J. C. Mottram and I. Doniach, Nature, 140, 588, (1937)
- 50b. S. Epstein, M. Small, H. L. Falk and N. Mantel, Cancer Res.,
24, 855, (1964)
- 50c. S. Epstein, M. Small, I. Bulon, I. Kaplan and N. Mantel,
Nature, 204, 750, (1964)
51. G. von Foerster, J. Chem. Phys., 40, 2059, (1964)
52. H. M. McNair and E. J. Bonelli, "Basic Gas Chromatography",
Varian Aerograph. 1964, pp. 116-117.
53. e.g. H. Tsubomura and R. S. Mulliken, J.A.C.S., 82, 5966, (1960)
54. e.g. C. A. Parker, "Advances in Photochemistry", Vol. 2, pp.
327, Interscience 1964.
55. W. H. Melhuish, Nature, 184, 1933, (1959)
56. W. S. Metcalf, private communication.
57. W. R. Busing and H. A. Levy, "General Least Squares Program",
ORNL-TM-271.
58. T. G. Bissel and A. G. Williamson, private communication.
59. A. C. Ling and J. E. Willard, J. Phys. Chem., 72, 3349, (1968)
60. E. McLaughlin, Trans. Faraday Soc., 55, 28, (1959)
61. G. M. Badger, Adv. Cancer Res., II, 73, (1954)

62. e.g. (a) R. L. Berger, J. Jorden, E. Ackerman, J.A.C.S.,
78, 2979, (1956).
(b) W. Ware, J. Phys. Chem., 66, 455, (1962).
(c) B. Smaller, J. McMillan, and J. Remko, Bull. Am.
Phys. Soc., 8, 238, (1963).